AVRADCOM
Report No. 81-F-15

AD 81-F-15

MANUFACTURING METHODS AND TECHNOLOGY
(MANTECH) PROGRAM

TITLE: MANUFACTURING METHODS AND TECHNOLOGY PROGRAM FOR STABILIZED LINE OF SIGHT COMPOSITE GIMBAL

Author (s)	J.T. Johnson, W.B. Lloyd, T.F. Grapes, R.L. Kolek and R.S. Zucker
Organization	Westinghouse Defense & Electronic Systems Center
Organization Address	Systems Development Division Baltimore, Maryland 21203

Date: December 1981

FINAL REPORT

Contract No. DAAK80-80-C-0528

Approved for public release;
distribution unlimited

United States Army
AVIATION RESEARCH AND DEVELOPMENT COMMAND

DISCLAIMER NOTICE

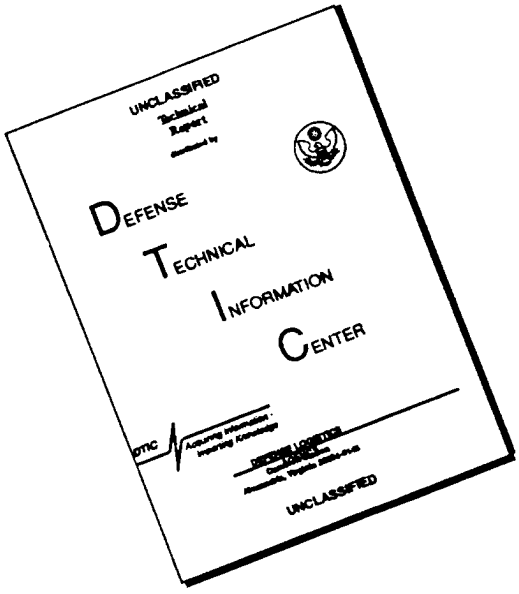

THIS DOCUMENT IS BEST QUALITY AVAILABLE. THE COPY FURNISHED TO DTIC CONTAINED A SIGNIFICANT NUMBER OF PAGES WHICH DO NOT REPRODUCE LEGIBLY.

REPORT DOCUMENTATION PAGE

READ INSTRUCTIONS BEFORE COMPLETING FORM

1. REPORT NUMBER: 81-F-15 Final Technical Report
2. GOVT ACCESSION NO.:
3. RECIPIENT'S CATALOG NUMBER:

4. TITLE (and Subtitle): Manufacturing Methods and Technology Program for Stabilized Line of Sight Composite Gimbal
5. TYPE OF REPORT & PERIOD COVERED: Technical
6. PERFORMING ORG. REPORT NUMBER: 80-1160A

7. AUTHOR(s): J.T. Johnson, W.B. Lloyd & T.F. Grapes, R.L. Kolek and R.S. Zucker
8. CONTRACT OR GRANT NUMBER(s): DAAK80-80-C-0528

9. PERFORMING ORGANIZATION NAME AND ADDRESS: Westinghouse Defense and Electronic Systems Center, Systems Development Division, Baltimore, Maryland
10. PROGRAM ELEMENT, PROJECT, TASK AREA & WORK UNIT NUMBERS: MANTECH Project 1797315 7315 (XM9)

11. CONTROLLING OFFICE NAME AND ADDRESS: US Army Aviation Research and Development Command, ATTN: DRDAV-EGX 4300 Goodfellow Blvd., St. Louis, MO 63120
12. REPORT DATE:
13. NUMBER OF PAGES:

14. MONITORING AGENCY NAME & ADDRESS (if different from Controlling Office): US AVRADA, DAVAA-E (HUN) Ft. Monmouth, NJ 07703
15. SECURITY CLASS. (of this report): UNCLASSIFIED
15a. DECLASSIFICATION/DOWNGRADING SCHEDULE:

16. DISTRIBUTION STATEMENT (of this Report): Approved for public release. Distribution unlimited.

17. DISTRIBUTION STATEMENT (of the abstract entered in Block 20, if different from Report):

18. SUPPLEMENTARY NOTES:

19. KEY WORDS (Continue on reverse side if necessary and identify by block number):

Advanced Composite
Composite Materials
Gimbals
Graphite Epoxy
Manufacturing Methods

20. ABSTRACT (Continue on reverse side if necessary and identify by block number):

The program effectively applied graphite epoxy composite to an electro-optical gimbal system resulting in a lighter gimbal with higher inherent damping. In addition, the coefficient of thermal expansion of the composite gimbal is more closely matched to the stainless steel bearings used in the assembly than is the case for an aluminum gimbal.

In the composite gimbal, weight was reduced by 1/3. The stiffness-to-

#20)

weight ratio has been increased by a factor of two. The damping ratio has been improved by a factor of 4. The stiffness was designed to provide natural frequencies of 150 Hz or higher. The lowest measured resonance was 136 Hz for the first sample, which was dimensionally similar to the aluminum design.

The composite gimbal cost factor, when compared to an aluminum gimbal, came out at 1.5X. However, the fact that the sample gimbal had to be designed to fit within a previously designed aluminum system represented a cost driver. Study indicates that in an entirely new, all composite design, using pitch base material, the cost factor could be reduced to 1.3.

Also in the area of cost, this program demonstrated that the use of low cost tooling allowed design changes to be incorporated without experiencing high cost impacts. The second gimbal sample allowed for the use of a larger mating gimbal in the final assembly. The change was accomplished by a few hours effort to change the drawings, and then the piece parts were fabricated accordingly with minimal tooling changes. It was not necessary to redesign a casting and then go through the casting procurement and checkout cycle. In a typical system where design improvement changes are incorporated on a fairly regular basis, the savings in the tooling area could more than offset the premium associated with the use of graphite epoxy.

The program developed and exercised design procedures for composite materials as applied to electro-optical gimbals. These procedures took advantage of the method of construction used, that is, the use of basic composite material shapes bonded together to form a light, rigid structure. This construction approach not only made attaining functional requirements straight forward, but permitted flexibility with respect to design changes.

Machining the composite parts prior to assembly, and machining the final assemblies did not present any serious problems. Carbide cutting tools were used since the quantity was small. In a production run, diamond tools would be appropriate. The main caution in the machining procedure is handling the dust which must be vacuumed away immediately. When machining wet, the filtration system must be serviced more frequently.

The quality control aspects of composites are advancing rapidly. The program developed a fairly standard approach in this area. However, since the actual implementation of a quality control system is very dependent upon the actual parts being manufactured and the state of the art at the time of implementation, future production programs would require a review of the proposed quality system.

Process flow charts and factory layout concepts were developed for a 1000 gimbal-per-year production rate. The basic premise was that all raw material would be purchased from industry sources and then processed within the facility to form the basic shapes needed for gimbal production.

The program was successfully concluded with the vibration and thermal evaluation of the two samples. The low cost tooling approach proved to be effective. The basic production planning for a 1000-gimbals-per-year has been completed. The next step, which would be a new program, is to build a complete gimbal system using advanced composites and subject it to flight tests.

TABLE OF CONTENTS

LIST OF ILLUSTRATIONS

LIST OF ILLUSTRATIONS (CONT.)

LIST OF TABLES

PREFACE

This Final Report covers work performed under Army Contract DAAK80-C-0528 by the Westinghouse Defense and Electronic Systems Center, Systems Development Division, Baltimore, Maryland, 20203.

All of the work was conducted at the Baltimore facility, with the exception of testing materials, coupons, and windings and machining two complex gimbal parts. The coupon tests and winding work was accomplished at the Westinghouse Research and Development Center in Pittsburgh, PA. In addition, some of the raw material was processed into plates and rectangular cross-section tubes by Exxon Enterprises Material Division, Fountain Inn, S.C. (Formerly Graftek Division of Exxon).

This project was accomplished as part of the U.S. Army Aviation Research and Development Command (AVRADCOM) Manufacturing Technology program. The primary objective of this program is to develop, on a timely basis, manufacturing processes, techniques, and equipment for use in production of Army material. Comments are solicited on the potential utilization of the information contained herein as applied to present and/or future production programs. Such comments should be sent to: U.S. Army Aviation Research and Development Command, ATTN: DRDAV-EGX, 4300 Goodfellow Blvd., St. Louis, MO., 63130.

Work was performed under the technical direction of Mr. Alfred Kleider of the Army Aviation Research and Development Activity, Ft. Monmouth, N.J., and Mr. Fred Reed of HQ, AVRADCOM, St. Louis, MO.

1. INTRODUCTION

This program developed manufacturing methods for applying advanced composite materials, such as high modulus graphite-epoxy, utilizing low cost tooling in gimbal structures in such a way that the cost impact of design changes are minimized. With implementation of the results, it will be possible to produce small sized lots of gimbal structures, and then make design changes and produce additional small lots without incurring prohibitive tooling costs. The program also demonstrated that the use of low weight, high stiffness and high damping material is very appropriate to electro-optical applications.

The sample fabrication and test program was divided into three phases. Material samples were initially fabricated and tested to help establish the materials base line for the gimbals. A thermal sample was designed and tested to demonstrate the adequacy of the design. Finally, two full gimbal samples were manufactured and subjected to vibration and thermal tests. The second gimbal sample represented a design change from the first and provided a design change experience.

This report is organized to present the program in approximately the order in which it was accomplished - Design, Fabrication, Test, and Production Planning. It should be pointed out that there were major beneficial overlaps between the various disciplines throughout the program. Manufacturing Engineering was involved in the design process just as Design Engineering and Quality Engineering were involved in the assembly process. All disciplines participated in the production planning. Material selection was based on the contribution made by the R&D Center's, Plastics and Elastomers group.

2. DESIGN AND ANALYSIS

2.1 COMPOSITES FOR GIMBALS

It can be shown[1] that the lowest natural frequency in a gimbal set is a good measure of the inherent acceleration sensitivity of the set. There is an inverse relationship between the lowest natural frequency and the sensitivity to acceleration, thus it is desirable to design the gimbal to force the lowest natural frequency, and all the others that accompany it, to be as high as possible. For gimbal sets which are used in airborne vehicles, it is especially important to resist the effect of vibrational g's as well as manuevering g's. The vibration is particularly bothersome because it can produce jitter which can cause image degradation.

Since the gimbal mass reduces the natural frequency while the gimbal rigidity increases it, it is desirable to obtain the highest possible stiffness to weight ratio, which makes the gimbal structure a logical application for high modulus composite materials. This is the accepted reason for using composites in gimbals. A lesser known but equally important reason is damping, or diminished amplitude of the oscillations because each of the resonances within the spring mass system is perturbed by the vibrational input. Since more damping causes less response at each of the resonances, the jitter is reduced.

A third reason for use of composites is the capability to change the design in the course of the development of the system. For example, with the built up construction described in this report, it is possible to build two gimbals with short yoke arms and then quickly change to build several more gimbals with long yoke arms, with only modest changes in the tooling.

2.2 DESIGN APPROACH

Figure 1 shows the unmachined aluminum casting for the gimbal structure which was chosen to be redesigned to use composite materials. It is, in essence,

[1] AFFDL-TR-76-145 "Vibration Control for Airborne Optical Systems" by W.B. Lloyd, et al, March 1977.

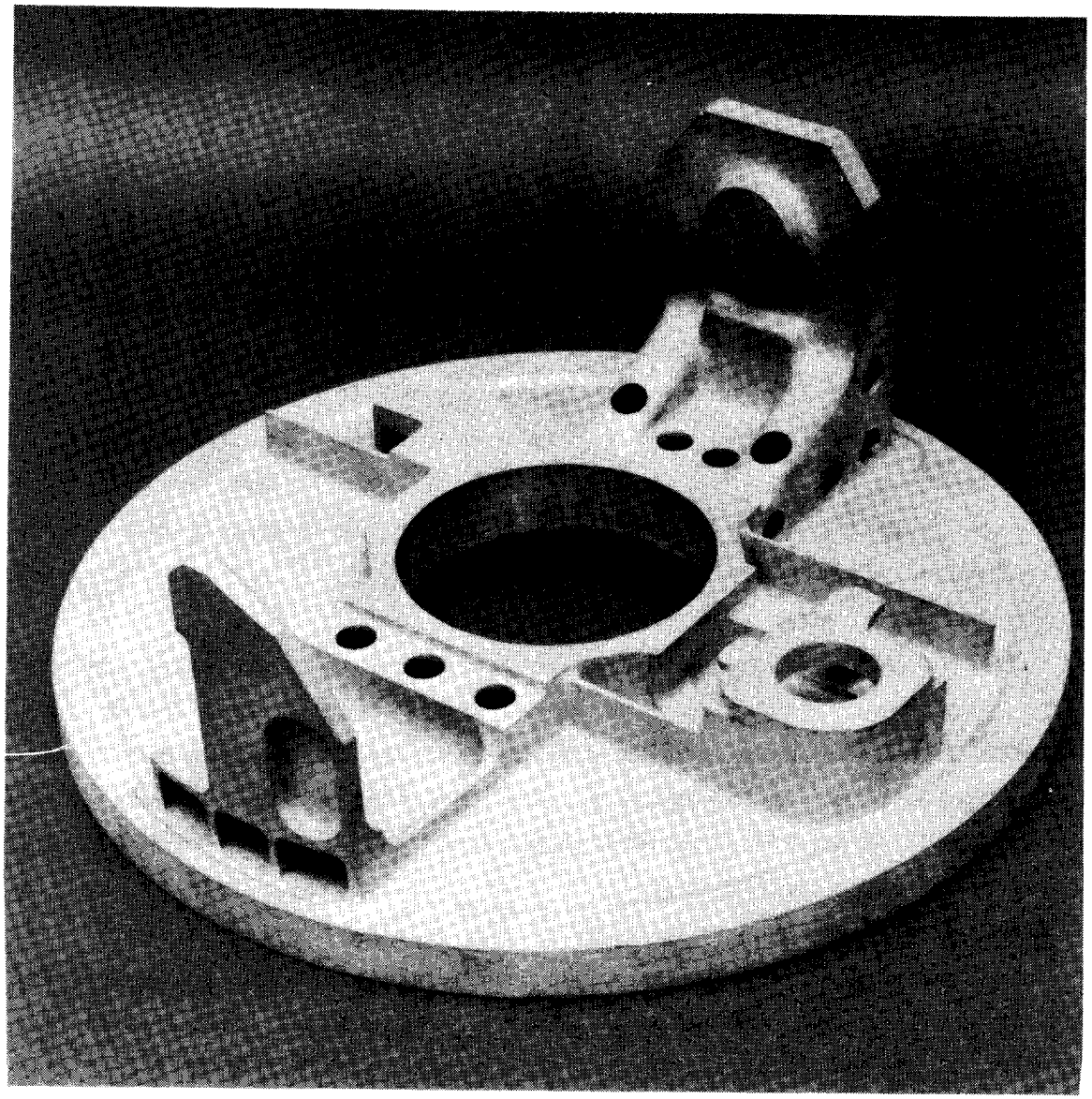

Figure 1. Aluminum Gimbal

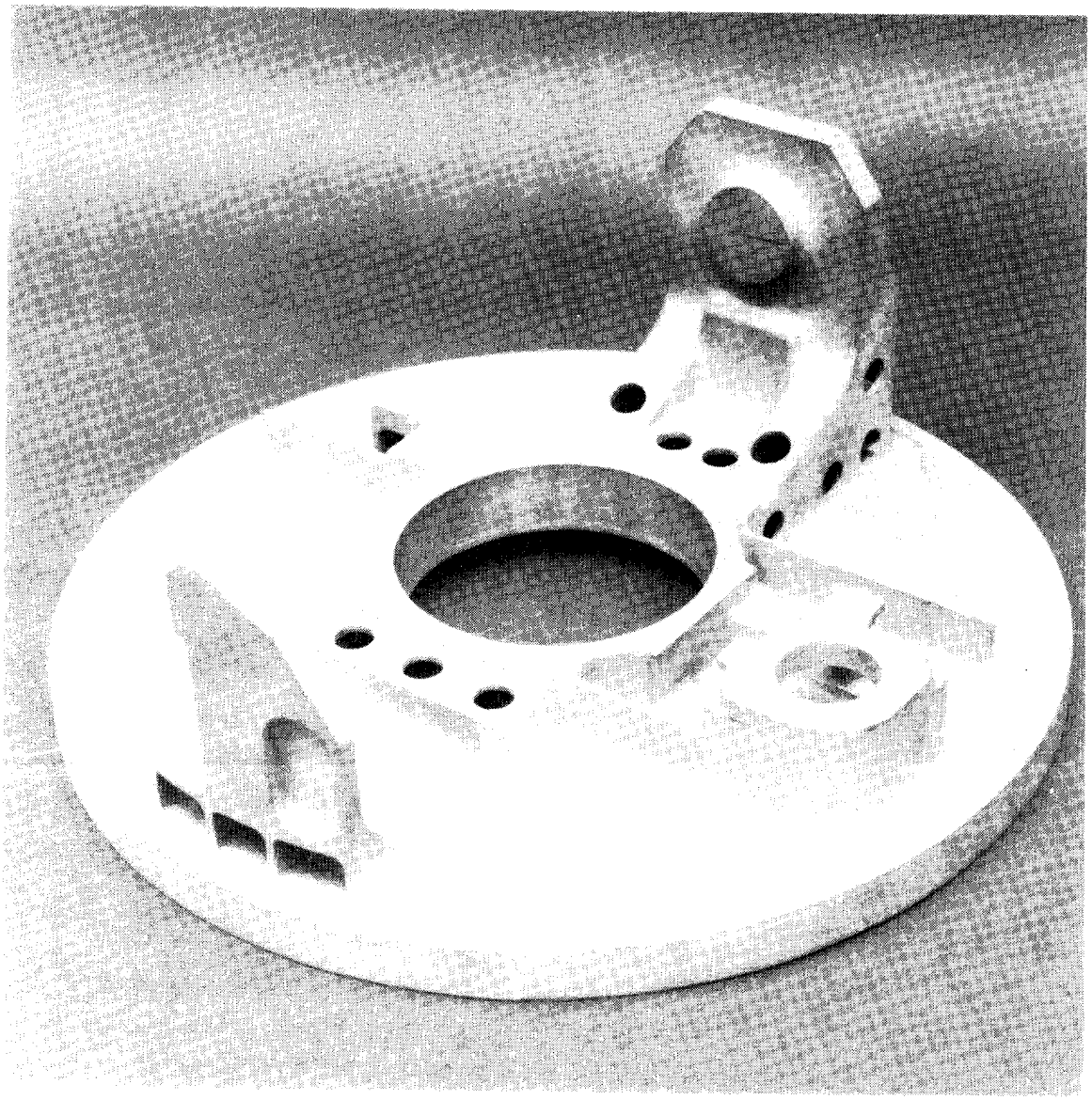

Figure 1. Aluminum Gimbal

a yoke structure with a 13.2 inch diameter base-plate made integral with the cross-piece of the yoke. The center of the cross-piece is penetrated by a 4.125 inch diameter hole which accommodates optical elements, and which is provided with a duplex ball bearing to create the azimuth axis for the gimbal set involved. It is seen that the cross-piece must maintain structural integrity although penetrated by the large bore. The yoke arms, which point upward in figure 1, support the elevation gimbal which pivots on shafts which rotate using bearings fitted into the bosses evident on the yoke arms. The elevation gimbal is shown schematically in figure 2. The integral base-plate, which is quite thin except for the circular rim, provides a mounting base for a pressurized dome. The azimuth drive motor mounting base and gear box frame are also made integral with this base-plate.

The actuator support arm (upper right in figure 1) is the more massive of of the two yoke arms. This is true because the elevation gimbal is axially constrained by this arm by means of a thrust-carrying bearing, whereas it has axial freedom with respect to the half arm (lower left in figure 1). The half arm is volume-limited because it must be cut away to provide clearance for the stabilizing mirror. Loads on the yoke arms and cross-piece are derived from the mass of the elevation gimbal assembly. These elevation gimbal loads on the yoke arms are carried radially inward to the bearing support ring by cross-piece box structures which are effective in resisting both bending and torsional loads. The box structures also stiffen the base plate and assist in carrying the dome loads inward to the bearing support ring. The integral gear box frames further strengthen the base plate against dome loading.

2.2.1 Problem Definition

The basic problem was to redesign the above-described gimbal structure using advanced composite materials and low cost tooling. One objective was to achieve a weight less than the aluminum gimbal, with resonant frequencies equal to or greater than those associated with the aluminum version while staying within envelope constraints determined by the prior design. Specific problem areas included load analysis to determine optimum filament orientation, development of subelement fabrication techniques, bonding, alignment during bonding, and metal inserts.

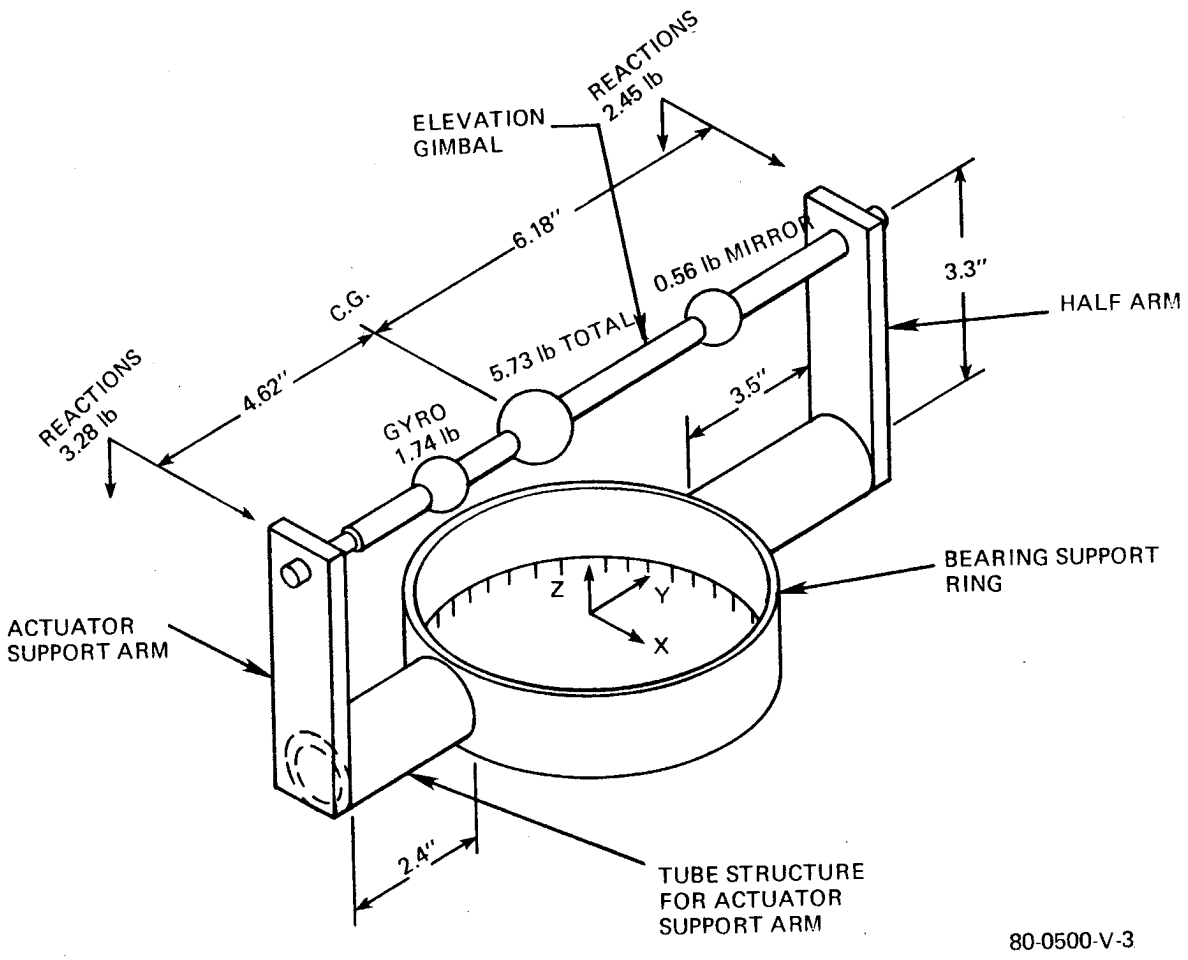

Figure 2. Idealized Gimbal Yoke Structure

2.2.2 Idealized Yoke Structure

Figure 2 shows an idealized yoke structure having the same basic dimensions as the original design shown in figure 1. In this configuration, the structure has been simplified to facilitate visualization of the overall problem. The elevation gimbal is assumed to be a rigid shaft with concentrated loads as shown with end reaction to the support arms also as shown. The bearing support ring is assumed to be rigidly attached to the frame, which assumes infinitely rigid rolling element bearings except, of course, for rotation about the azimuth axis. The mode shapes at the fundamentals for each of the input axis can be easily visualized by considering frame vibration in each of the axis X, Y, and Z. For example, excitation in the X direction will cause a mode which involves combined torsion and bending of the indicated tube structures. This means that the composite material used in this location must have a layup which achieves a good compromise between flexural rigidity and torsional rigidity.

The basic idea for designing with composites was to fabricate individual elements from plates and box sections, and then to join the parts together to form the gimbal. To accomplish this, it was necessary to engineer the mating surfaces of the elements to form highly reliable joints. The idealized structure of figure 2 suggests methods of designing for use with composites, and it serves to highlight problem areas in doing so. One such problem is joining a composite tube to the bearing support ring. An unreinforced butt joint as shown in figure 2, would not provide sufficient bonding area and is thus to be avoided.

2.2.3 Layout

In the composite gimbal structure shown in figure 3, six of the subelements are displaced away from the main structure for purposes of clarity, although the main structure is complete as drawn. The structure employes a base-plate onto which the major structural elements are bonded. These bonded elements are the bearing support ring, the actuator arm box structures, the half arm box structures (top and bottom), the main gear box, the cross-plane stiffeners, and the base-plate stiffener ring.

The bearing support ring, shown in cross-section in figure 4 consists of a titanium inner ring, a composite outer ring, and a composite top plate bonded together to form a closed ring having a hollow section. The bearing support ring is bonded to the base plate and to the cap plate.

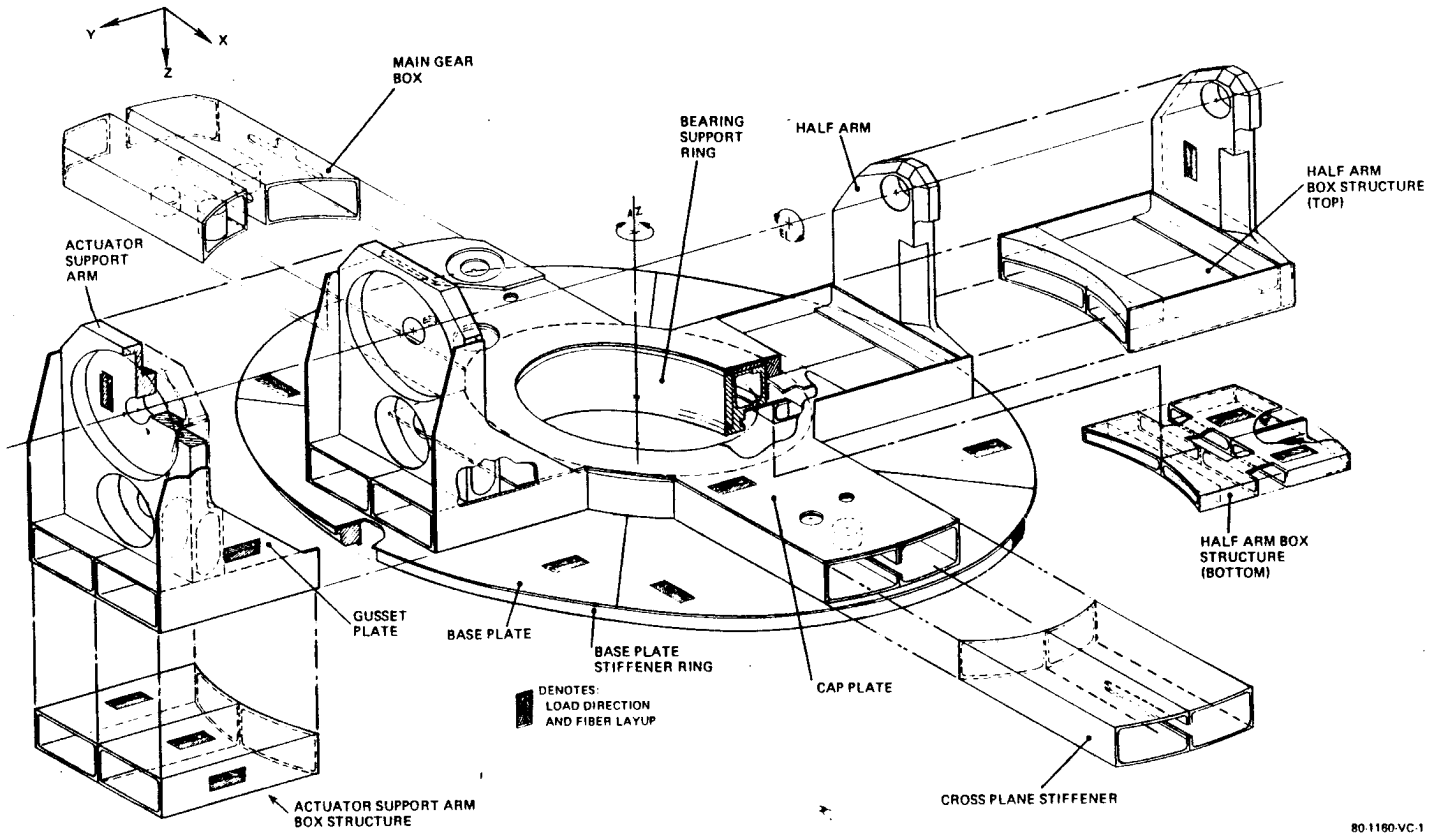

Figure 3. Isometric of Complete Gimbal

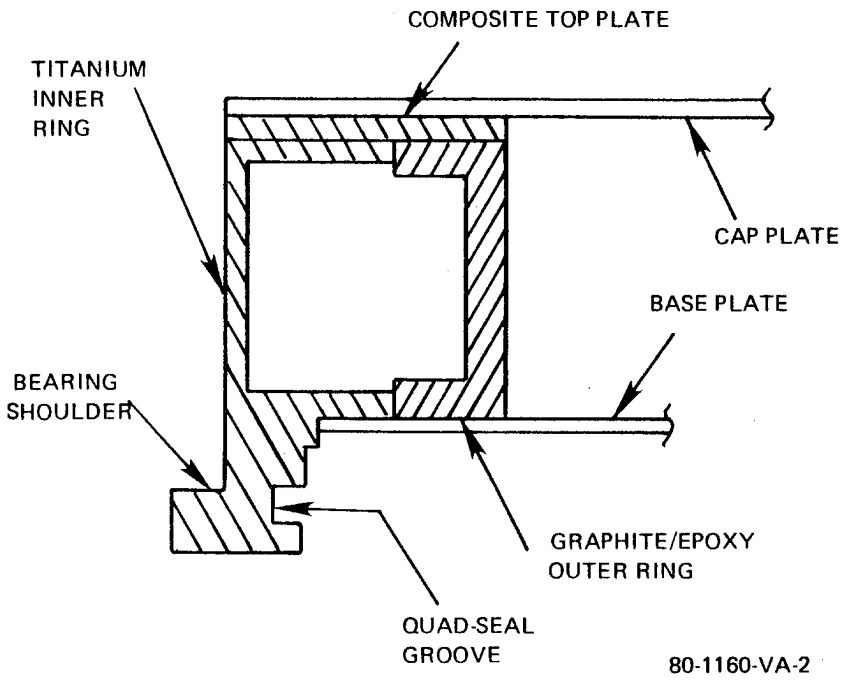

Figure 4. Bearing Cross Section

The actuator support arm box structures, having inboard ends contoured to match the radius of the bearing support ring, are bonded to the O.D. of this ring and the joint is reinforced by the cap plate which is bonded to the top of the bearing support ring as well as to the tops of the actuator support arm box structures. It will be appreciated that the joint between the box structures and the bearing support ring is in the form of a classical double strap joint, with the cap plate and base plate being the straps. A similar situation ensues where the half arm box structures (top) are bonded to the bearing support ring on the half arm side, although the cap plate area is not as great in this case. The cross-plane stiffener boxes and the main gear box are also attached to the bearing support ring in the manner of a double strap joint.

The two actuator support arm boxes are bonded together on the adjoining sides, and the actuator support arm, which is in essence a bulkhead with a broadened base, is bonded to the tops of the box structures. The actuator support arm is buttressed by gusset plates, one on each side, which serve to strengthen and rigidify the joint between the arm and the boxes in all three axes. Reinforcement of this arm is more critical than for the half arm because

the rotatable elevation gimbal is axially anchored to the actuator arm while being free to slide in the half arm. The half arm also has gusset plates on each side to reinforce the joint between it and the half arm box structures on top. The half arm box structures (bottom) are bonded to the base plate but are not attached to the bearing support ring.

2.2.4 Filament Orientation

The actuator support arm boxes, the half arm boxes and the bearing support ring were the first parts to be designed to obtain sufficient rigidity to obtain the required resonant frequencies for vibration in the X,Y, and Z directions. For this requirement the boxes are subjected to both bending and torsion, which means that a good compromise between Young's modulus, E, and shear modulus, G had to be achieved. Plots of E and G versus θ, where θ is the angle between filaments and the load axis (grain), showed that a $\pm$ 25 degree layup would result in values of both E and G which are significantly higher than those for an isotropic layup. Subsequent calculations of the resonant frequencies, using the composite properties determined by the computer program SPACEWOUND for the $\pm$ 25 degree layup, confirmed that this is a good choice as compared to an aluminum structure (in terms of stiffness to weight ratio). This layup was found to be suitable for all the other box structures and thus became the most frequently used layup.

The base plate was designed to use the $\pm$ 25 degree layup to achieve thermal expansion compatibility with the boxes to which it is bonded. To do this requires a four segment base plate with each segment having its load axis oriented as shown in figure 3. The seams in the base plate are reinforced by doubler plates on the bottom surface.

Table 1 gives a summary of measured weights for each of the major parts of the composite gimbal. The total weight of 2.75 lb. compares to a weight of 4.0 lb. for the equivalent aluminum gimbal.

TABLE 1
COMPOSITE GIMBAL WEIGHT BREAKDOWN

1. Base Plate (0.032 thick)	0.339
2. Actuator Support Arm	
Tubes	0.541
Vertical Arm	
Side Plates	

Table 1 (Con't)

3. Lip Seal Ring	0.154
4. Half Arm	0.392
Tubes Top Solid Vertical Arm	
Angle Side Plates Bottom Solid	
5. Synchro Tubes (Cross plane stiffeners)	0.141
6. Gear Box	0.148
7. Cap Plate	0.227
8. Bearing Support Ring	0.746
9. Hardware	0.0617
	2.750

2.2.5 Thermal Analysis

The configuration of the bearing support ring involves differential thermal expansion between the composite and the metal over a wide range of temperature. The differential expansion can induce shear stress which may break the bond, and it can induce changes in curvature which may affect critical alignment.

Analysis of an assembly of two annular flat plates, one of titanium and the other of graphite epoxy composite, bonded together with high strength adhesive has shown that the problem can be solved using circular spring theory. In this approach, the rings are first considered to be of equal diameter and unattached. Thermal expansion is then allowed to occur, which causes the diameter of the titanium ring to become larger than that of the composite ring. This, in effect, reestablishes the free diameter of circular springs which are to be subsequently forced to have the same diameter. The rings are then assumed to be brought into diametral coincidence by a uniformly distributed, radially oriented array of relative force vectors which expand the composite ring and shrink the titanium ring. Using the ring spring constant for the two rings and equating the diameters, it is possible to solve for the shear force as a function of the initial difference in expanded diameters. The final diameter of the combined plates can also be determined.

For circular plates in a typical assembly, the thermally induced bond stress is only a few hundred psi for each 100^{o} F change in temperature. Since

the adhesive has a shear strength of approximately 3000 psi, there is sufficient bond strength to avoid bond breakage over the normal range of temperatures encountered. Thermally induced warping may occur but it can be controlled by adequate moment of inertia of the sections of the joined materials.

The thermal characteristics of the bearing support ring and its adjoining structures were studied experimentally by tests of a thermal sample (shown in figure 5). This sample was subjected to temperature changes comparable to those expected in use, and measurements were of its rigidity and dimensional stability. The thermal sample also served as a structural sample useful in validating the structural analysis described in Section 2.2.6.

2.2.6 Resonant Frequency Analysis

A resonant frequency analysis was carried out for the gimbal structure. The bearing support ring was assumed to be rigidly attached to a frame, which assumes infinitely rigid rolling element bearings. The model analyzed is shown schematically in Figure 6.

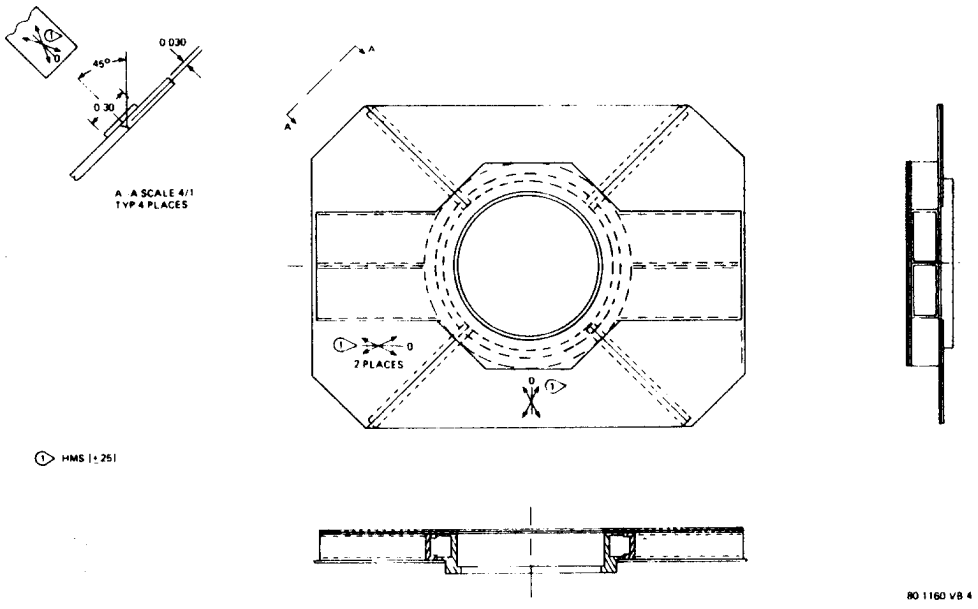

Figure 5. Thermal Sample Design

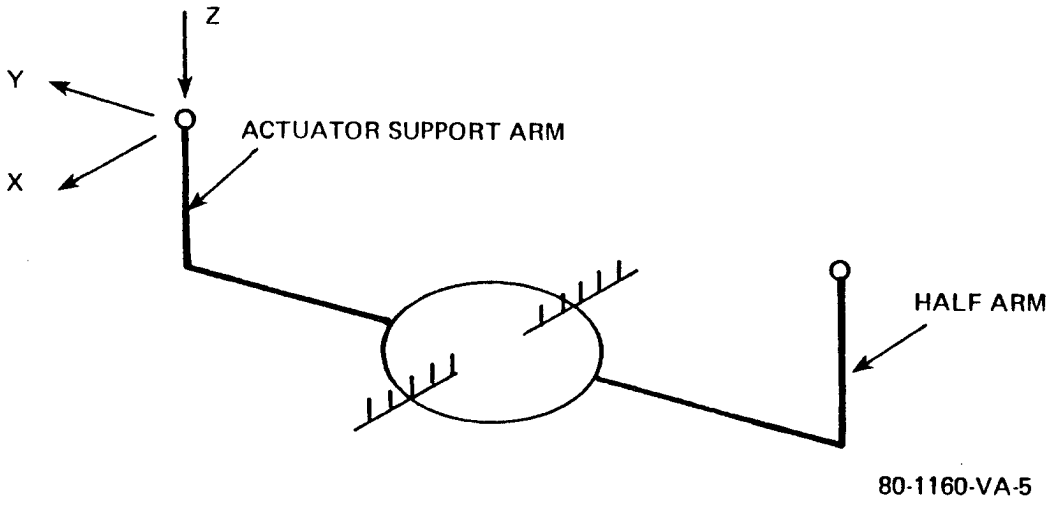

Figure 6. Gimbal Yoke Structure Schematic

In the X direction, the spring rate at the end of the actuator arm is given by

$$K_X = \frac{K_{RM} K_{BT}}{(K_{RM}+K_{BT})\, r^2}$$

where K_{RM} = Torsional spring rate of the ring, lb-in/rad

K_{BT} = Torsional spring rate of the boxes, lb-in/rad

A similar relationship holds for the spring rate at the end of the half arm.

In the Y direction, the spring rate at the end of the actuator arm is

$$K_Y = \frac{K_B\, K_R}{(K_B+K_R)\, r^2}$$

K_B = torsional spring rate at the end of the boxes, with respect to moments around an axis parallel to the X axis, lb-in/rad

K_R = torsional spring rate of the bearing support ring with respect to moments around an axis parallel to the X axis, lb-in/rad

r = length of actuator support arm, in.

In the Z direction

$$K_Z = \left(\frac{1}{K_B} + \frac{1}{K_{T\theta}/\ell_B^2} + \frac{1}{K_{RTD}/\ell_B} + \frac{1}{K_{RF}/\ell_B} \right)^{-1}$$

K_B = displacement stiffness of beam (bending), lb/in

K_{RFD} = displacement stiffness of ring to force, lb/in

K_{RT} = rotational stiffness of ring to twisting torque, lb-in/rad

K_{RTD} = displacement stiffness of ring to twisting torque, lb/in

K_{RF} = rotational stiffness of ring to force, lb/in

B = length of beam, in.

Spring rates with R in the subscript pertain to the bearing support ring which was treated as a curved beam using the Roark formulas [2] for such beams. Owing to the complexity of the formulas, a small Fortran Program was written and used to analyze various cases for the design evolution. The spring rates with B in the subscript pertain to the box structures and were also evaluated using formulas from Roark. In some cases these formulas were programmed on a programmable calculator for better efficiency in carrying out design iterations.

A summary of the calculated spring rates follows.

TABLE 2
GIMBAL SPRING RATES

	Actuator Arm Side	Half Arm Side
K_x(lb/in)	28,710	9,385
K_y(lb/in)	12,646	N.A.
K_z(lb/in)	17,520	9,792

2.2.6.1 Rigid Body Modes

The elevation gimbal was assumed to be a rigid body having I_x = 0.25 lb-in-sec^2, weight = 6.1 lb, $\overline{X} = \overline{Z} = \overline{0}$, and $\overline{Y}$ = 0.1 in. so that the stiffness of the azimuth gimbal could be studied more easily, for vibration inputs in the X and Z directions this results in the classical case in which a rigid beam is spring suspended at each end with springs having unequal spring rates. The solution yields two resonant frequencies in each direction. For the Y direction, only one resonance exists. The results of this analysis are tabulated in table 3.

TABLE 3
RIGID BODY RESONANCES

Input Axis	Frequency, F(Hz)	
X	205.8,	355.4
Z	201.4,	289.8
Y	142.4	

[2] R.J. Roark and W.C. Young, "Formulas For Stress and Strain", 5th Edition, McGraw Hill (1975) pp. 252-280.

These calculated frequencies are well above the minimum requirement of 100 Hz, and all but the Y direction resonance are well above the 150 Hz design goal.

3. FABRICATION AND TOOLING

3.1 SELECTION OF MATERIALS

Graphite-Epoxy was selected for the advanced composite gimbal structure based upon the following advantages in comparison to aluminum:

- o Stiffness to weight-greater than aluminum
- o Modulus - greater or equal to aluminum
- o Damping Coefficient - greater than aluminum

Consideration of other materials such as glass, Kevlar and metal matrix did not offer all these advantages.

A comparison of the physical properties of various graphite compsites with aluminum is shown in table 4.

The material selected for use in the manufacture of the plates and the box sections was high modulus graphite fibers. A typical material supplied by Hercules is HMS high modulus graphite and 1908 epoxy resin. Typical properties of this system when fully cured are shown in Table 5.

Another material of the same category supplied by Exxon's Fiberite is Courtauld's 10 K HY-E high modulus graphite with 1248-A1 epoxy resin system.

High modulus graphite Hercules HMS is compared with pitch graphite, Union Carbide P-50, in table 6.

Pitch graphite offers a cost advantage over high modulus graphite while maintaining high stiffness. However, the handling characteristics are slightly poorer.

3.2 FABRICATION OF BASIC SHAPES

The test sample gimbal design is made up of 33 items or styles of parts. The 33 styles of parts were organized into 5 categories as follows:

1. Box Sections
2. Plates
3. Windings
4. Individual fabrications
5. Metal

TABLE 4. Property Comparison Of Graphite Composites

Material	Tensile ksi 0°	Tensile ksi 90°	Compression ksi 0°	Compression ksi 90°	Tensile Modulus psi x 10^6 0°	Tensile Modulus psi x 10^6 90°	Tensile Strain % 0°	Density Lb/In^3
AS Fiber	220	7-12	220	40	18	2	1.5	0.056
HM Fiber	150	5-10	150	30	25	1.5	1.0	0.059
UHM Fiber	130	3-5	100	27	37	1	0.75	0.060
6061-T6 Al	45		--		10		17	0.098

TABLE 5. HMS-1908 Composite Properties

Property	HMS-1908
Tensile, ksi	130
Compression, ksi	140
Tensile Modulus, psi x 10^6	27
Tensile Strain, %	0.5
Density, Lb/In^3	0.059

TABLE 6. Support Ring Test Results

Property	HMS (90°)	P-50 (90°)	HMS (90°/+45°)
Tensile Strength, ksi	97	89	67
Tensile Modulus, msi	26	21	18
Tensile Strain, %	0.40	0.38	0.50
Short Beam Shear, psi	4,200	4,200	5,600

Methods of fabrication are discussed for each of these categories in the following sections.

3.2.1 Box Sections

The box sections or rectangular tubes have to have good external surface finish to facilitate alignment and bonding to other parts during later operations. Therefore they were formed on expandable internal mandrels. After these mandrels were wrapped with Courtauld's 10K HY-E 1248-1A graphite prepreg at the proper angles such as $\pm 25^{\circ}$, $\pm 45^{\circ}$, and/or $\pm 90^{\circ}$, the mandrel was positioned inside a form tool and then expanded. After curing, the external form was dissassembled and the internal mandrel contracted and removed. The box section was then machined for the next operation.

Photographs of the tooling used to produce the small box sections used in the gimbal fabrication are shown in figure 7, 8, and 9.

A large rectangular box tube which was twice the area of the small rectangular box tube was also fabricated. The tooling for this tube is shown in figure 10.

3.2.2 Plates

Twelve plies of Courtauld's HMS 10K HY-E 1248-1A graphite oriented at $\pm 25^{\circ}$ and Fiberite 984A1 epoxy resin were used to produce the 0.063 thick plates. These were cured in an autoclave at 100 psi and 250°F. The other thickness plates were fabricated using the appropriate ply counts and angles as required. For example, the 0.030 thickness plates require 6 plies and the 0.100 thick plates require 10 plies. Only these three thickness were used in the design of the gimbal. Other thicknesses when required were fabricated by stacking plates together and bonding with FM73 adhesive.

3.2.3 Filament Windings

Two parts were fabricated using filament winding combined with manual layup. These parts were the Bearing Support Ring shown in figure 11 and the Base-Plate Stiffener Ring shown in figure 12. These are also shown as H17 and H26 respectively in drawing 687R259 in Appendix A.

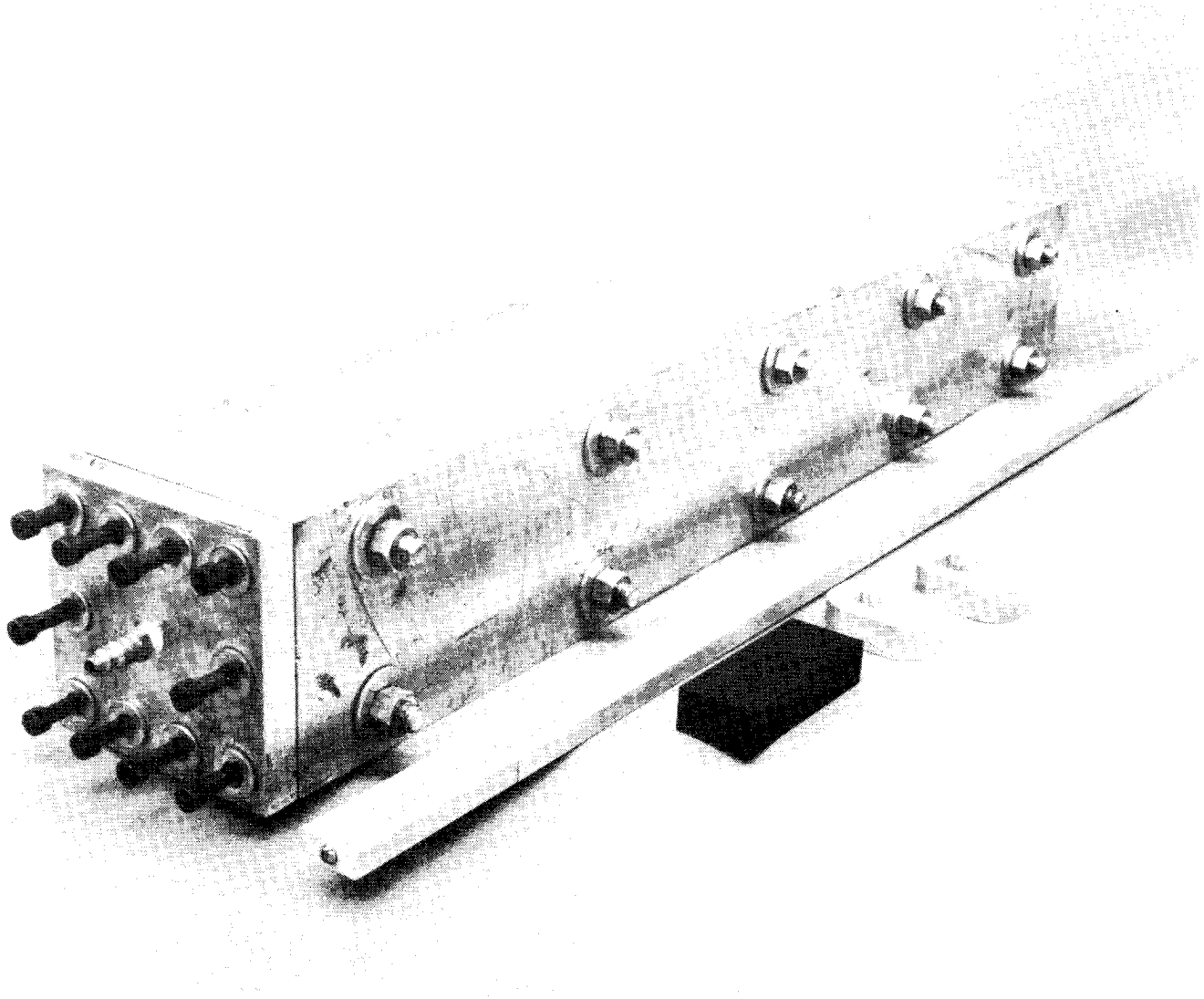

Figure 7. Small Rectangular Tube Mold

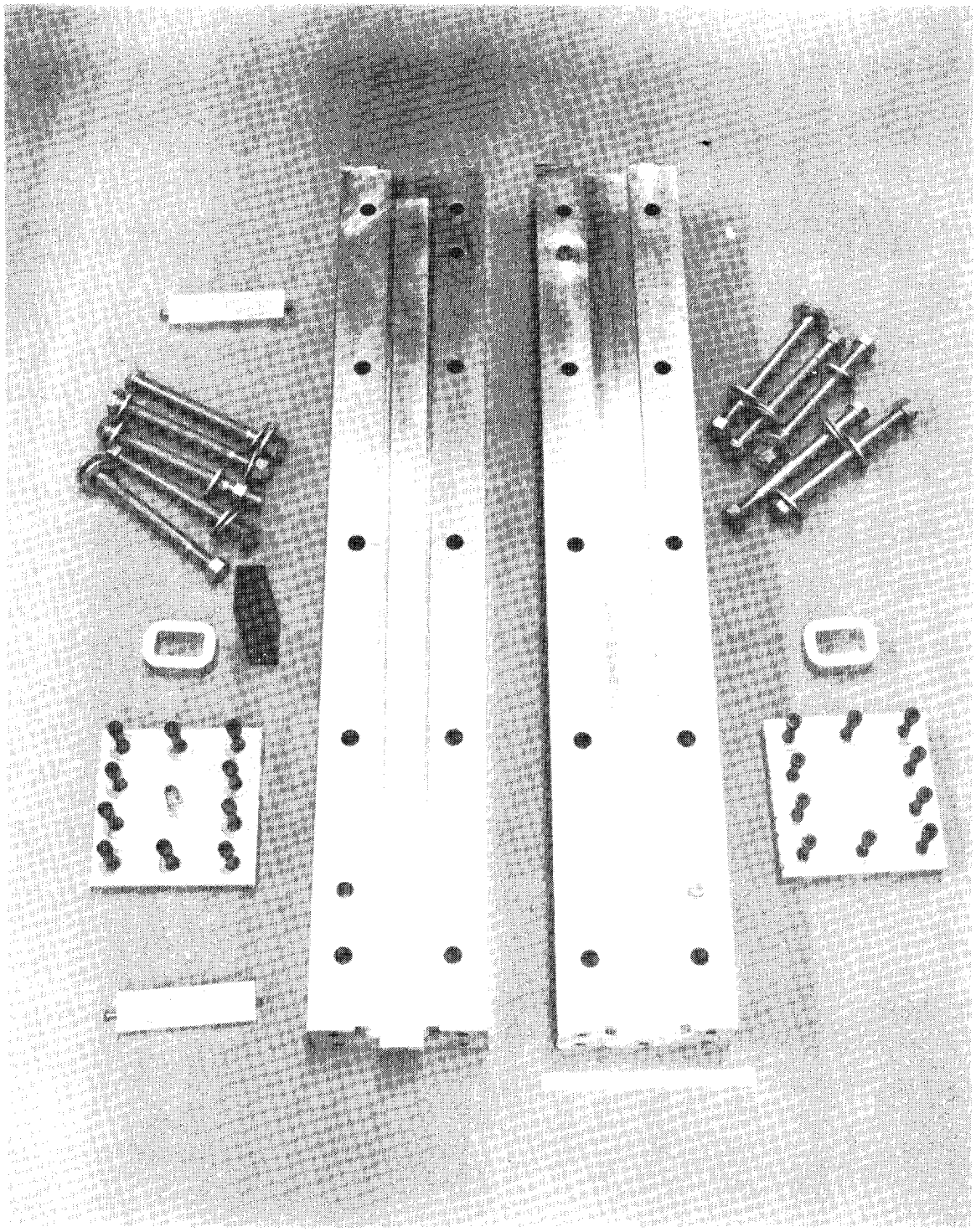

Figure 8. Spiral Tube Mold Open

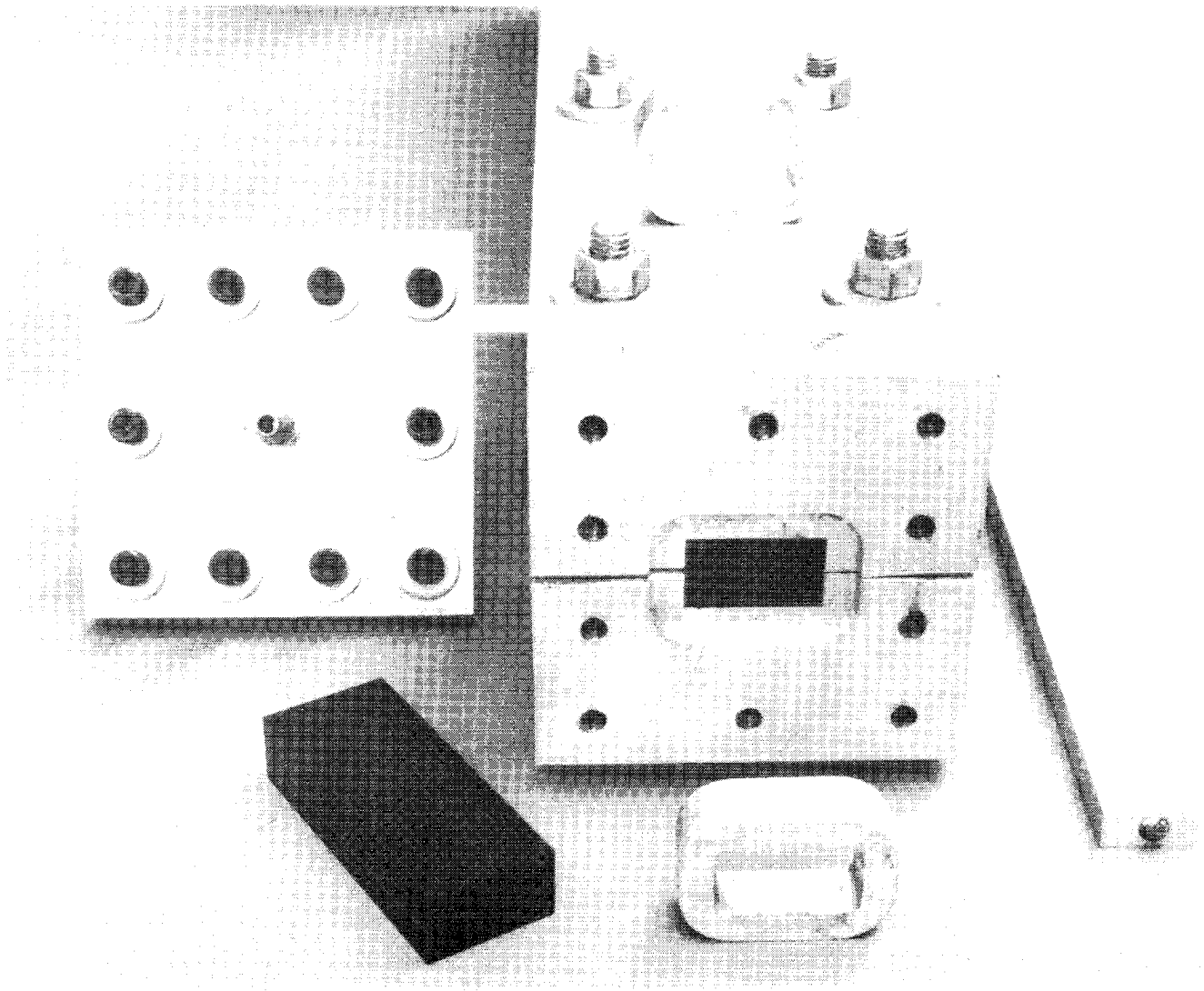

Figure 9. Small Tube Mold, End View

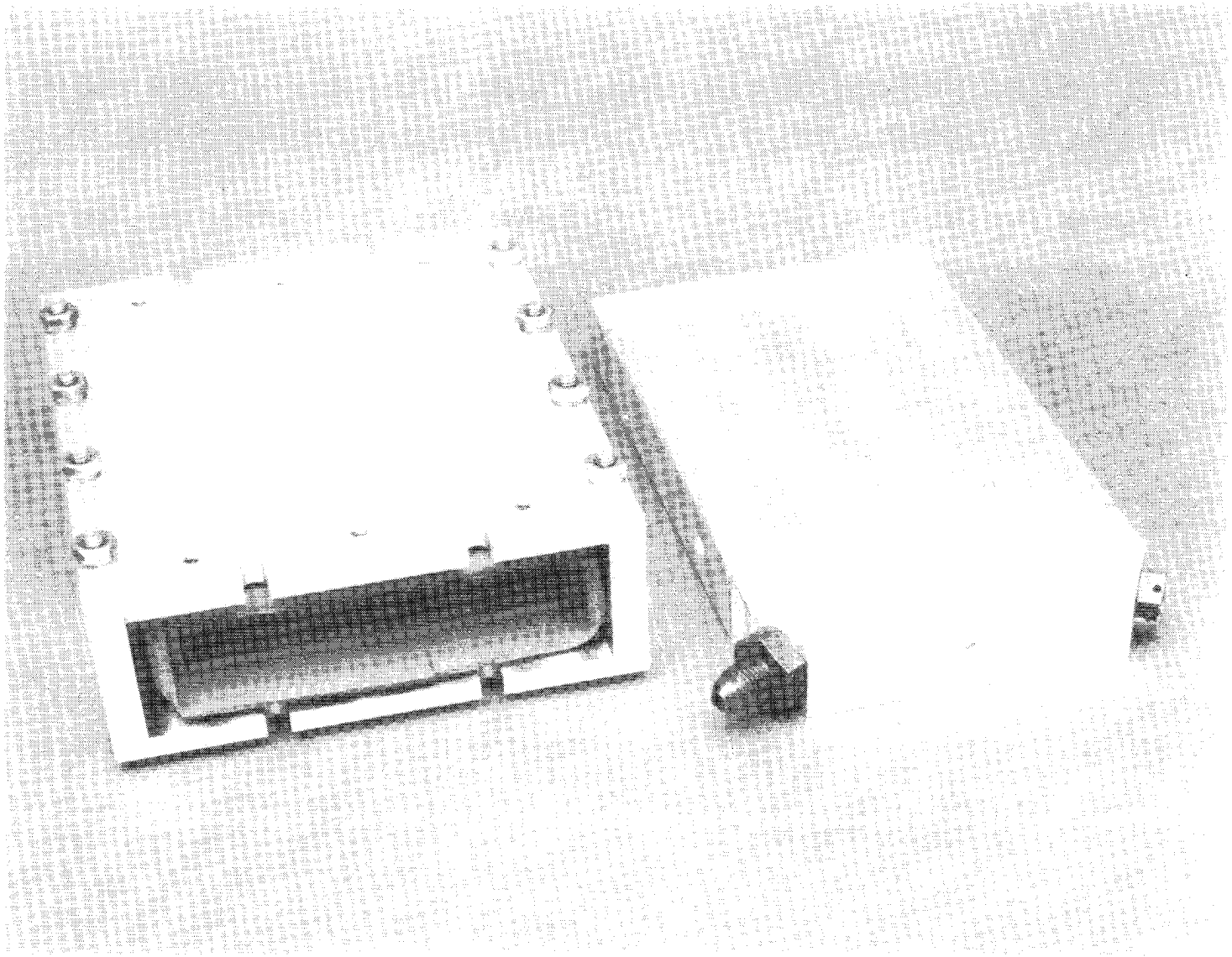

Figure 10. Large Rectangular Tube Mold

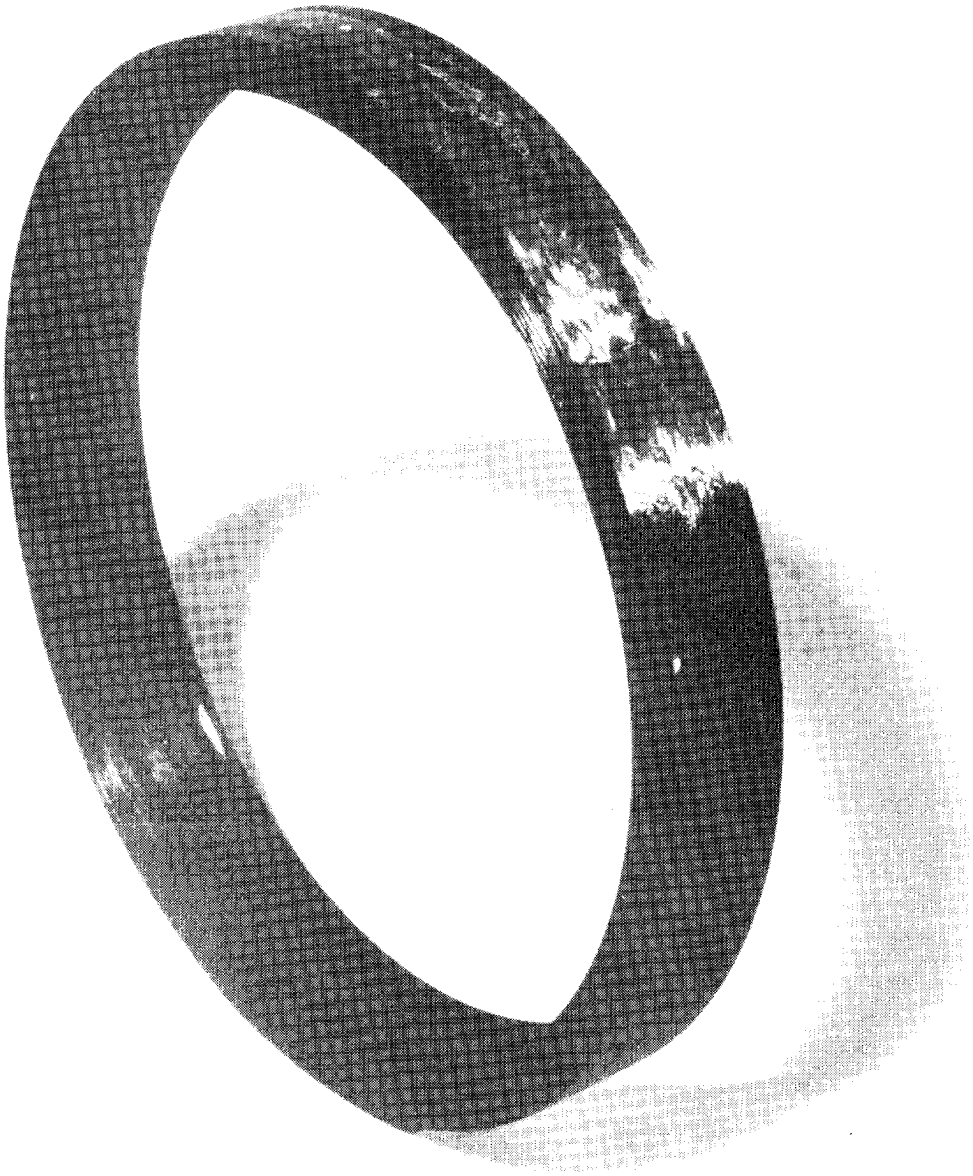

[illegible] Support Ring

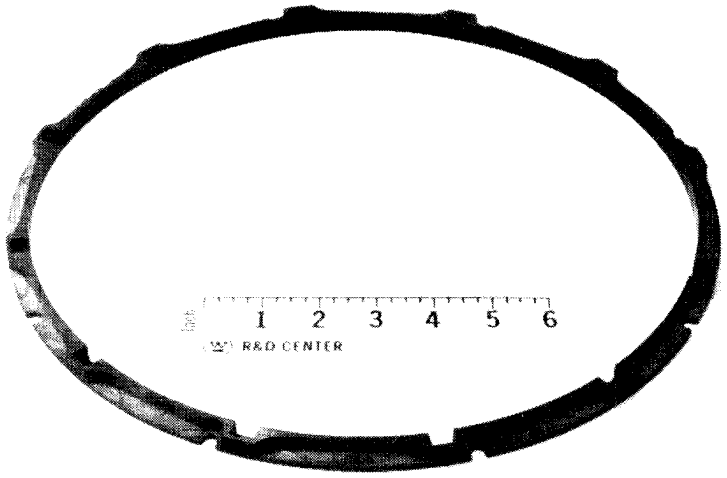

Figure 12. Base Plate Stiffener Ring

3.2.3.1 Bearing Support Ring

The bearing support ring is made up of both composite material and titanium. Figure 4 shows this in cross-section. The graphite/epoxy outer ring was fabricated in three parts and then bonded together using Hysol EA 9320 adhesive to form the circular channel section. Machining the composite part as a single piece was considered but it was believed to be too risky due to the thin flanges.

The support ring laminate construction uses Hercules HMS graphite with a bisphenol epoxy-aromatic amine resin system containing Epon 826 epoxy resin, Celanese 5022 reactive diluent, and Tonox 60/40 hardener. The graphite tow is passed through the warmed resin bath and wound on a mandrel-60% in the hoop direction (90°) and alternatively 40% in the 45° direction. The web structure for the support ring is as follows:

$$\left[90^{\circ}_3 \; / \; \pm 45^{\circ} \; / \; 90^{\circ}_2 \; / \; \pm 45^{\circ} \; / \; 90^{\circ}_2 \; / \; \pm 45^{\circ} \; / \; 90^{\circ}_2 \; / \; \pm 45^{\circ} \; / \; 90^{\circ}_3 \right]$$

12 plies (60%) - 90°

8 plies (40%) - 45°

The flange structure for the support ring is slightly different, but still shows the same ratio of hoop to bias plies as shown below:

$90^{\circ}_3/ \pm 45^{\circ}/90^{\circ}_2/\pm 45^{\circ}/90^{\circ}_3$

8 plies (60%) - 90°

4 plies (40%) - 45°

The web structure forms the length of the support ring, and the flange structure forms the ends of the support ring which are carefully machined to slip fit inside the web structure. A radially reinforced cylinder is formed which constitutes the bearing support ring.

Hercules HMS fiber was used for the 90° layers and Hercules HMS-1908 prepreg was used for the $\pm 45^{\circ}$ layers. The resin formulation for the 90° fibers was:

Epon 826	80 parts by weight
Celanese 5022	20 parts by weight
Tonox 60/40	24 parts by weight

Curing was accomplished using:

Gel	1 hours, 200°F, 1 hour, 250°F
Cure	2 hours, 350°F

Prior to bonding the composite and titanium parts together, the titanium was pretreated to improve bondability with PASA JELL SOLUTION[3]. Ciba Geigy adhesive XU235/205 was used for the bonding.

3.2.3.2 Base-Plate Stiffener Ring

A number of constructions were tried which were not successful due to wrinkling and buckling of the laminate. The final structure which was satisfactory is based upon the use of carbon fiber mat, Stackpole Panex CFP. The hoop fibers are Hercules AS4 graphite. The actual ring structure is shown as follows:

$$\left[\text{Panex CFP}_2 \ / \ 90^{\circ}_2\right]_{12}$$

The resin system and cure schedule used is the same shown in 3.2.3.1 for the bearing support ring. Test Results of an AS-4 graphite composite test sample are shown in table 7.

[3] DoD/NASA Structural Composite Fabrication Guide, 2nd ED, Vol. 2, Sec B-4-2, May 1979.

TABLE 7. Stiffener Ring Test Result

Property	AS-4 (90°)	AS-4/Panex CFP 30-05 (70%/30%)
Tensile Strength, ksi	203	173
Tensile Modulus, msi	17.4	14.0
Tensile Strain, %	1.2	1.2
Short Beam Shear, psi	9,800	18,000

Stiffener ring test results are shown in table 7 and compare favorably to the predicted values based upon test specimens previously examined. The test methods used for the analysis are shown in table 8.

This ring was wound using 70% by wt. of resin in the mat layers and 30% by wt. of resin in the AS-4 12K layers.

The measured thickness of the as-wound layers were as follows:

Panex CFP 30-05 (2 Layers) - 0.010 inch

AS-4 12K (2 Layers) - 0.020 inch

The continuous 90° layers of AS-4 12K fiber were applied with a tension of 5 lbs per tow. Two tows were used for the winding, giving a band width of 0.15 inches. The wound part used the same resin and cure schedule described previously. The cured part is shown in figure 13. The O.D. was measured at 13.00 inch. The ring was edge trimmed with a diamond cut-off saw and examined visually. Excellent composite compaction was achieved. The void content was measured at 3.5% and the resin content at 45% by wt.

A second back up ring was fabricated in the same way as the one just described except that a tension of 8 lbs-per-tow was applied to the AS-4 12K fiber. The higher tension was used in order achieve greater composite compaction in the event machining problems were encountered with the second ring. Wet weight measurements on the as-wound layers removed from the mandrel indicated a resin content of 40% by wt. This data point indicates that greater consolidation and lower void content was achieved. It was not necessary to utilize this ring for gimbal fabrication.

TABLE 8. Summary of Plate Tests Performed

Tensile Strength and Modulus	-	ANSI/ASTM D-3039-76
Compression Strength	-	ASTM D-3410-75
Flexural Strength	-	ASTM D-790-71
Short Beam Shear	-	ANSI/ASTM D-2344-76
Hardness	-	ASTM D-2583
Void Content	-	HI HD-SG-2-6002C
Fiber Volume	-	HI HD-SG-2-6002C

Two finished rings were produced from the second as-wound ring. This operation was viewed primarily as a milling operation which required continual support of the composite part during the milling and drilling operations. Two 0.41 inch wide rings were wet cut from the as-wound part using a diamond cut off wheel. A finished ring is shown in figure 12.

Aluminum support tools were fabricated to fixture the composite rings for the milling operations. Solid carbide four flute routers were used for the milling operation. The called-out holes were pre-drilled using carbide drills and were used to attach the composite ring to the aluminum bed plate. All of these operations were done dry.

This composite ring represents one of the most complicated machined composite items ever attempted and represents also a breakthrough in machining parts with tight tolerances.

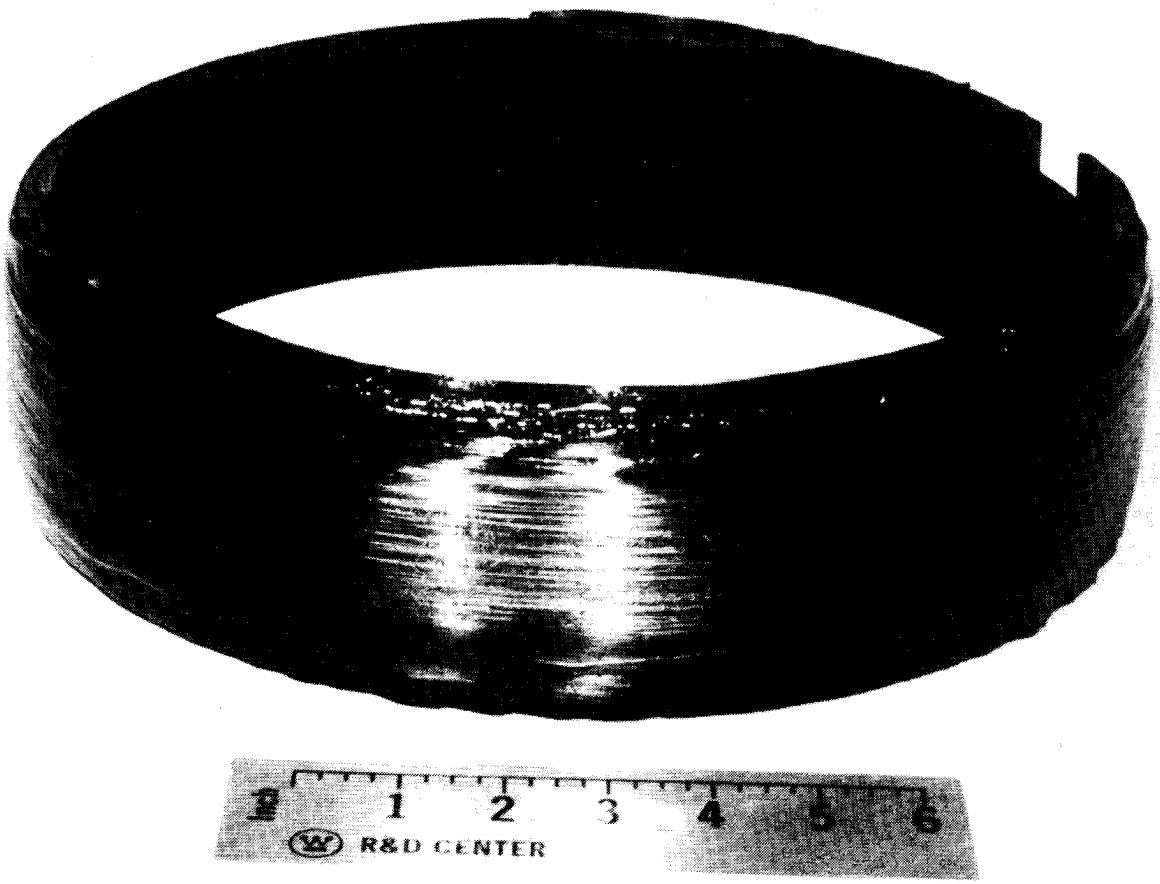

Figure 13. Winding for Base Plate Stiffener Ring

The W-60 McClean-Anderson filament winding machine fitted with the aluminum mandrel is shown in figure 14.

3.2.4 Individual Fabrications

Parts that had unusual configurations or that had to be built up out of several components were put in this category. Parts designed H08, H12, H13 and H14 as shown on drawing 687R259 in Appendix A are examples. In a production situation, these items would be evaluated for optimized manufacturing. They were fabricated using available material and methods consistent with the engineering requirements.

3.2.5 Metal Parts

The metal parts consist of threaded stainless steel inserts H32 and H33 as shown in drawing 687R260 and titanium washers H19 and H20, and the titanium ring H16 as shown in drawing 687R259 in Appendix A. The development work associated with the inserts is shown in an earlier report.[4] Manufacturing of these metal parts using standard machining procedures has not presented any problems.

3.3 ASSEMBLY OF THERMAL SAMPLE

The assembly procedure for the thermal sample required the development of a number of processes for adhesive bonding of metals and composites and was designed as shown in figure 5. Photos of this sample are shown in figure 15.

Thermal cycling of the sample, from -65F to + 160F, showed no loss of stiffness, and it therefore can be concluded that the bonded joints were not adversely affected by the temperature extremes.

3.4 ADHESIVE BONDING OF METAL AND COMPOSITES

3.4.1 Procedure A

The most widely used process bonding composite pieces together is based upon the Primary Aircraft Bonded Structures Technology (PABST) report test results, which showed that the American Cyanamid Adhesive Film FM73 was superior to others tested and was recommended for moisture resistant applications over the temperature of -67 to +250F for adhesive bonding of metals and composites. The adhesive is used directly on composites and stainless steel but required a phenolic primer BR127 over aluminum for corrosion resistance. A summary of the key features is shown here:

[4] Composite Gimbal Program, Technical Report No. 2, P. 13.

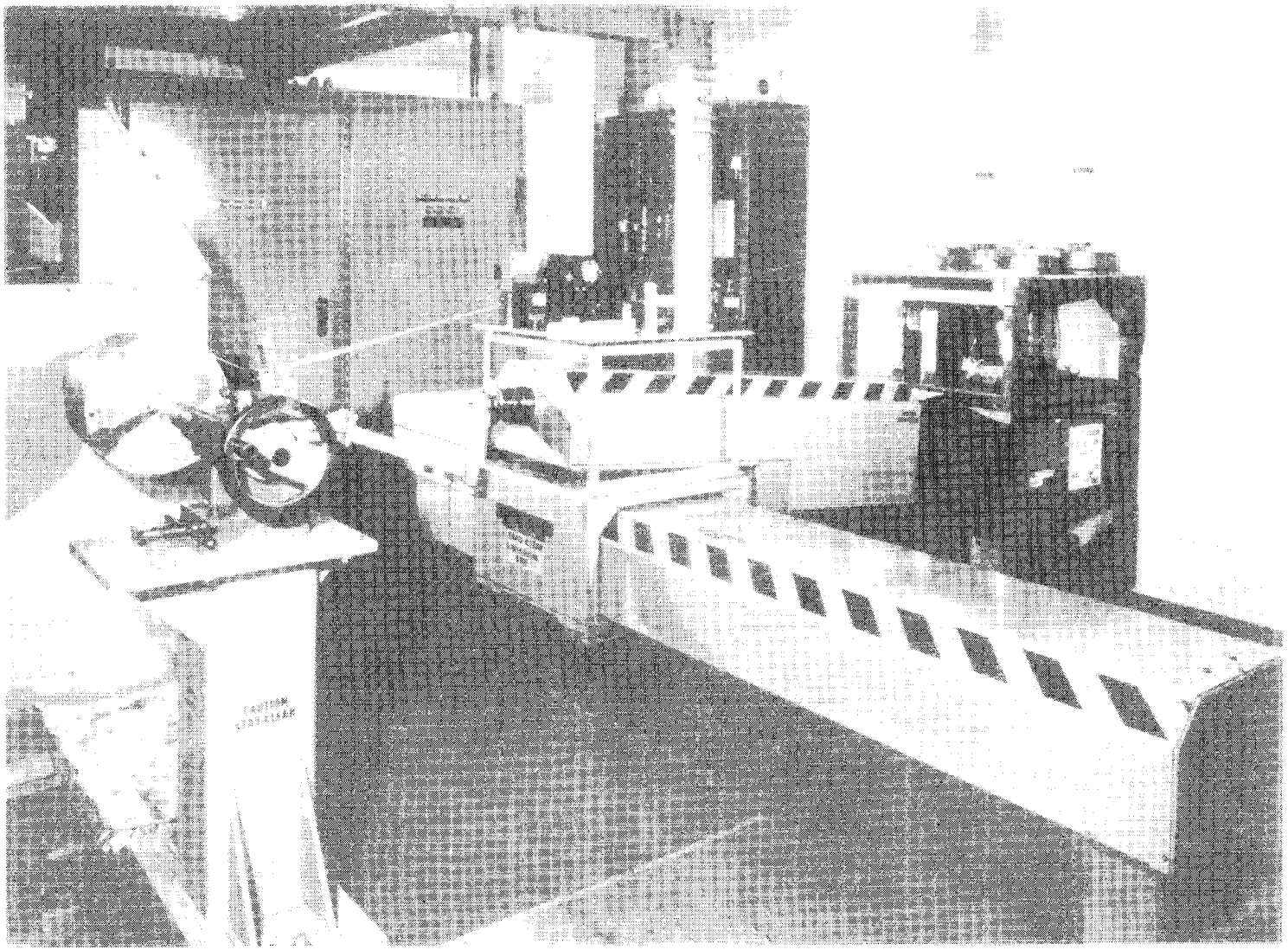

Figure 14. W-60 Winding Machine

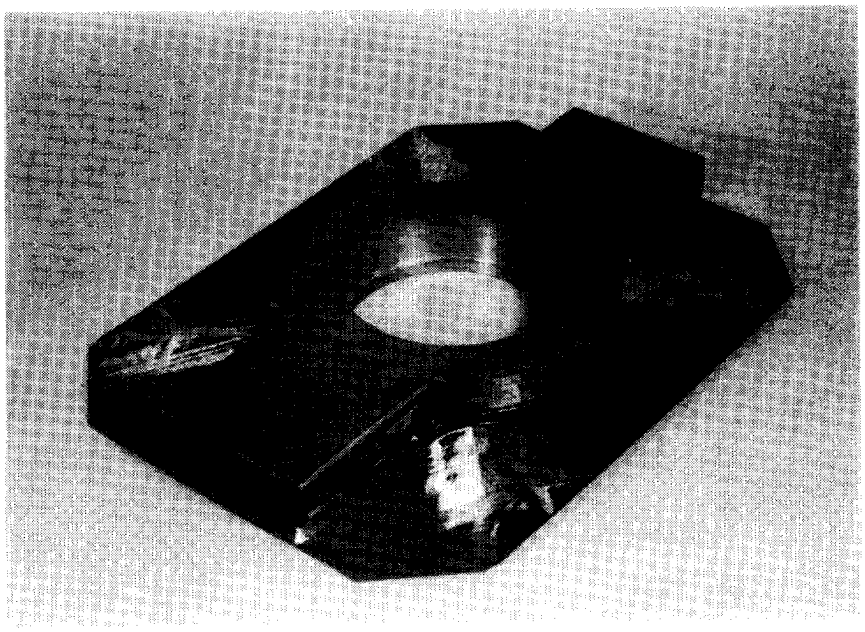

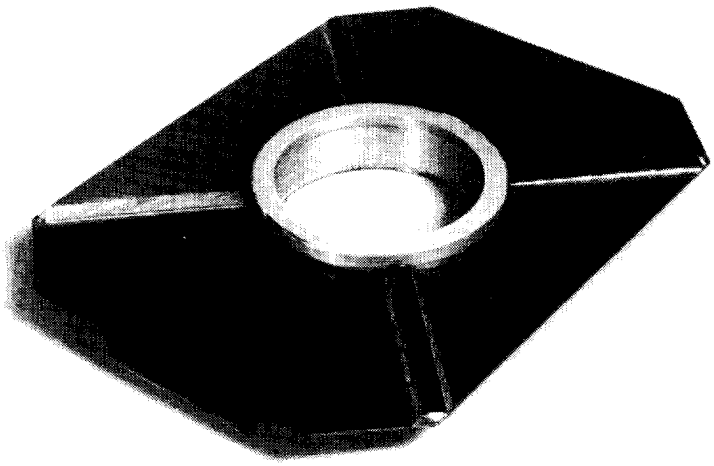

Figure 15. Thermal Sample Views

- o American Cyanamid FM73 Adhesive Film
- o Standard thickness 0.007 inch
- o Standard weight 0.045 pounds per square foot
- o Shop life 30 days at 75°F
- o Storage conditions 40F or below
- o Shelf life 6 months at 40F or below
- o Bonding conditions 1 hour at 250F under 40 psi pressure

3.4.2 Procedure B.

For applications where Procedure A can not be used because of heat sensitivity of the component parts, Procedure B is recommended. This procedure requires a lower temperature cure compared to Procedure A or even a room temperature cure may be used, although better physical properties will be obtained if the higher temperature cure is used. Highlights of the process are shown here:

Procedure B/Hysol Aerospace Adhesive EA 9320

(2-component amine cured, asbestos-filled epoxy resin system)

- o High shear and peel strength from -67F to +200F
- o Property retention after salt-spray, water and organic chemical exposure.
- o Recommended cure: 5 minutes at 140 F
- o Alternate Cure: 7 days at 77 F
- o Parts may be handled after 5 hours at 77 F

3.4.3 Procedure C.

For applications where Procedures A and B do not have high enough bond strength, Procedure C is recommended. Procedure C is also used as a repair adhesive for graphite-epoxy composites. This procedure has shown exceptional results with titanium or stainless steel fasteners in graphite-epoxy composites with bond strengths actually greater than the strength of the metal material itself. The fastener is destroyed during tensile pull tests due to superior hardness and toughness of the fully cured adhesive. Provided it is used in the elastic region of the stress-strain tensile curve; it is not affected by micro-cracks or subjected to a major fracture. Procedure C was developed as a matrix adhesive for graphite epoxy composite use and is especially useful in filament winding operations because of its low viscosity and high wettability of the graphite

fibers. A summary of the procedure is shown here:

- o Ciba-Geigy (XU235/XU205) 100/52 Parts By Weight (polyfunctional epoxy resin/low viscosity aromatic amine)
- o Glass transition temperature (fully cured) 177°C
- o Cure Cycle 1 hour at 100°C followed by 2 hours at 150°C, followed by 2 hours at 200°C

Advantages

- o Moderate curing temperature
- o Low coefficient of thermal expansion
- o Low moisture absorption
- o High elastic modulus
- o Good elevated temperature properties
- o Good chemical resistance
- o Good radiation resistance

3.5 ASSEMBLY OF CONFIRMATORY SAMPLE

3.5.1 Assembly Plan

Table 9 shows the assembly plan for the test sample in accordance with the drawing shown in figure 3.

TABLE 9

Confirmatory Sample Assembly Plan

1. Assemble mirror arm-2 steps
2. Assemble base plate-3 steps including bearing & top plate
3. Assemble all 4 arms to Base Plate Assembly incl. top plates except for vertical parts of motor arm - 1 step
4. Assemble vertical parts of motor arm-2 steps
5. Assemble bottom parts of motor arm-2 steps
6. Assemble bottom half box to motor arm/base plate assembly
7. Drill/2 holes for rivnut clearance on rim of base plate
   Enlarge 8 slot for rivnut clearance on rim of base plate
   Drill 8 holes and c/bore for bearing mount
8. Bond all 28 pcs. of hardware
9. Grind bearing bore to size

A flow diagram for the parts as shown in drawing 687R259 in Appendix A is given below in figure 16. Photographs of the confirmatory sample parts before assembly are shown in figure 17. The same parts after partial assembly are

shown in figure 18, 19, with assembly testing. The fully assembled confirmatory sample is shown in figure 20.

3.5.2 Assembly tooling

Tooling for the various steps shown in Table 9 is listed in Table 10.

TABLE 10

Tooling

Step
No.

1. SK-RZ-070181-1 Plate for centering plates @4.687 Dia. plug

4. SK-TFG-080581-1 Plate for cementing Ti Ring @4.70 Dia. I.D. Hole

5 SK-TFG-081781-1 Alignment tool for centering four arms
replaces 5A SK-TFG-073181-1 Alignment tool for centering two arms

5A SK-TFG-080781-1 Thread stock + nuts + washers

5A SK-TFG-080781-2 Flex arm

5A SK-TFG-080781-3 Pressure block

6 SK-TFG-082081 H01, H02, H03, Pressure Plates

10 SK-TFG-091581-1 Plate

10 SK-TFG-091581-2 Plate

Photos of the tooling are shown in figures 21, 22, and 23.

Tooling drawings are shown in Appendix B.

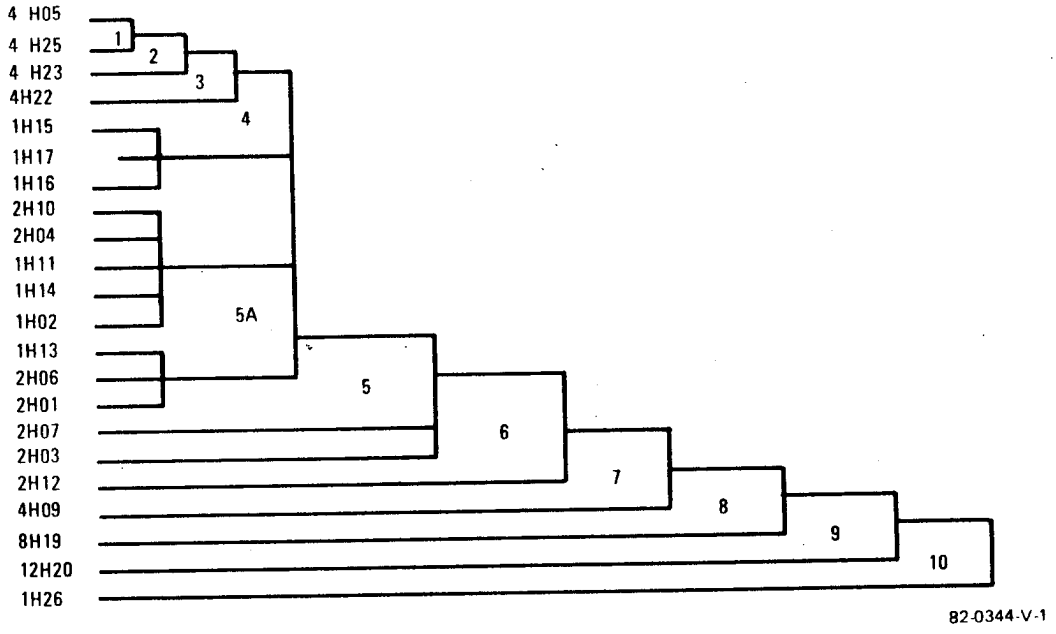

Figure 16. Flow Diagram of Parts Shown in 687R259 in Appendix A

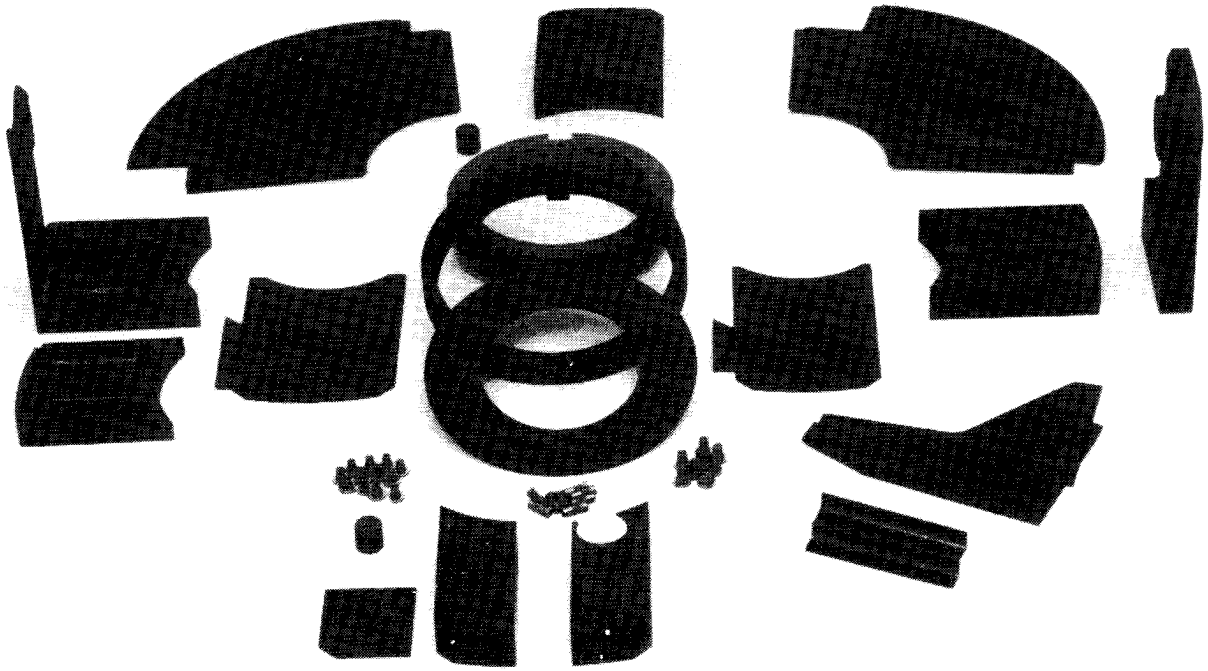

Figure 17. Confirmatory Sample Parts

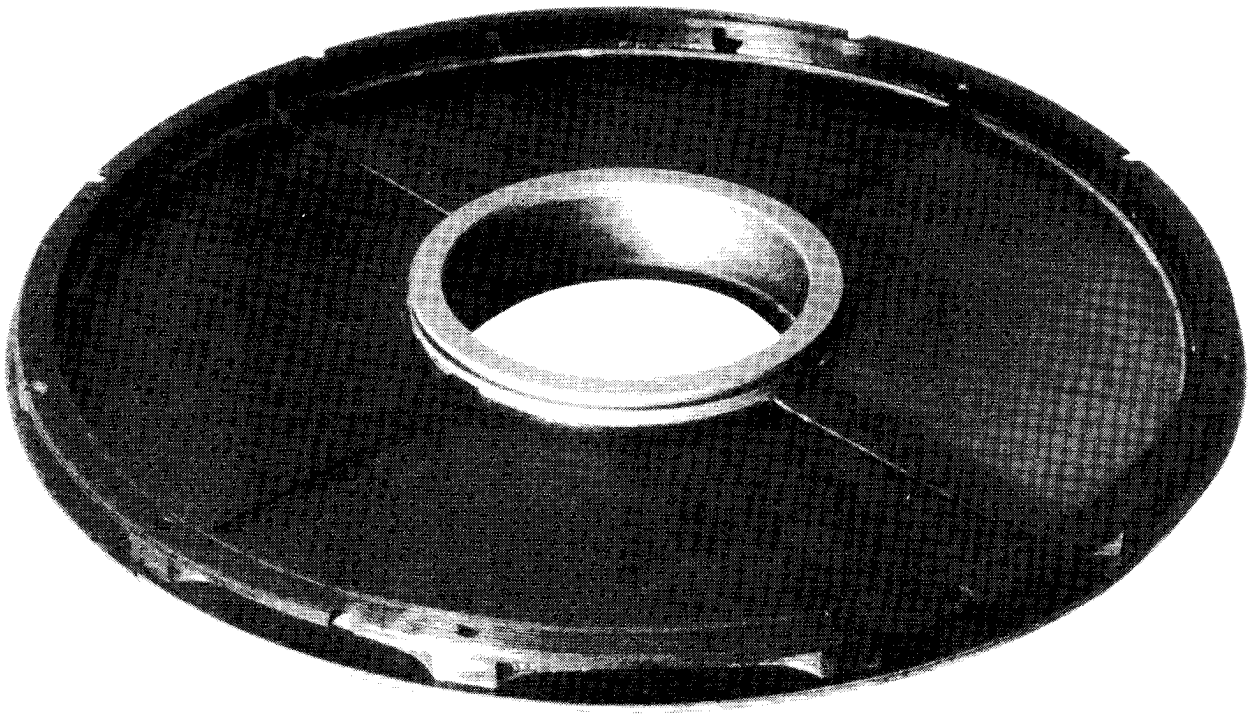

Figure 18. Gimbal Partial Assembly

Figure 19. Gimbal Partial Assembly

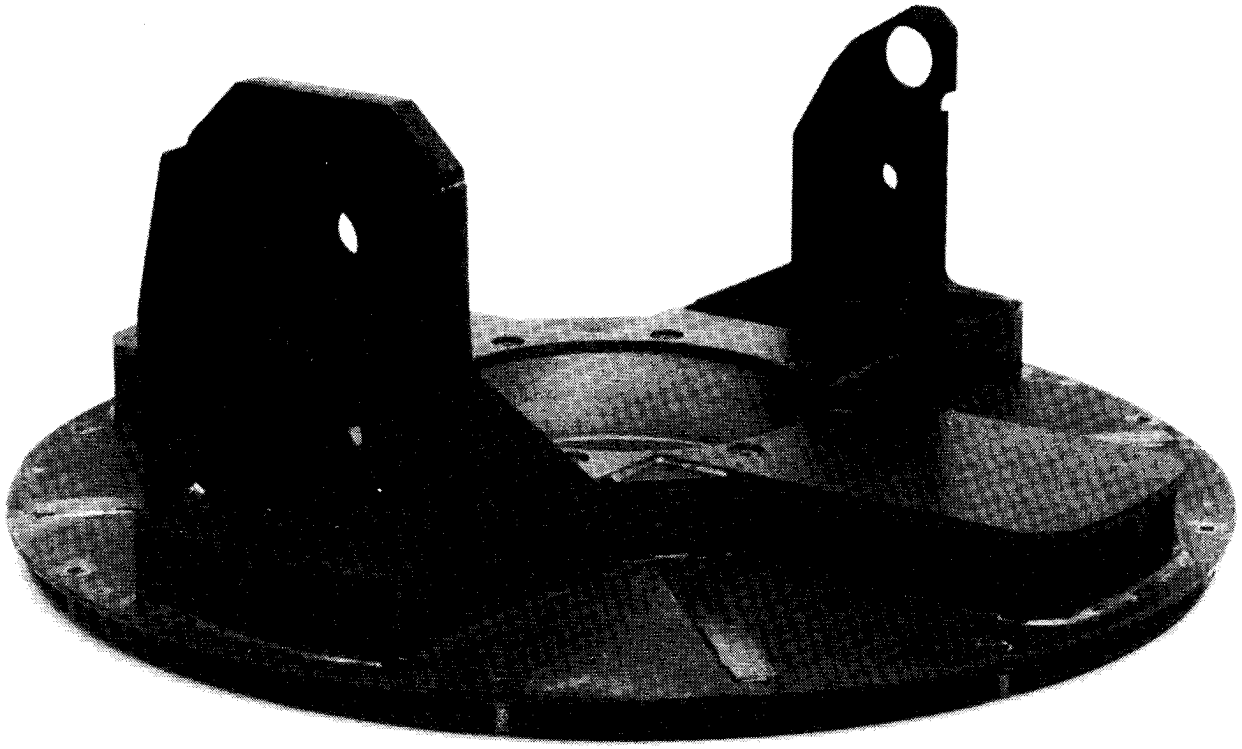

Figure 20. Gimbal Completed Assembly

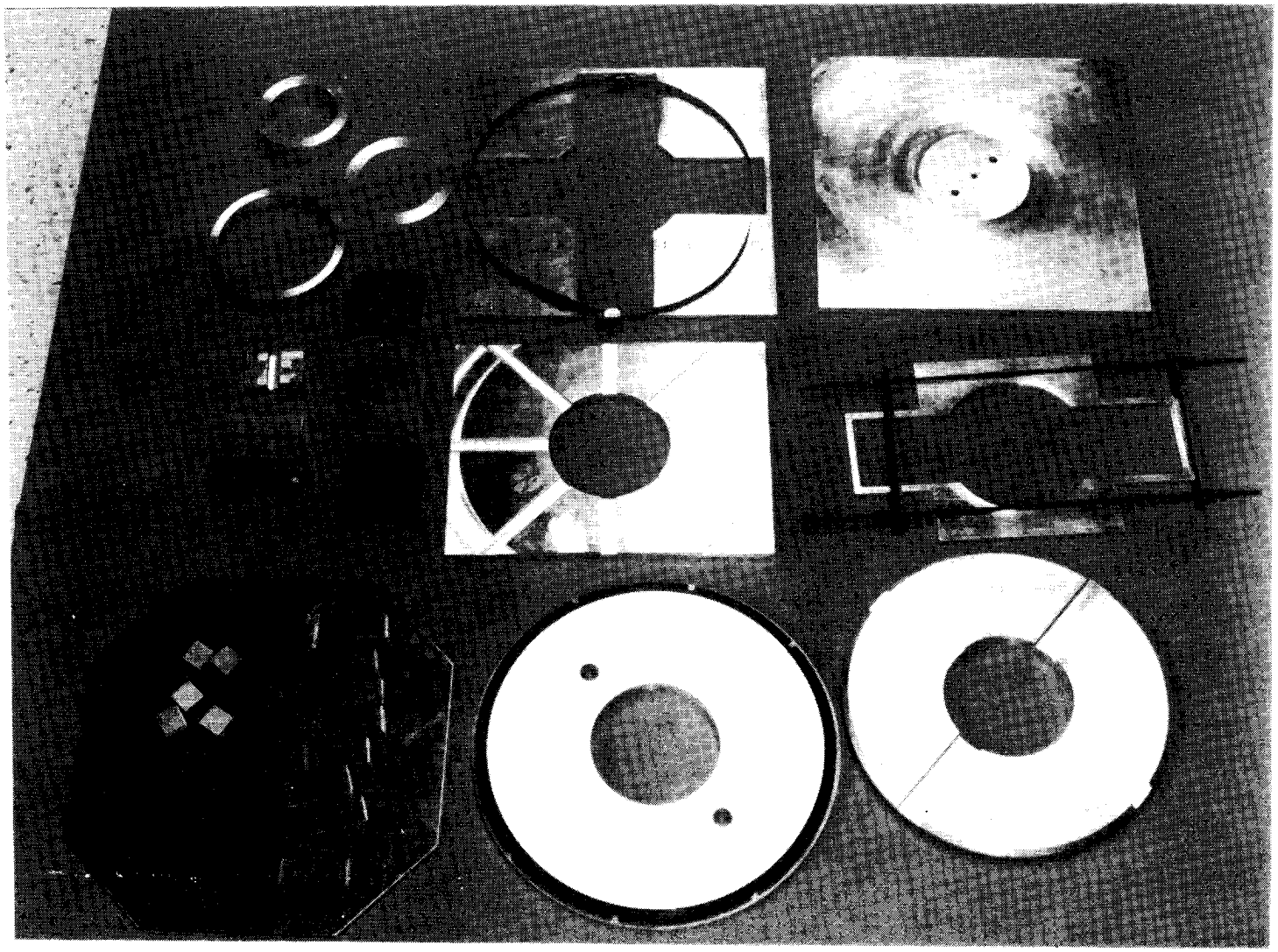

Figure 21. Gimbal Tooling

Figure 22. Gimbal Tooling

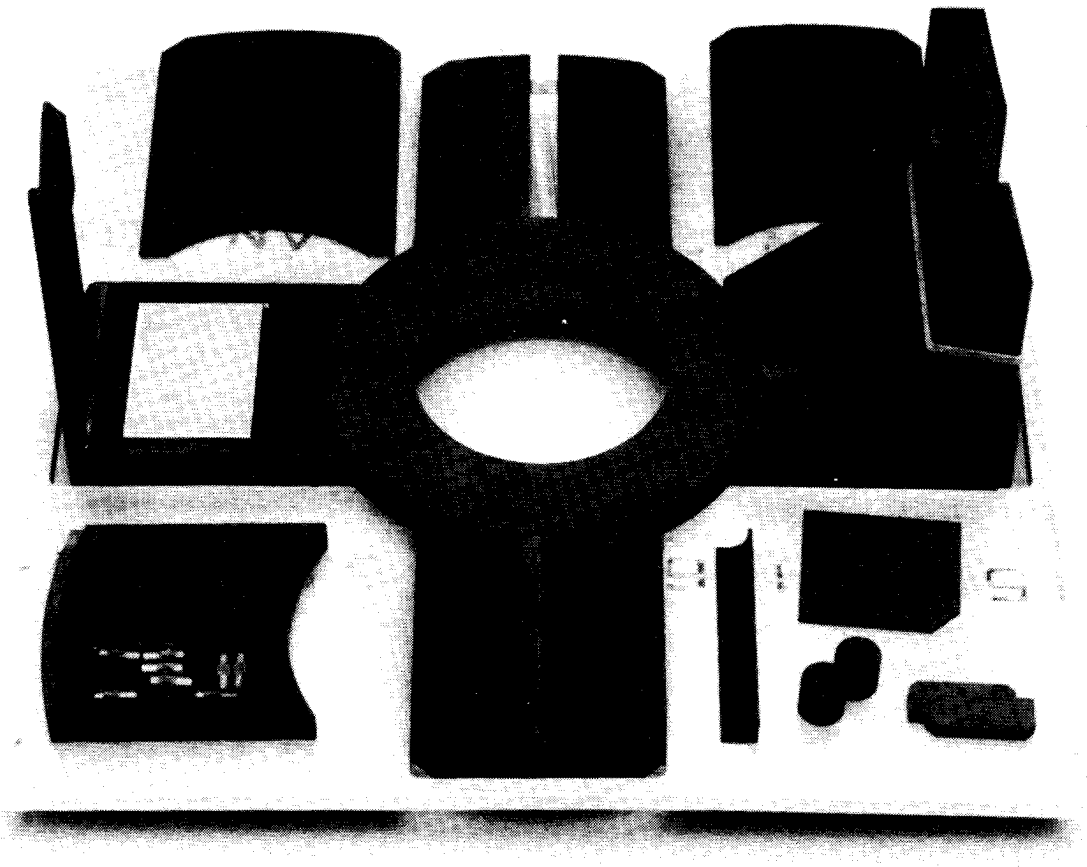

Figure 23. Gimbal Tooling

4. EVALUATION

4.1 GENERAL PURPOSES OF EVALUATION TESTING

Tests were used at different times during the program to verify analytical predictions and to measure properties too difficult to predict. During the design phase, tests were performed to evaluate physical properties of graphite-epoxy materials, to measure adhesive joint properties, and to measure insert strengths. Later, when the design was more complete, a partial prototype of the confirmatory sample was tested to measure the coefficient of thermal expansion of the bearing bore and to evaluate the adhesive bond joint condition after thermal extremes. Finally, the completed confirmatory samples were tested to determine structural resonances and temperature related boresight changes.

4.2 TESTS INVOLVING ENGINEERING SAMPLES

4.2.1 Tests of Material Samples

Tests of ten physical properties of HMS/1908 graphite epoxy composite (supplied by Graftek, Inc.) were conducted at the Westinghouse R&D Center. The results of the tests along with the theoretical values are given in table 11. The theoretical values were computed using the computer program "SPACE-WOUND", which was developed at the Westinghouse R&D Center. The program uses as inputs the resin and fiber properties along with the layup angles. The test values in the table are an average for 5 specimens for each category of test. Variation of test results between specimens was quite small; for example, the range of the tensile strength was 7,100 psi compared to the mean of 60,000 psi, while the spread of tensile modulus results was $1.06 \times 10^{+6}$ psi compared to the mean of $9.7 \times 10^{+6}$ psi.

The explanation for the variations between the analytic predictions and the tests results was not determined. It is noted that laminate analysis is subject to error of greater magnitude than the analysis of isotropic materials due to the much greater complexity of laminates. In perspective, the variations of design-critical properties were moderate and not large enough to jeopardize

the outcome of the design. Greatest emphasis was placed on maximizing the achieved Young's modulus because stiffness was the driving factor in this gimbal design rather than strength.

TABLE 11
COMPARISON OF TEST RESULTS AND THEORETICAL PREDICTIONS FOR HMS/1908 MATERIAL

Test	Experimental Value	Predicted Value
Tensile (0^o)	60,000 psi	67,833 psi
Compressive (0^o)	44,190 psi	31,797 psi
Flexure (90^o)	60,050 psi	67,833 psi
Shear 90^o	5,610 psi	12,235 psi
0^o	5,250 psi	12,235 psi
Density	1.5649 gm/cc	1.587 gm/cc
Fiber Volume	57.02%	
Void Content	0.0%	0.0%
Hardness	55,60,60,58,57	
Tensile Modulus	$9.7 \times 10^{+6}$ psi	$11.6 \times 10^{+6}$ psi
Shear Modulus	Not Tested	$4.437 \times 10^{+6}$ psi
Thermal Coef. of Expan.	Not Tested	1.080×10^{-6} in/in/^oF
Poisson's Ratio (tension)	0.319	0.3072
Poisson's Ratio (compression)	0.300	0.3072

Table 12 is a list of the test standards used in each test, along with the dimensions of the samples. The specimens were machined from a 14" x 14" composite plate with an isotropic layup $(0,\pm 45,90)s$.

TABLE 12
TEST STANDARDS

Test	Standard	Sample Dimensions
Tensile	ANSI/ASTM D-3039-76	8.0" x 0.50" x 0.085"
Compression	ASTM D-3410-75	4.5" x 0.50" x 0.085"
Flexure	ASTM D-790-71	4.25" x 0.50" x 0.085"
Shear	ANSI/ASTM D-2344-76	0.75" x 0.25" x 0.085"
Density	ANSI/ASTM D-792-66	0.50" x 0.50" x 0.085"
Hardness	ASTM D-2583	2.0" x 2.0" x 0.085"

4.2.2 Tests of Metal Inserts

Corrosion resistance is an important consideration in the mating of metals with composites; for example, aluminum is subject to galvanic corrosion when in intimate contact with graphite composites. Other metals, closer to carbon on the galvanic scale, show greater resistance to corrosion. Titanium is an excellent material to use in contact with graphite as are some stainless steels. Titanium in contact with graphite does not show noticeable corrosion after long-term exposure to corrosive conditions.

Threaded titanium inserts bonded to graphite composite test pieces are shown in figure 24. Failure of the threaded insert during torque testing showed the superiority of the adhesive bond. Two two adhesives used showed the superiority of Ciba-Geigy XU235/XU215 over Hysol EA 9320 in this type of application.

The second type of threaded insert tested is shown in figure 25. Good results were obtained with the addition of a thin stainless steel washer on the side where the clinch nut sleeve collapses when being set.

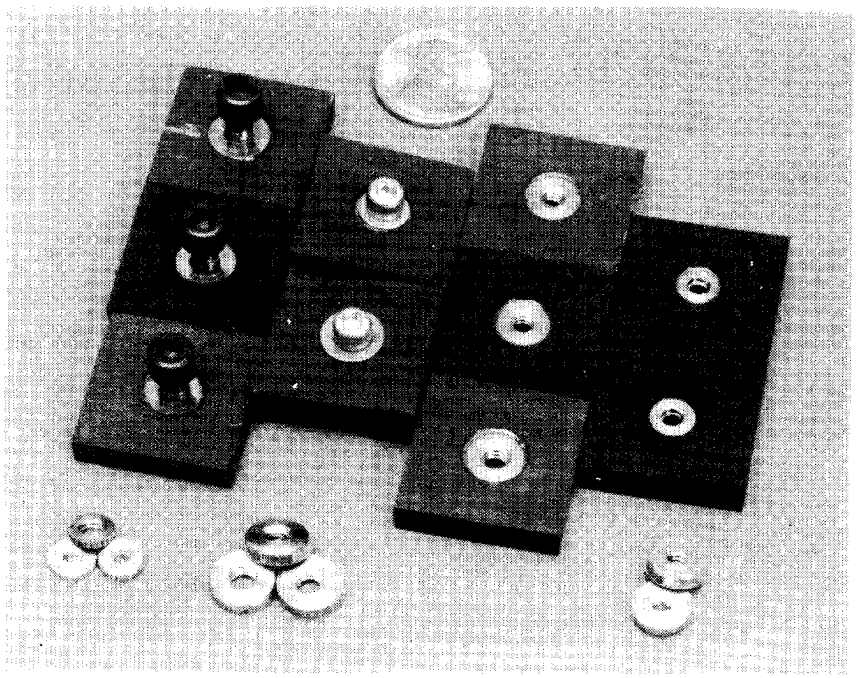

Figure 24. Bonded Titanium Cylindrical Inserts

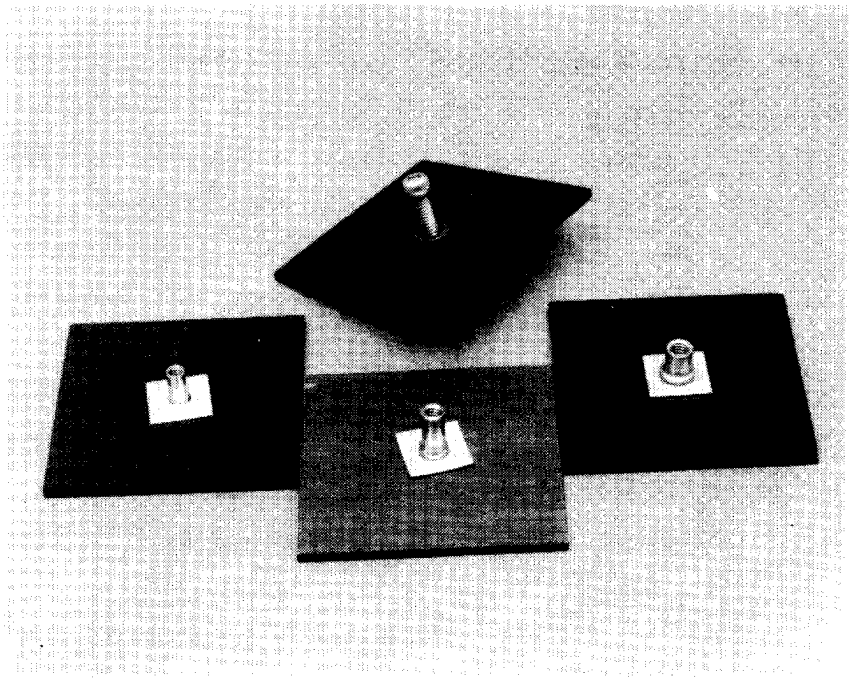

Figure 25. Threaded Insert Clinch Nut

A combination of both insert methods was chosen for the fabrication of the confirmatory samples. A titanium washer was clinched on a stainless steel clinch-nut and the combination was bonded to the graphite epoxy by means of XU235/XU205 adhesive. This proved to be entirely satisfactory.

4.2.3 Bond Shear Strength Tests

Available adhesives suitable for bonding the various structural parts together to form the complete gimbal were reviewed. The most promising adhesive was the film adhesive FM73 (American Cyanamid) and tests were conducted to determine the shear strength and shear rigidity (Section 4.2.4) of this adhesive. Shear strength data was available from the manufacturer but shear modulus was not.

The shear ultimate for the FM73 adhesive was tested using the standard lap shear test. The specimens were prepared as shown in figure 26.

The test results were about one half that of the manufacturer's test data of 6400 psi lap shear at 75°F. The difference was attributable to delamination of the adherend, which was HMS/1908 graphite epoxy plate with an isotropic layup.

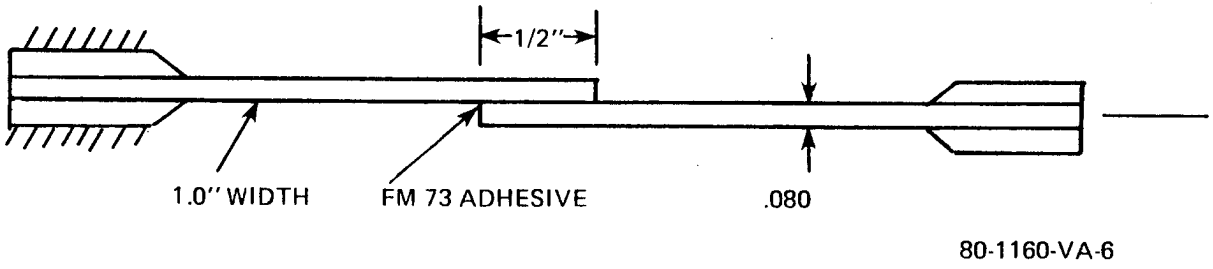

Figure 26. Lap Shear Specimen

In the absolute sense, the measured shear strength was judged more than adequate for the gimbal design.

4.2.4 Bond Shear Rigidity

In view of the critical nature of the rigidity of bonded joints in the gimbal design, a special vibration test was devised to determine whether a structural member composed of parts bonded together can approach the rigidity of a unitary member. Two pieces of graphite composite were attached together using a double strap joint. The doublers, or straps, were of the same composite material and the adhesive was FM73. The test specimen, shown in figure 27, was rigidly clamped in a vise-like fixture of very high mass and rigidity such that the specimen experienced vibration as a near-ideal cantilever beam when excited at its free end. Using the expression for the first vibration mode of an end-fixed cantilever (after Hartog) and solving for Young's modulus E, the resulting expression is

$$E = \frac{4\pi f_n^2 \mu_1 \ell^4}{a_n^2 I}$$

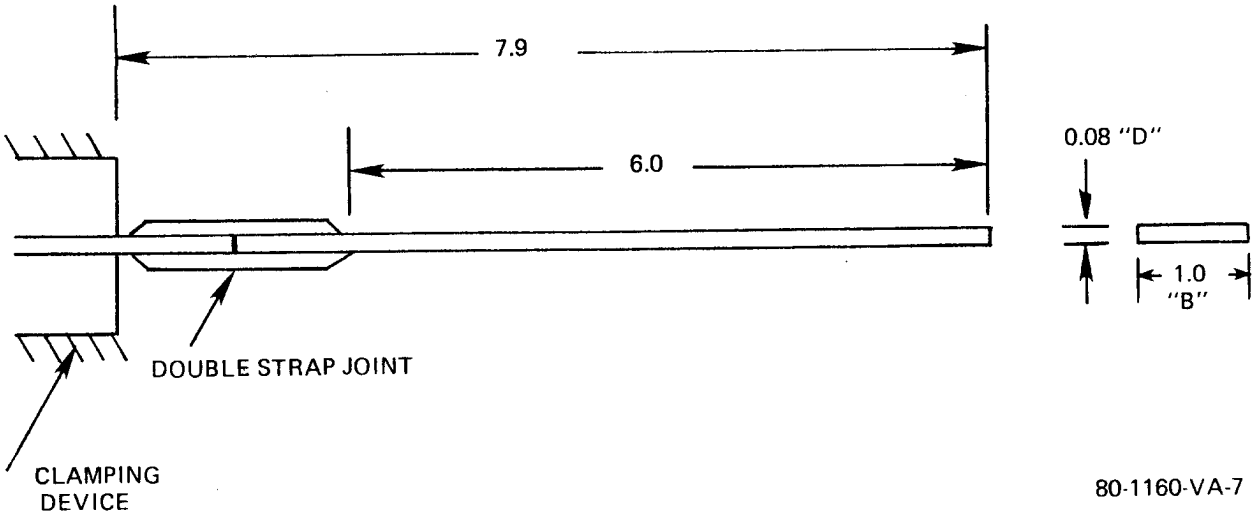

Figure 27. Bond Rigidity Specimen

where f_n = the resonant frequency, Hz

μ_1 = mass per unit length of the beam, lb-sec^2/in^2

ℓ = length of the beam, in

I = moment of inertia of the beam section, in^4

a_n = a constant (for the lowest frequency, the fundamental, a_n = 3.52)

For f_n = 92.48 Hz, material density = 0.056 lb/in^3 and ℓ = 7.9 in. (the total length of the specimen including the double strap joint), the value of E calculated from the formula is 28.87 x 10^{+6} psi, which is much higher than a unitary structure of 0.08 in thickness should be. For ℓ = 6.0 (the length of the specimen outboard of the double strap joint) the calculated value of E is 9.607 x 10^{+6} psi.

The specimen material was HMS/1908 graphite epoxy, isotropic layup, from the same batch tested at the Westinghouse R&D Center. The E found from those tests for a unitary specimen was approximately 9.7 x 10^{+6} psi (table 12). It was concluded from the vibration test that the test specimen behaved as if it was fixed at the beginning of the double strap joint. It was then inferred that the shear modulus of the FM73 does not adversely affect the fixity of

members bonded in a manner similar to the bond rigidity specimen (double strap).

The shear flexibility of the FM73 was detected in a three-point ending test. The two specimens were graphite composite beams of the same material. One specimen was twice as thick as the other, with FM73 adhesive between the two halves. In this test, the thicker beam did not realize the full increase in flexural stiffness associated with the increase in area moment of inertia. This was due to the flexibility of the adhesive, located in the plane of maximum shear stress, which reduced the overall stiffness of the bonded beam. However, this test configuration was not representative of the actual gimbal design whereas the vibration specimen of figure 27 was. The double strap joint showed no loss of rigidity due to bonding.

4.3 TESTS OF THE THERMAL SAMPLE

The "thermal sample" was built and tested to evaluate two temperature related phenomena; (1) bearing bore coefficient of thermal expansion, and (2) adhesive bond durability. It was constructed from composite materials similar to those which were to be used in the confirmatory samples. Structural features of the azimuth bearing housing assembly were included exactly and structure surrounding the bearing assembly was represented closely. The thermal sample is shown in figure 15.

4.3.1 Bearing Bore Coefficient of Thermal Expansion Test

It is usually desirable to match as closely as possible the coefficient of thermal expansion (CTE) of bearings and bore. This is definitely the case for the preloaded bearing pairs that are typically used in gimbals. For significantly mismatched CTE's, an undesirable tradeoff must be made between excessive sloppiness in bearing fit and overstresses in the bearings. The bearing bore of the composite gimbal was designed to have a CTE close to the CTE of the steel bearings.

The bearing bore CTE over three temperature ranges was calculated using the relationship shown below. The CTE values are listed in Table 13.

$$CTE = \frac{\Delta D}{D_R \, \Delta T}$$

where ΔD = diameter - reference diameter

delta ΔT = temperature - reference temp.

D_R = reference diameter

The composite gimbal bearing bore average CTE was measured as $+4.51 \times 15^{6}$ in/in/^{o}F. The bore CTE of the composite gimbal is better matched to the steel bearing CTE ($+5.6 \times 15^{6}$ in/in/^{o}F) than is the bore CTE of the cast aluminum gimbal ($+8.7 \times 10^{-6}$ in/in/^{o}F).

TABLE 13

BEARING BORE COEFFICIENT OF THERMAL EXPANSION

Temperature Range	CTE (in/in/^{o}F)	Variation from overall CTE
-14^{o}F to $+78^{o}$F	5.184×10^{-6}	+14.8%
$+78^{o}$F to $+162^{o}$F	3.784×10^{-6}	-16.4%
-14^{o}F to $+162^{o}$F	4.516×10^{-6}	

4.3.2 Adhesive Bond Durability Test

The composite gimbal, being an assemblage of composite and metal parts, has numerous bonded interfaces between parts with different coefficients of thermal expansion. The effects of both high and low temperatures on the bond joints were evaluated using the thermal sample.

The stiffness of the thermal sample as determined by a three-point bend test was the evaluation criterion of adhesive bond integrity.

The test setup is shown in figure 28.

The bending stiffness was measured before the test sample was exposed to temperature cycling. Initial thermal exposure was 10 cycles between -20^{o}F and $+160^{o}$F, after which the bending stiffness was measured again. The test sample was then exposed to single cycles from -40^{o}F to $+160^{o}$F, -55^{o}F to $+160^{o}$F, and -65^{o}F to $+160^{o}$F. After each cycle the bending stiffness was remeasured. Each of the last three tests had a lower minimum temperature so that the damage threshold temperature, if one were found, would be detected. Table 14 presents the results of the bond durability test.

No statistically significant change in the bending stiffness of the thermal sample occured which indicated that the structural design of the composite gimbal would be tolerant of the temperature extremes it would be subjected to in service. The operating temperature range for the ARPV Mission Payload System is within the range tested (-65^{o}F to $+160^{o}$F).

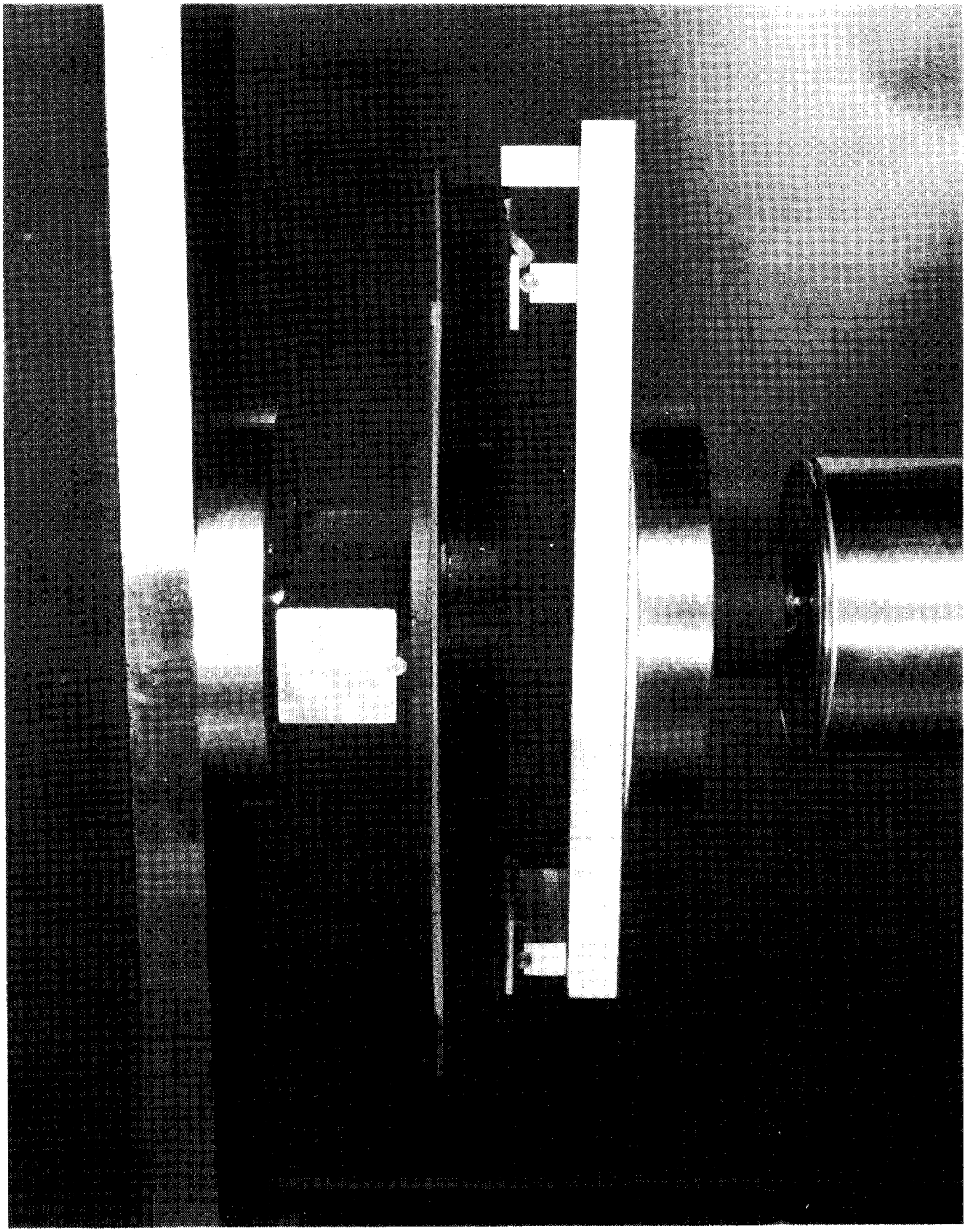

Figure 28. Three Point Bend Test

TABLE 14

ADHESIVE BOND DURABILITY TEST RESULTS

Status of Thermal Sample	Average Measured Stiffness(lb/in)x10^3
1. before thermal cycling	16.1
2. after 10 cycles between -20°F and +160°F	15.4
3. after 1 cycle between -40° and +160°F	16.9
4. after 1 cycle between -55° and 160°F	16.4
5. after 1 cycle between -65° and +160°F	16.3

4.4 TESTS OF THE CONFIRMATORY SAMPLES

The finished composite gimbals, or confirmatory samples, were tested for performance critical characteristics. The first confirmatory sample, which had the same functional dimensions as the cast aluminum gimbals, was tested for natural frequencies/mode shapes and for thermally induced boresight changes. The second confirmatory sample, with lengthened elevation gimbal support arms, was evaluated for natural frequencies and mode shapes.

4.4.1 Modal Analysis of Confirmatory Samples

Natural frequencies and mode shapes of the confirmatory samples were determined by analysis of multiple transfer functions recorded from the samples while white noise excitation was being applied. For meaningful natural frequencies, the mass and attachment interfacing of an elevation gimbal were simulated. The simulated gimbal had the proper weight and center of gravity location, but neither the rotational inertia nor the stiffness of actual elevation gimbal was simulated. Both of these characteristics were difficult to obtain without the use of an actual gimbal and neither was greatly significant.

The confirmatory samples were mounted to a shaker by a flanged shaft inserted into the azimuth bearing bore. The shaft was attached to the gimbals with hardware engaging the bearing retainer threaded inserts in the gimbal while a shoulder on the shaft was driven against the bearing step in the bore. This support represented the actual attachment of the gimbal to the real shaft without using bearings. The first confirmatory sample, ready for modal analysis, is shown in figure 29.

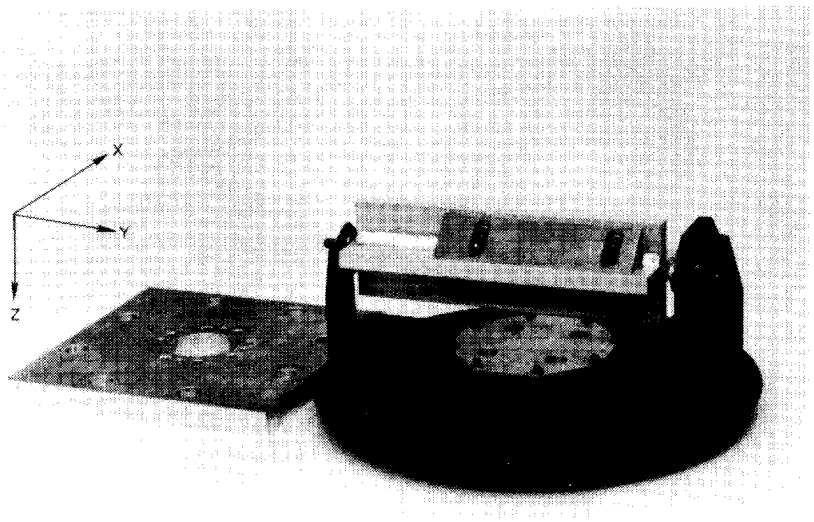

Figure 29. Gimbal with Test Fixture

Transfer functions between various points on the gimbals and the input excitation were measured and recorded. Transfer functions in each of three orthogonal directions were taken at each point. Analysis of the transfer functions after data collection was completed yielded the natural frequencies and the mode shapes associated with them. A Hewlett-Packard 5451C system was used for data collection and transfer functions analysis.

The natural frequencies determined for both confirmatory samples are listed in table 15 along with the predicted values for the first confirmatory sample. A typical transfer function from the first confirmatory sample for Y axis input excitation (see figure 29) is shown in figure 30. The fundamental translational mode in the Y directions, 136 Hz, appear as the large peak on this transfer function. A greatly exaggerated representation of the deflection which occurs at this frequency is shown by the two extreme positions shown in figure 31.

TABLE 15

Natural Frequencies of Confirmatory Samples

Mode Description	Measured Frequency (Hz)		Predicted Frequency (Hz)
	First Confirmatory Sample	Second Confirmatory Sample	First Confirmatory Sample
Y axis translation of elevation gimbal	136	110	142
X axis translation of elevation gimbal	Not observed	126	206
Z axis translation of elevation gimbal	159	191	201
X axis rotation and Z axis translation of elevation gimbal combined	196	Not observed	Not predicted
Z axis rotation of elevation gimbal	296	266	290
X axis rotation of elevation gimbal	389	379	355

All structural resonances were greater than the original design minimum set at 100 Hz. The agreement between the predicted and achieved lowest natural frequency of the first confirmatory sample was good. Since the structure of the second confirmatory sample was the same as the first, except for the lengthening of the elevation gimbal support arms, it was expected that the resonances of the second would be less than the first. The measured resonances of the second confirmatory sample confirmed this expectation.

4.4.2 Thermal Stability of Confirmatory Samples

It is possible, in optical gimbal systems, for thermal dimensional changes to cause shifts in boresight between various sensor/devices in the optical path. This is not relevant to the system of which the confirmatory samples are conceivably parts of, since the sensors/devices are located off gimbal. However, gross thermal instability of the gimbal, if great enough, could cause functional problems associated with strength and bearing friction. The thermal stability of the elevation arms with respect to each other was determined by test, for the first confirmatory sample.

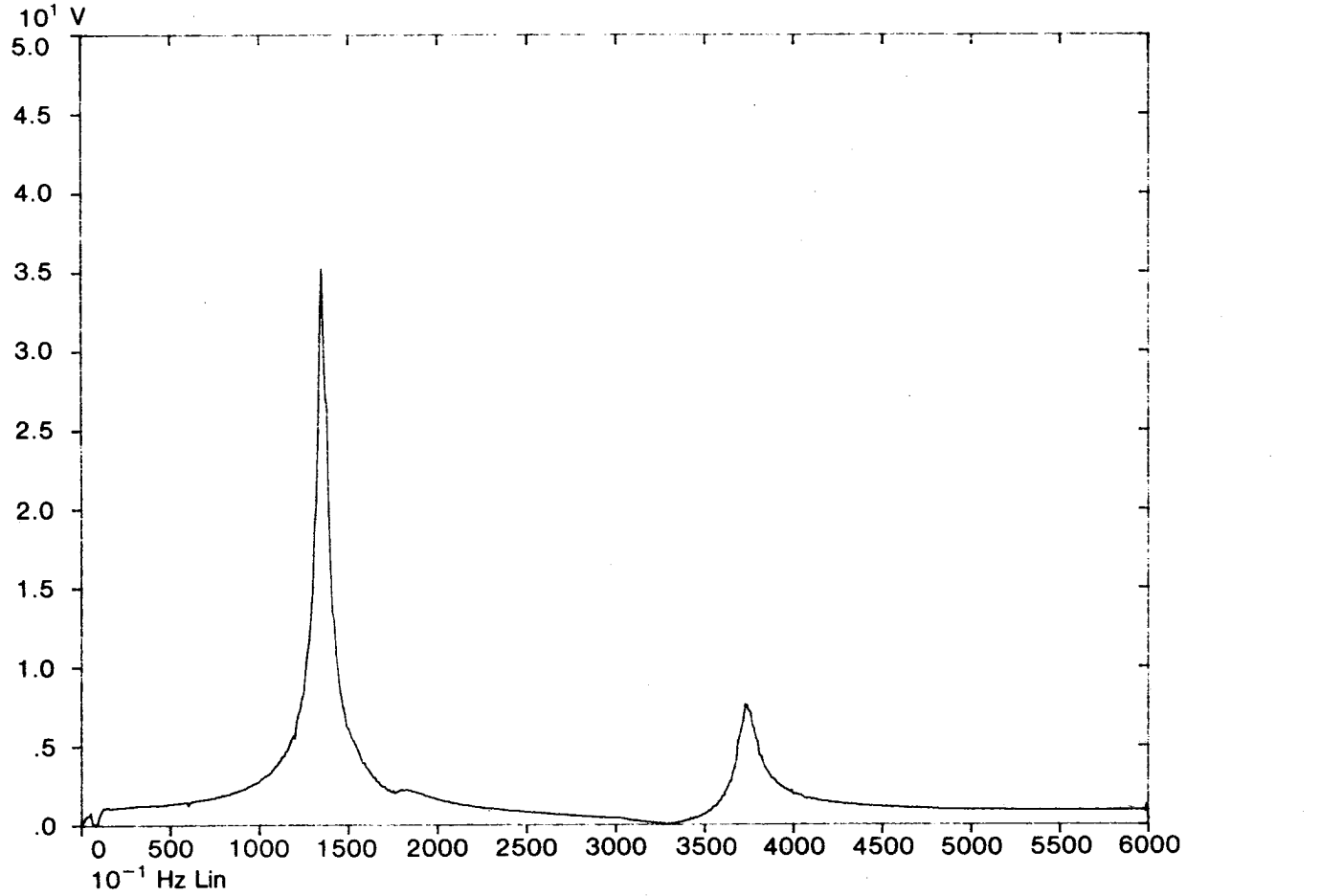

Figure 30. Typical Y-Axis Transfer Function (Magnitude) for First Confirmatory Sample

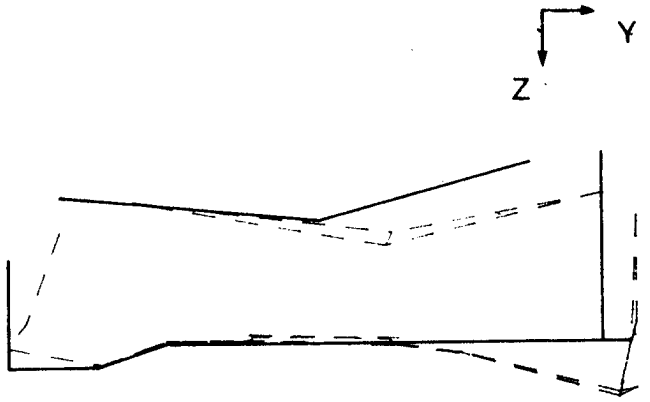

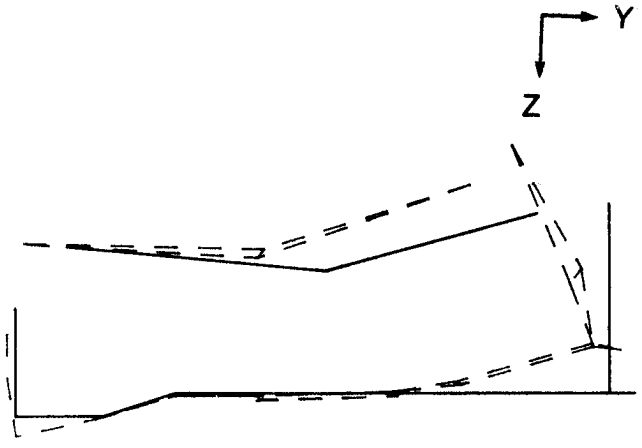

Figure 31. Exaggerated Modal Deflection at 136 Hz

A half-silvered mirror was attached to one gimbal arm and a fully-silvered mirror to the other. A helium-neon laser was positioned to pass the beam through the first mirror through the elevation shaft hole, and to the second mirror. A return beam was reflected from both mirrors. The gimbal was placed in a chamber, with a viewing port, capable of both heating and cooling.

The return spots from both mirrors were charted with the gimbal at $-25^{o}C$, $+25^{o}C$, and $+65^{o}C$. The angulation of the mirrors with respect to each other was found using the spread between the spots, the distance from the target to the mirrors, and accounting for the 2 to 1 effect of the reflecting surfaces.

In going from $+25^{o}C$ to $-25^{o}C$, the arms shifted with respect to each other by 1.4 milliradians or 0.03 milliradians per degree C. The angular shift between the gimbal arms during the $+25^{o}C$ to $+65^{o}C$ excursion was 1.1 milliradians or 0.03 milliradians per degree C.

The measured relative motion between arms was judged to be acceptable for the gimbal application. It is also likely that the motion would have been less in a fully assembled gimbal, with an elevation gimbal in place between the arms.

5. PRODUCTION PLAN

The production plan is based on an anticipated quantity of 1000 gimbals per year with design changes expected after every 150 to 200 gimbals. It should be mentioned that this plan is structured to accommodate the gimbal developed for this program. Although the plan is fairly universal, it would have to be reviewed and possibly modified for a different gimbal design. The planned facility will procure raw materials in the form of resin, tow, prepreg, and mat. This raw material will be processed within the facility to form the basic shapes required to manufacture the gimbals.

5.1 PROCESS FLOW

The process flow will be as shown in figure 32. Received material, after passing through the quality control station, is directed to the filament winding operation or the formed shapes operation. The completed windings are rough machined, final machined and then bonded as necessary to form the final detail parts. In the case of shapes, they are machined to size, bonded as necessary and machined again to complete the detail parts.

The detail parts are then brought together at the sub-element assembly station where they are bonded to form the gimbal sub-elements. Following this, the sub-elements are machined and submitted to the gimbal assembly station.

The gimbal assembly station processes all of the sub-elements and some remaining detail parts into a full gimbal assembly. Appropriate tooling is used during both sub-element and full gimbal assembly to insure proper alignment of all the parts.

Two machine operations are performed on the gimbal. The first is essentially a rough machining to establish all the necessary datums and to complete the less critical operations. This is followed by a precision machining operation of the close tolerance features.

Prior to submission to final inspection, the fasteners and miscellaneous hardware are installed.

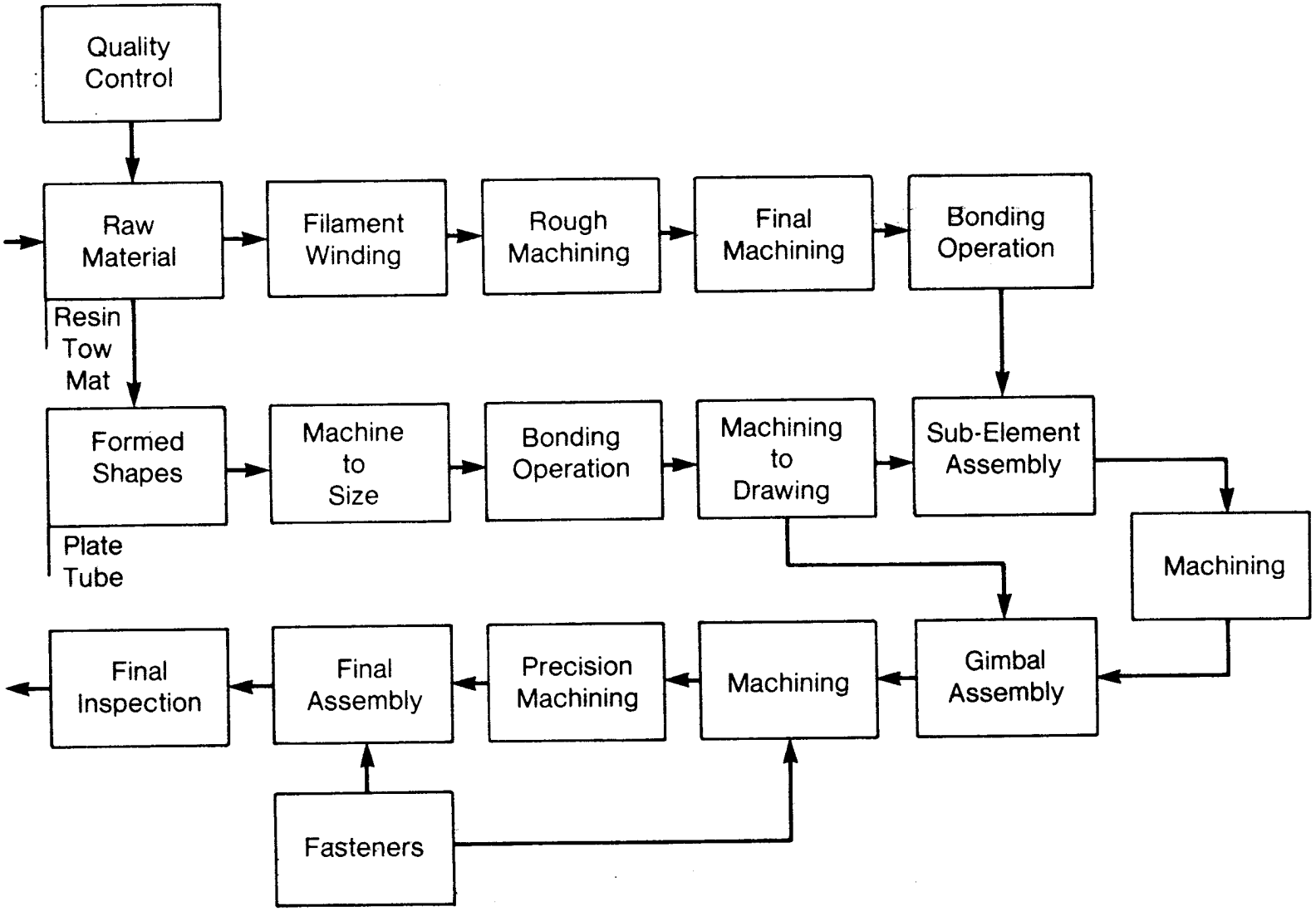

Figure 32. Production Plan Processor Flow

Not shown in figure 32 are the quality control stations which are located at appropriate points in the process.

5.2 MATERIAL REQUIREMENTS

The cost of material necessary to fabricate 1000 gimbals has been estimated at $435 per gimbal. Of this, $360 is associated with nonmetal type material such as resin, tow, prepreg and mat. The remaining $75 is for metal items such as titanium, stainless steel and fasteners.

A breakdown of the major raw material is as follows:

Titanium	$ 60
HMS/1908 Graphite Epoxy	
Rings	140
Plates, Box Sections	220
Fasteners	15
	$435

5.3 TOOLING REQUIREMENTS

The tooling required to produce 1000 gimbals per year will cost approximately $22,000 exclusive of large scale equipment such as filament winding machines, machine tools, etc. The breakdown is as follows:

Winding mandrels, small, 2	$1200
Winding mandrels, large, 2	3000
Fixtures, machining, 2	5000
Mold, box	3000
Fixtures, plate molding, 6	3000
Machining tools, special	1000
Installation tools, fasteners	1000
Alignment tools, sub-element, 4	2000
Alignment tools, gimbal assembly,4	2000
	$21200

5.4 LABOR REQUIREMENTS

	Hours	Cost
Winding and fabricating basis shapes	9	$ 310
Machining of windings and shapes	17	600
Bonding to form detail parts	4	140
Sub-element assembly	4	140

	Hours	Cost
Machining of sub-elements	6	210
Assembly of gimbal	12	420
Machining of gimbal	30	1050
Final assembly	4	140
		$3010

5.5 TOTAL COSTS

Combining the tooling, material and labor costs results in a total gimbal cost of $3467 on a 1000 lot basis.

Material	$435
Tooling	22
Labor	3010
	$3467

The cost drivers are the raw material and the machining labor. It should be possible to reduce both of these factors on future designs.

In the case of raw materials, the pitch base epoxy graphites are becoming more available and the techniques used to process the materials into finished parts are becoming better developed. Future designs should be able to use a greater amount of the pitch base material. The cost of pitch material is currently $27/pound which is 50 percent less than the cost of the non-pitch base material used for this production plan. A review of the material breakdown indicates that substituting pitch material would reduce the material costs from $435 to $325.

Machining costs on the gimbal were somewhat higher because the interfaces were dictated by the existing aluminum design. In a new all composite design it is estimated that about $200 of machining costs can be eliminated by designing interfaces that lend themselves to composite fabrication.

Taking advantage of both of the cost reductions discussed above, the gimbal cost tabulation would be:

Material	$325
Tooling	22
Labor	2810
	$3157

The 1000 lot cost of the orginal aluminum gimbal is estimated as $2368. The composite gimbal is therefore from 1.3 to 1.5 more costly than the

comparable aluminum gimbal.

In considering this cost comparison, there is one additional and very important factor that needs to be discussed. This factor is the ease with which design changes can be incorporated into a composite design that employs low cost tooling. In this program, the second confirmatory sample was different from the first with respect to the length of the arms and corresponding bearing bore locations. To incorporate these changes, all that was required was a few drafting hours to change a set of drawings. Fabrication of the 2nd set of detail parts was based on the revised drawings. No expensive tooling had to be scrapped or changed. New tool try-outs were not needed. This would not have been the case if the design were based on a metal casting. These savings plus the added performance capability of advanced composites in electro-optical systems greatly reduce or eliminate the significance of the cost edge of the aluminum gimbal.

5.6 QUALITY CONTROL

The quality control aspects of the production plan incorporate the basic elements that have been proven to be necessary and appropriate to maintain quality throughout a production run. The key items to be considered are: Vendor evaluation and performance, in-process inspection and controls, and operator qualification.

5.6.1 Vendor Evaluation and Performance

Prior to the start of production, potential vendors will be identified and asked to submit documents describing their quality control system and the basis of compliance with the applicable military and contractor requirements. If this submittal indicates compliance or a desire to make the changes necessary to fully comply, a quality review team will visit the facility and perform an on-site audit of the system. Based on successfully meeting the requirements of the audit, the vendor will be approved for a trial lot.

The manufacture of the trial lot will be monitored and quality tests performed on samples. If production of the trial lot is satisfactory, the vendor will be approved for the program.

After the program is underway, appropriate samples of all incoming material will be subjected to tests to determine acceptability.

The results of all tests will become a permanent record. These records will be used in statistical analysis of vendor performance.

5.6.2 In-process Inspection And Controls

Optical scanning equipment will be used to continually inspect the pre-preg laying portion of the manufacturing cycle to monitor the level of contamination present and the fiber orientation. Final acceptance inspection of the product at this point will include acoustic emission/ultrasonic inspection for voids.

Machined parts will be inspected for dimensional compliance and for delamination of materials on the machined surfaces.

Bonded joints will be inspected for voids using acoustic/ultrasonic equipment (non-destructive). Destructive tests will be used periodically to check tensile properties.

Data generated at incoming and during manufacture will be transmitted to a central evaluation center. This data will be summarized and statistically plotted and used to monitor the condition of the various processes on a real time basis. This will serve to alert quality control that a vendor or process is deviating from the norm and that action must be taken to correct the situation.

5.6.3 Operator Qualification

Operators will be trained in the required methods and their performance evaluated. The operators demonstrating the ability to consistently perform to the requirements will be certified. Periodically these operators will have to demonstrate their ability in order to maintain their certification.

5.7 PLANT LAYOUT

Figure 33 shows a concept for a plant layout. The square footage required is estimated at 25,000. Arrows indicate the material flow direction out of the various areas. Robotics will be employed in the areas noted. It is anticipated that robotics could also be developed and applied in the molding and assembly areas. Although not developed as part of this program, mechanized computer controlled material handling will be used throughout the facility.

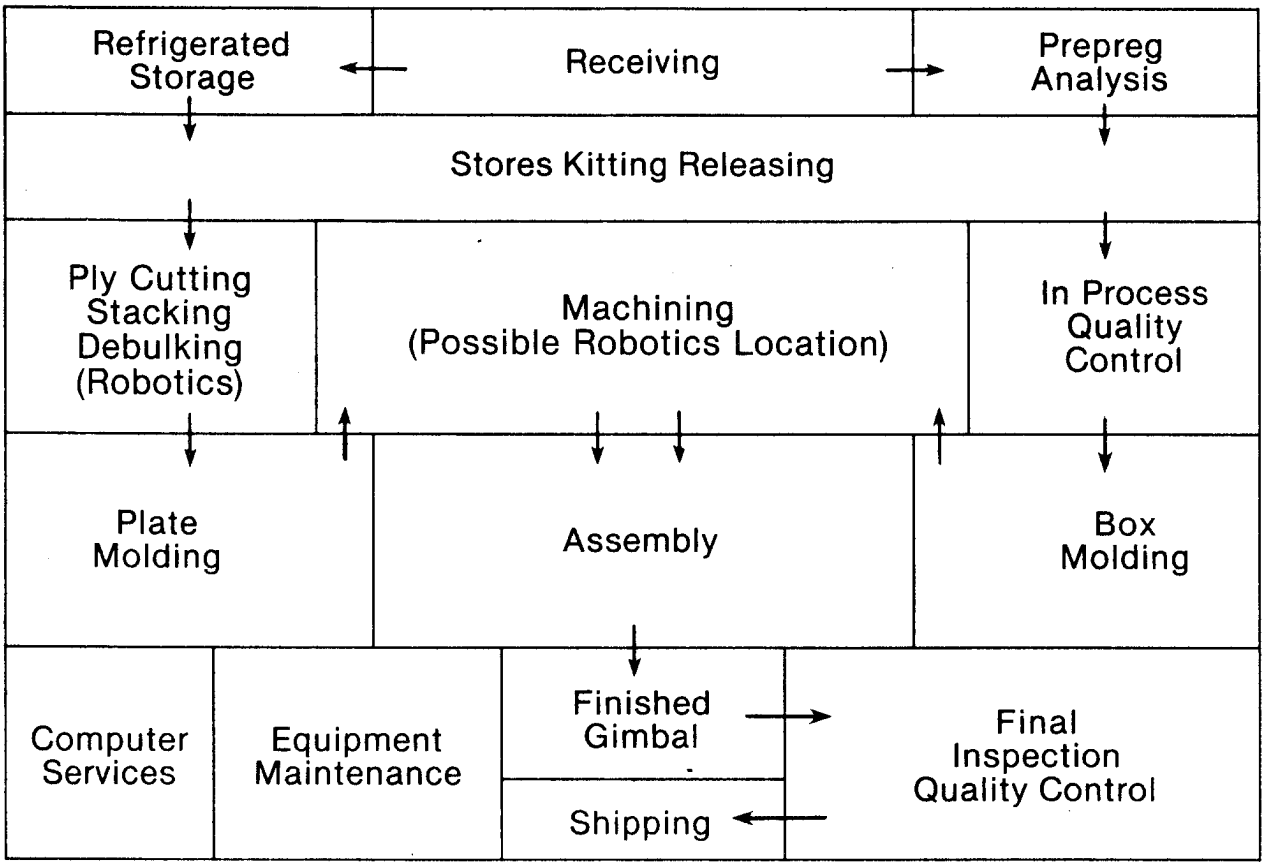

Figure 33. Plant Layout for Composite Gimbal

6. CONCLUSIONS AND RECOMMENDATIONS

This contract provided the opportunity to develop unique methods for applying advanced graphite epoxy composite materials to electro-optical gimbal systems and to demonstrate the viability of the methods. It also allowed the demonstration of the advantages associated with the use of low-cost tooling.

It is concluded that the application and use of advanced composites and low-cost tooling for stabilized line of sight gimbal systems is very appropriate. The functional advantages of composites are significant- reduced weight, increased stiffness to weight ratio, improved damping ratio, and lower coefficient of thermal expansion.

With regard to cost, although the composite design is 30 to 50% more costly than an aluminum design on a per-unit basis, the ease of design change will make the composite design less costly in the long run on typical programs. For this program, if a 40% per-unit cost adder for the composite gimbal is used and a $100,000 increased cost differential for an aluminum casting design change is assumed, the break-even point would be a design change every 100 units. Some estimates indicate the cost differential for a new aluminum casting through design, drafting, tooling and check-out would approach $500,000. This would increase the cross-over point to 500 units. In other words, the composite design would be less costly than an aluminum design if a design change were required before the 500th unit. It is believed to be unlikely that a program in today's technological environment would produce 500 units without one or more casting design changes.

Another consideration is the fact that the methods and tooling applied on this program lend themselves to the development of a family of gimbals. Once a basic design is established, it is straightforward to change the design to a larger or smaller size to suit a different application.

To continue the exploitation of advanced composites for electro-optical gimbal systems, the next obvious step which is recommended is the development and flight-test of a complete system. This would allow complete design control of the internal interfaces within the system, for more optimum material use, and reduced fabrication costs along with full documentation of the final system performance.

7. GLOSSARY OF TERMS

Actuator Support Arm: The azimuth yoke arm which supports the elevation actuator and which is adjacent to the gyro.

Actuator Support Arm Box Structure: The structural member which carries most of the load from the actuator support arm to the bearing support ring.

Base-Plate: The circular plate to which the azimuth yoke and the pressurized dome are attached.

Base Plate Stiffener Ring: The large diameter ring used to stiffen the base plate and provide support for the lip seal.

Bearing Support Ring: The central structural ring into which the azimuth bearings are fitted.

Cap Plate: A plate structurally analogous to the base plate. It is the top plate in the double strap joint concept and is bonded to the tops of several of the main structural subelements.

Cross-Plane Stiffeners: Box structures bonded to the base plate on the side opposite to the main gear box. These structures also serve as a housing for the synchro gears.

Half Arm: The azimuth yoke arm which supports the end of the elevation gimbal opposite the actuator end and which is adjacent to the stabilizing mirror. This arm is partially cut away to allow clearance for the mirror, hence the term "half arm."

Main Gear Box: The box structure bonded to the base plate perpendicular to the elevation axis. It houses the azimuth drive gearing.

Mirror Arm: Same as Half Arm

Motor Arm: Same as Actuator Support Arm

MPS: Mission Payload System

SLOS: Stabilized Line of Sight

Support Ring: Supports Titanium Bearing Mount

APPENDIX A

DRAWINGS 687R258 687R259 687R260 687R261

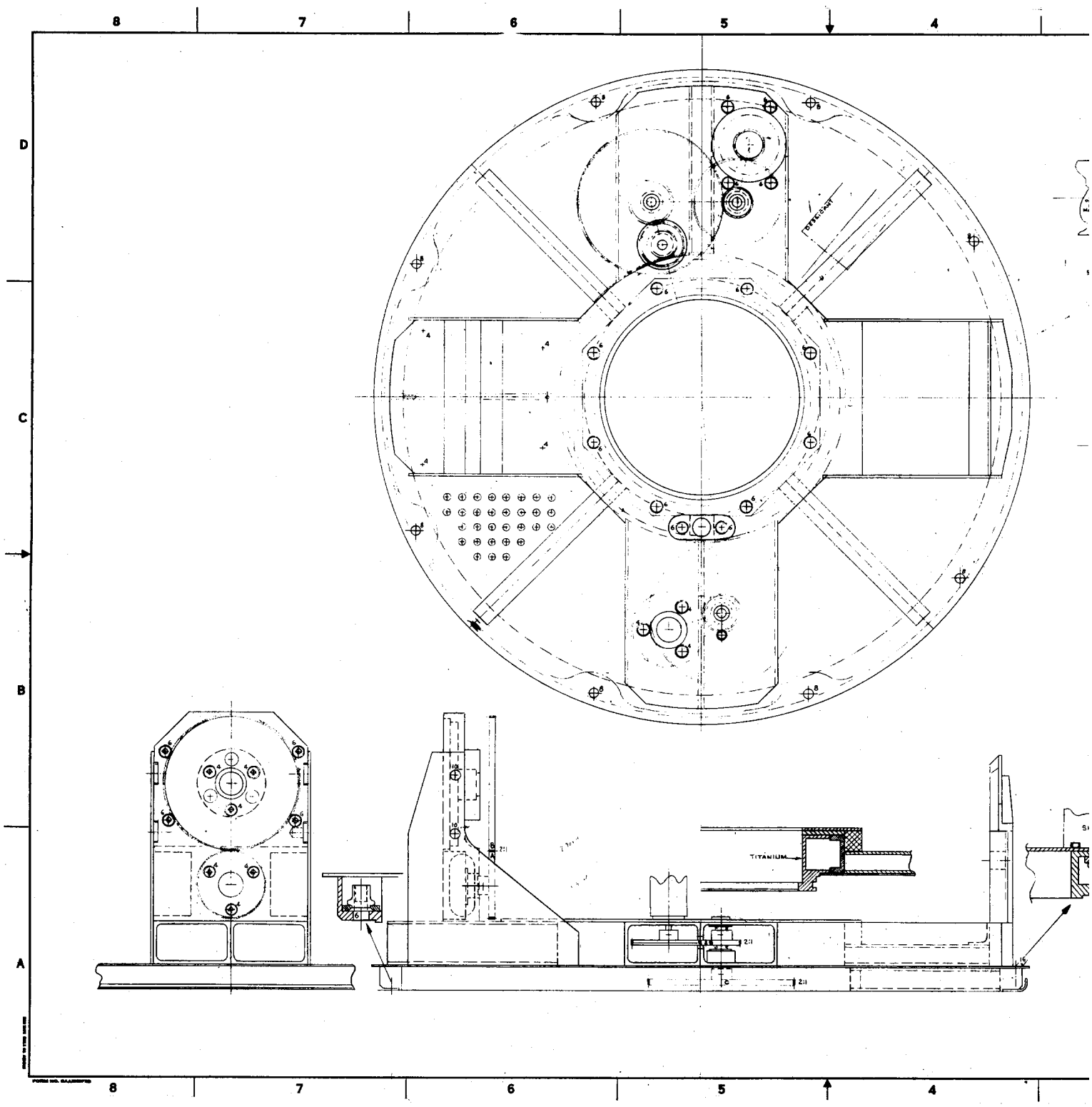
8
7
6
5
4
D
C
B
A
TITANIUM

DWG NO. 687R258 SH 1

REVISIONS				
ZONE	REV.	DESCRIPTION	DATE	APPROVED
	–	DRAWING RELEASED		

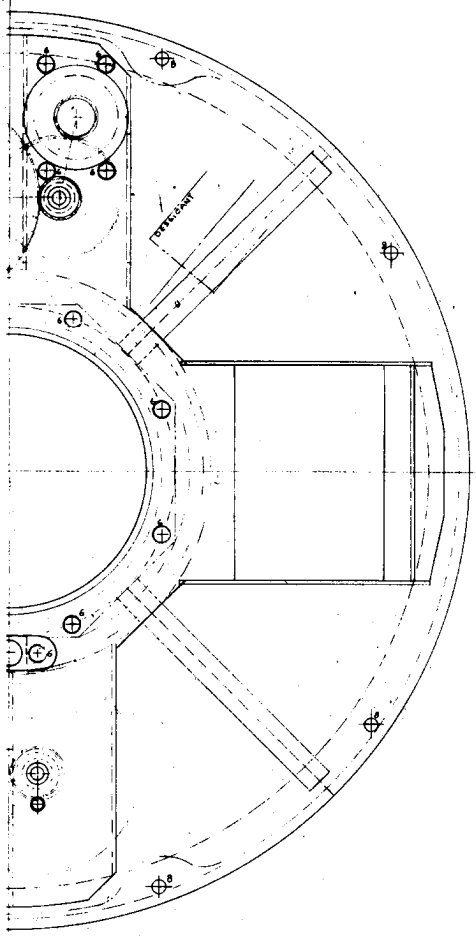

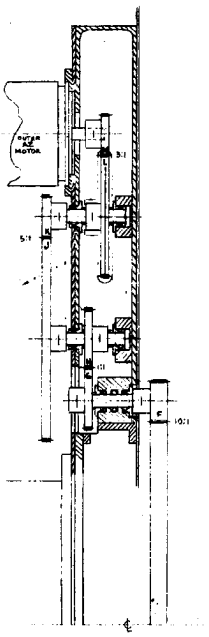

GEAR DATA
A - 1.3542 P.D.
B - 2.7084 P.D.
C - 2.9166 P.D.
D - .7500 P.D.
E - 1.5000 P.D.
F - .5833 P.D.
G - .8750 P.D.
H - .8750 P.D.
J - 2.9166 P.D.
K - .5833 P.D.
L - 1.7500 P.D.
M - .5932 P.D.

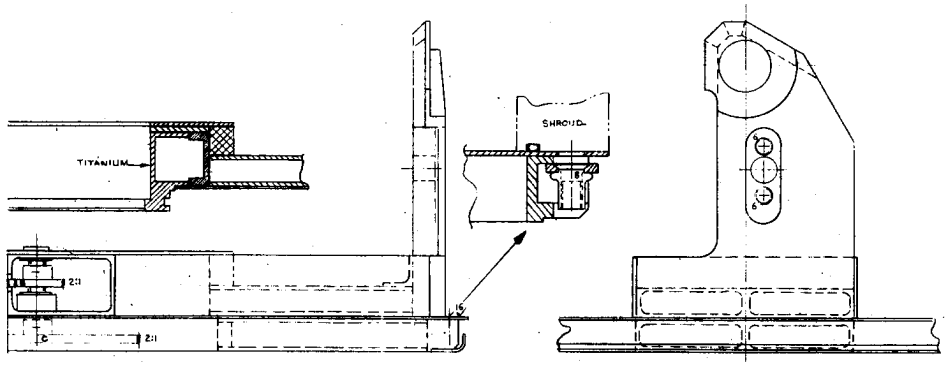

ADVANCED COMPOSITE
OF AZIMUTH GIMBAL
LAYOUT

REV. A

Westinghouse Electric Corporation	SIZE	FSCM NO.	DWG NO.
CONTR. NO.	D	97942	687R258
OPTION	SCALE 1/1		SHEET 1 OF 1
RELEASED			

PARENTHETIC IDENTITIES ARE FOR WESTINGHOUSE REFERENCE ONLY

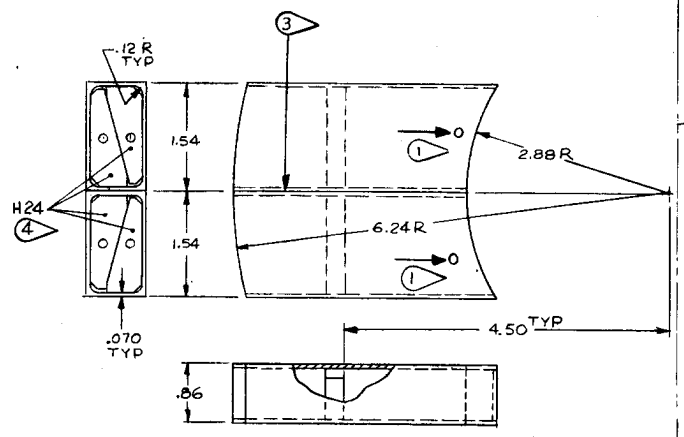

H01

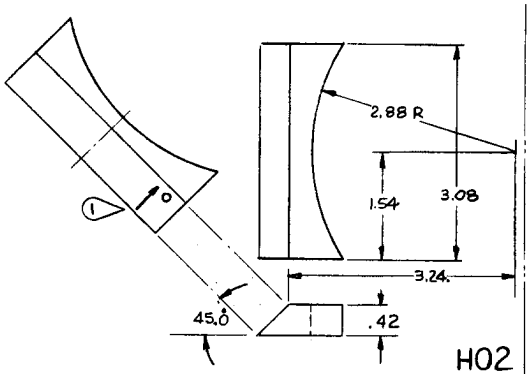

H02

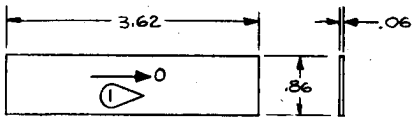

H0

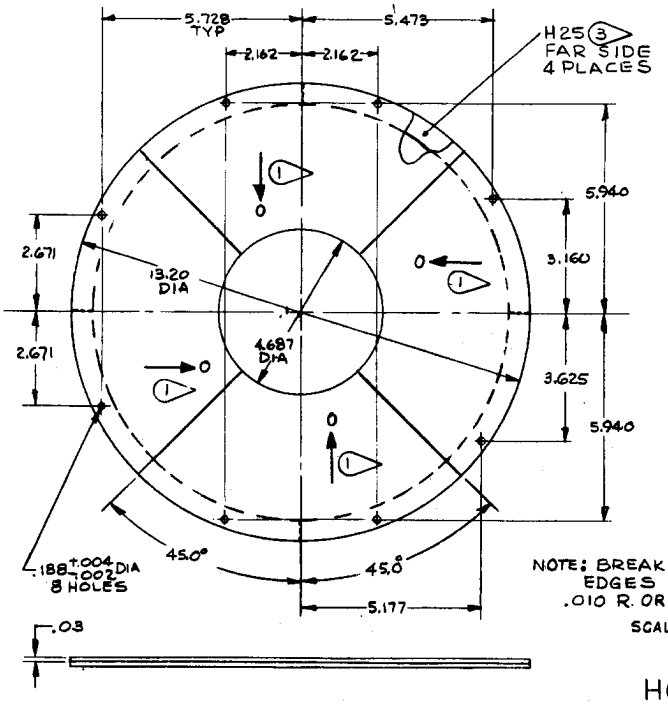

NOTE: BREAK ALL EDGES TO .010 R. OR CHAMFE

SCALE 1/2

H05

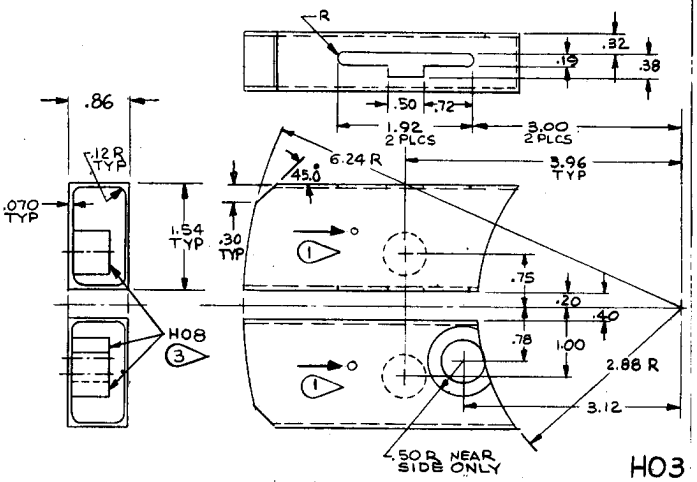

H03

NOTES

1. HMS/1908(±25°)
2. HMS/1908(0°/±45°/90°)$_S$
3. BOND WITH FM 73 THEN CURE FOR 1 HR. AT 250°F WITH 40 PSI PRESSURE APPLIED
4. BOND WITH EA9320, CURE AT ROOM TEMP
5. HMS/1908(0°60%/±45°40%)

NEXT ASSY	USED ON
APPLICATION	

DWG NO. 687R259 SH 1

SHEET REVISION STATUS					
5	4	3	2	1	SHEET NO.
	-	A	A	A	REV.

REVISIONS				
ZONE	REV.	DESCRIPTION	DATE	APPROVED
	-	DRAWING RELEASED		
	A	DR DATED 11 MAR 81 REV PER ENG INSTR	16 MAR 81	

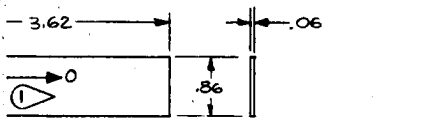

H04

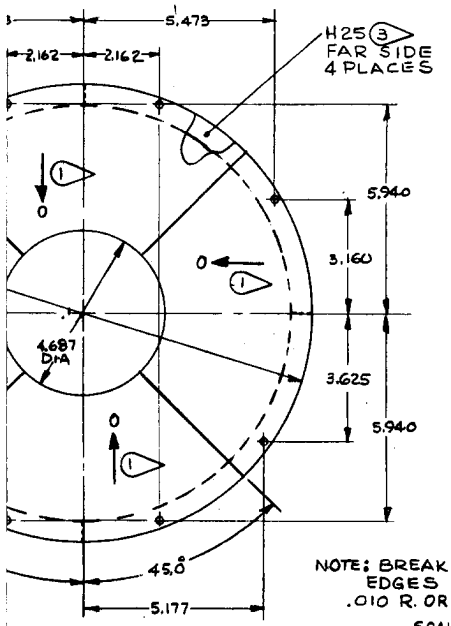

NOTE: BREAK ALL EDGES TO .010 R. OR CHAMFER

SCALE 1/2

H05

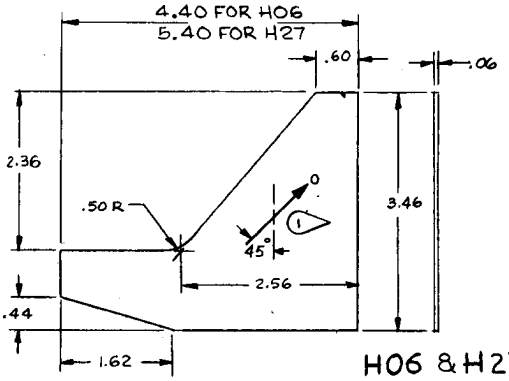

H06 & H27

-		687R259H29	GRAPHITE EPOXY			2	29
-		687R259H28	GRAPHITE EPOXY			2	28
-		687R259H27	GRAPHITE EPOXY			1	27
1		687R259H26	GRAPHITE EPOXY			5	26
4		687R259H25				1	25
1		687R259H24					24
4		687R259H23					23
4		687R259H22	GRAPHITE EPOXY			1	22
4		687R259H21		SST		PDS10701EG	21
12		687R259H20		TI		PDS17710BE	20
8		687R259H19		TI		PDS17710BE	19
1		687R259H18	GRAPHITE EPOXY			1	18
1		687R259H17	GRAPHITE EPOXY			5	17
1		687R259H16		TI		PDS17710BE	16
1		687R259H15	GRAPHITE EPOXY			2	15
1		687R259H14				2	14
1		687R259H13				2	13
1		687R259H12				1	12
1		687R259H11					11
1		687R259H10					10
1		687R259H09				1	9
4		687R259H08				2	8
1		687R259H07				1	7
2		687R259H06					6
1		687R259H05					5
2		687R259H04					4
1		687R259H03					3
1		687R259H02					2
1		687R259H01	GRAPHITE EPOXY			1	1
QTY REQD	FSCM NUMBER	PART NO.	SYM	DESCRIPTION	GOVT SPEC	Ⓜ SPEC	FIND NO.

SYM: B=BULK MATERIAL V=VENDOR ITEM SEE CONTROL DWG

PARTS LIST SEE PL

NEXT ASSY	USED ON
APPLICATION	

UNLESS OTHERWISE SPECIFIED DIMENSIONS ARE IN INCHES DO NOT SCALE. TOLERANCES ON DIM.

2 PLACE	3 PLACE	ANGLES
±.01	±.005	±0.5°

Ⓜ SPEC 90501 APPLIES

PROCESS SPEC

CONTR. NO.

ORIGINAL DATE OF DWG

DRAFTSMAN APPD

CHECKED APPD

APPD APPD

DESIGN ACTIVITY APPROVAL

PROCURING ACTIVITY APPROVAL

Westinghouse Electric Corporation
AEROSPACE AND ELECTRONIC SYSTEMS DIVISION
BALTIMORE, MARYLAND 21203

DETAILS
AZIMUTH GIMBAL ASSEMBLY
ADVANCED COMPOSITE STUDY

SIZE	FSCM NO.	DWG NO.
D	97942	687R259

SCALE / WEIGHT SHEET 1 OF 4

(90)S

THEN CURE FOR 1 HR. AT
51 PRESSURE APPLIED
20, CURE AT ROOM TEMP
(45°40%)

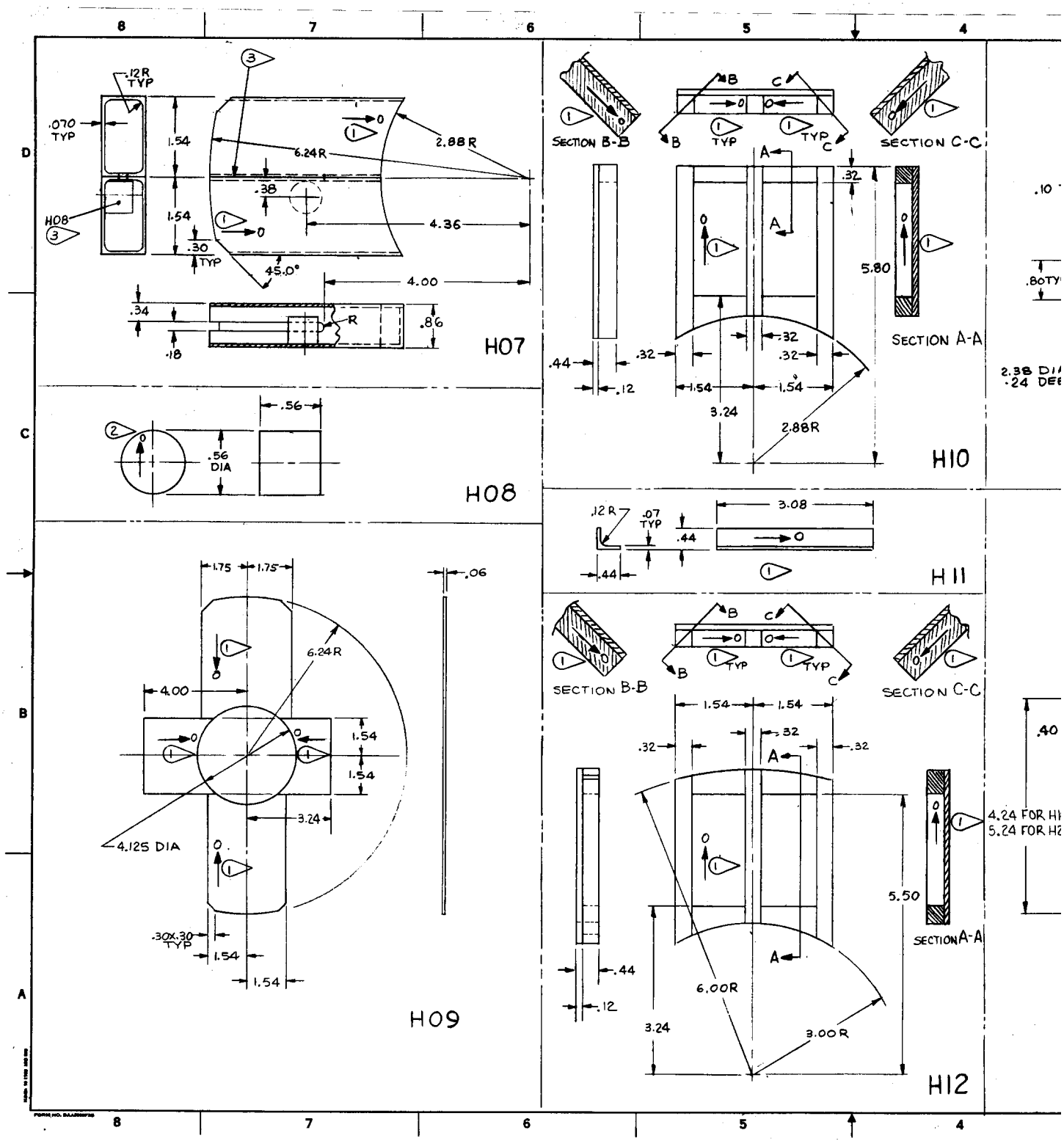
.12R TYP
.070 TYP
1.54
6.24R
2.88R
.38
1.54
4.36
H08
.30 TYP
45.0°
4.00
.34
.18
.86
R
H07
.56
.56 DIA
H08
SECTION B-B
SECTION C-C
TYP
.32
5.80
SECTION A-A
.44
.12
1.54
3.24
2.88R
H10
.12R
.07 TYP
3.08
.44
H11
1.75
.06
6.24R
4.00
1.54
3.24
4.125 DIA
.30X.30 TYP
H09
5.50
6.00R
3.00R
H12

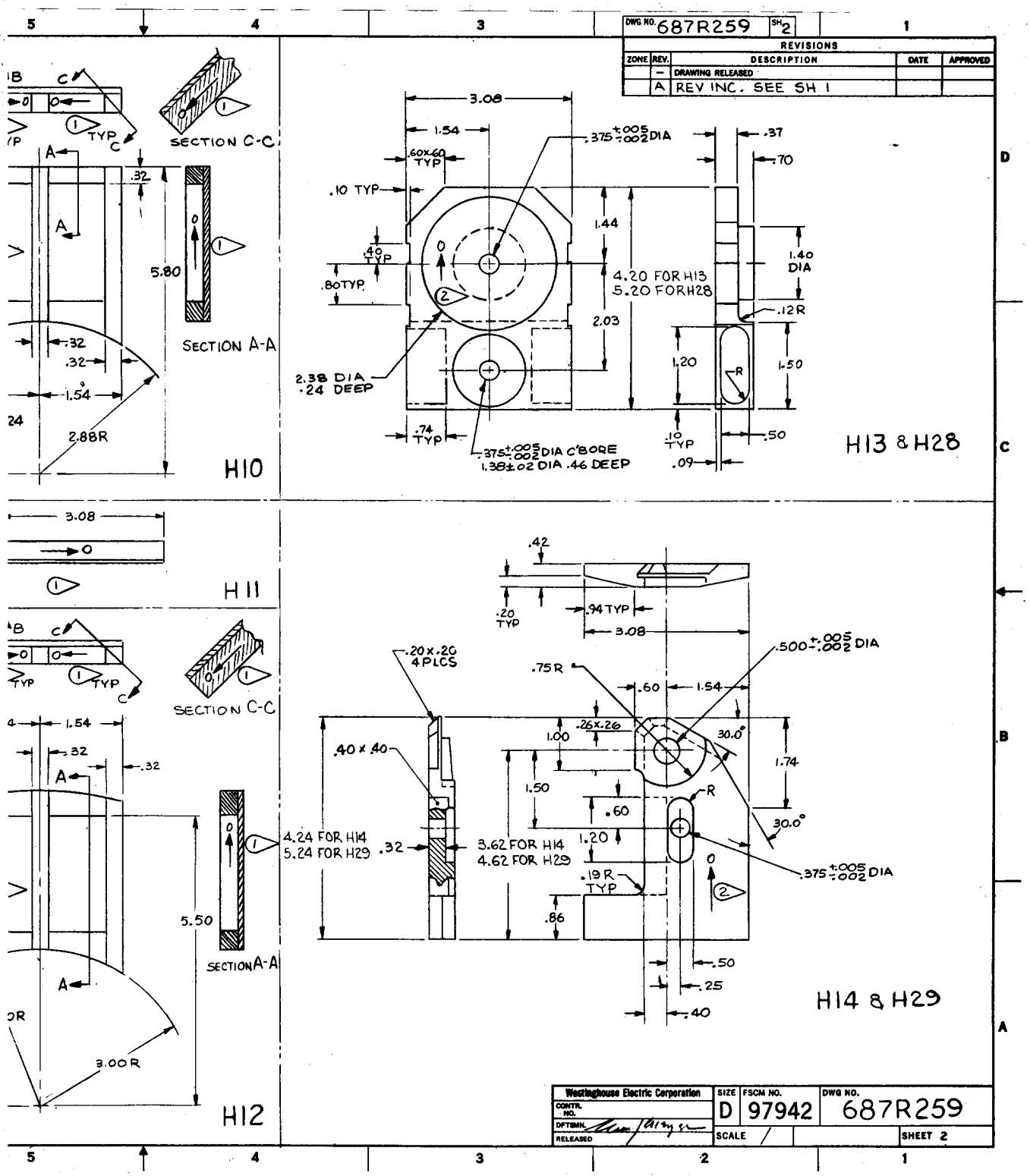
DWG NO. 687R259 SH 2
REVISIONS
ZONE REV. DESCRIPTION DATE APPROVED
– DRAWING RELEASED
A REV INC. SEE SH 1
SECTION C-C
SECTION A-A
H10
3.08
1.54
.60x.60 TYP
.10 TYP
.40 TYP
.80TYP
.375 +.005 -.002 DIA
.37
.70
1.44
4.20 FOR H13
5.20 FOR H28
2.03
1.40 DIA
.12R
2.38 DIA
.24 DEEP
1.20
R
1.50
.74 TYP
.375 +.005 -.002 DIA C'BORE
1.38±.02 DIA .46 DEEP
.10 TYP
.50
.09
H13 & H28
H11
.42
.20 TYP
.94 TYP
3.08
.20x.20 4PLCS
.75R
.60
1.54
.500 +.005 -.002 DIA
.26x.26
30.0°
1.00
.40 x .40
1.74
1.50
R
.60
30.0°
4.24 FOR H14
5.24 FOR H29
.32
3.62 FOR H14
4.62 FOR H29
1.20
.375 +.005 -.002 DIA
.19 R TYP
.86
.50
.25
.40
H14 & H29
1.54
.32
.32
5.50
3.00R
H12
Westinghouse Electric Corporation
CONTR. NO.
DFTSMN.
RELEASED
SIZE D
FSCM NO. 97942
DWG NO. 687R259
SCALE
SHEET 2

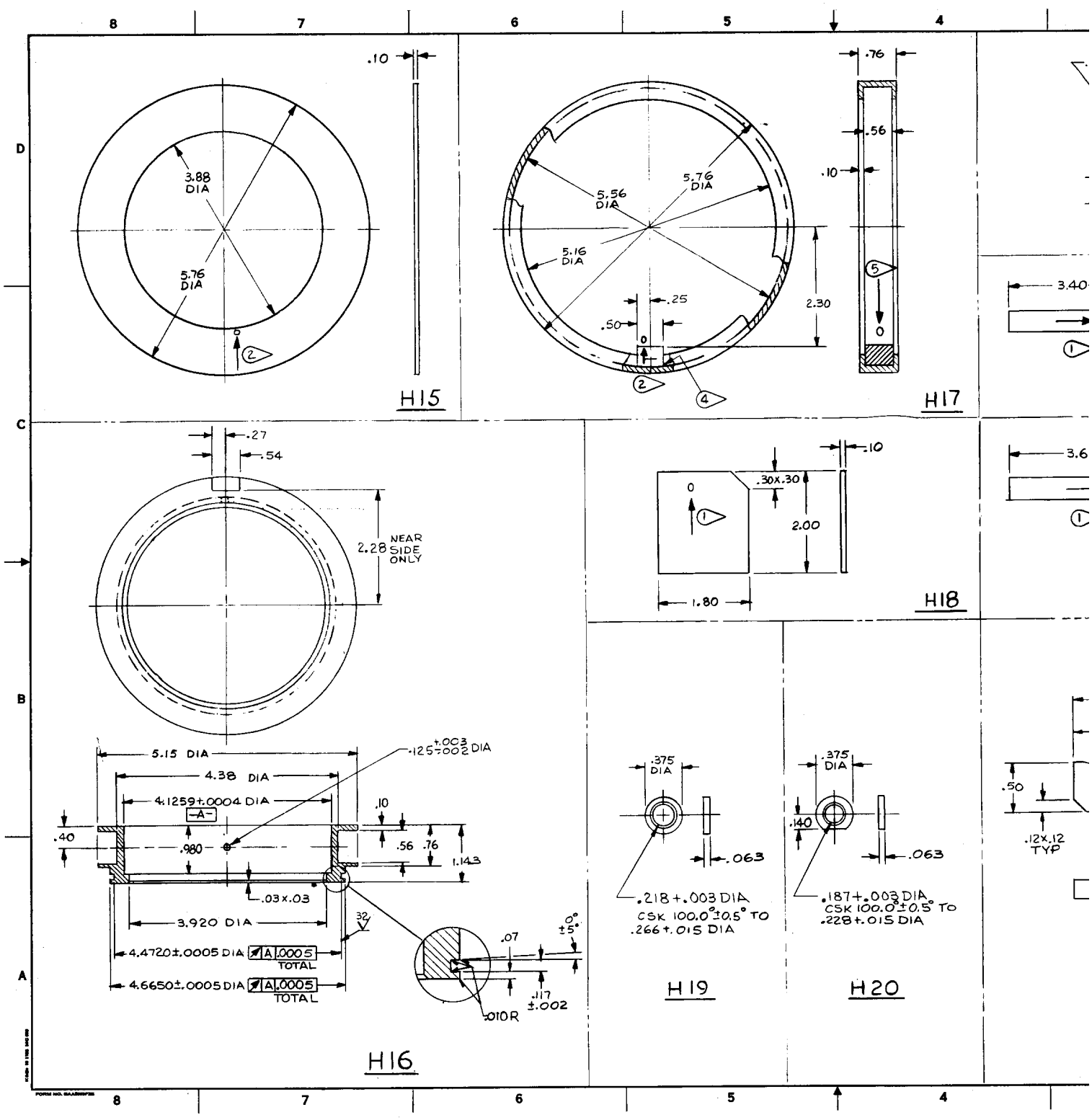
8
7
6
5
4
D
C
B
A
.10
3.88 DIA
5.76 DIA
H15
.76
.56
.10
5.56 DIA
5.76 DIA
5.16 DIA
.25
.50
2.30
H17
3.40
.27
.54
2.28 NEAR SIDE ONLY
.10
.30x.30
2.00
1.80
H18
3.6
5.15 DIA
.125 +.003 -.002 DIA
4.38 DIA
4.1259±.0004 DIA
-A-
.10
.40
.980
.56
.76
1.143
.03x.03
3.920 DIA
32
4.4720±.0005 DIA
A .0005 TOTAL
4.6650±.0005 DIA
A .0005 TOTAL
.07
0° ±5°
.117 ±.002
.010R
H16
.375 DIA
.063
.218 +.003 DIA
CSK 100.0° ±0.5° TO
.266 +.015 DIA
H19
.375 DIA
.140
.063
.187 +.003 DIA
CSK 100.0° ±0.5° TO
.228 +.015 DIA
H20
.50
.12x.12 TYP

DWG NO. 687R259 SH 3

REVISIONS				
ZONE	REV.	DESCRIPTION	DATE	APPROVED
	–	DRAWING RELEASED		
	A	REV INC. SEE SH 1.		

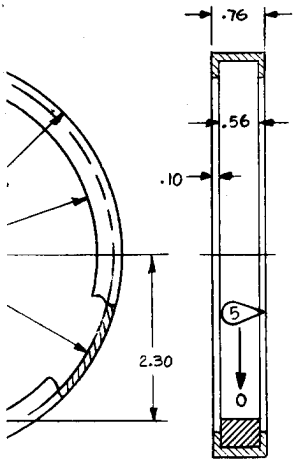

H17

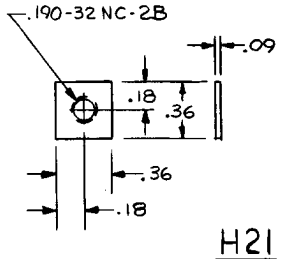

H21

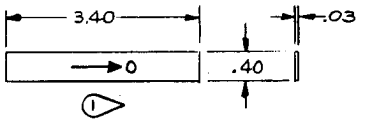

H22

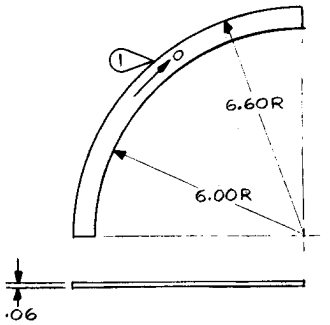

H25

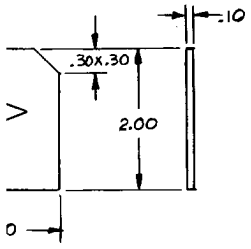

H18

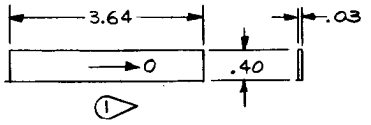

H23

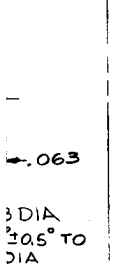

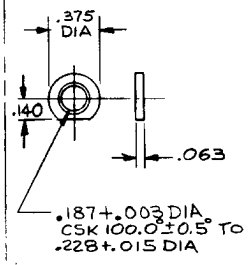

H20

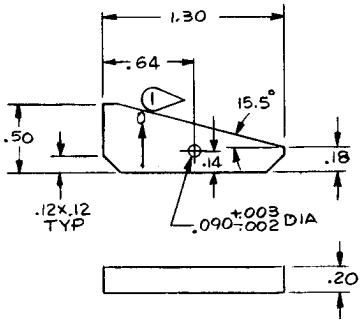

H24

Westinghouse Electric Corporation	SIZE	FSCM NO.	DWG NO.
CONTR. NO.	D	97942	687R259
DFTSMN. RELEASED	SCALE		SHEET 3

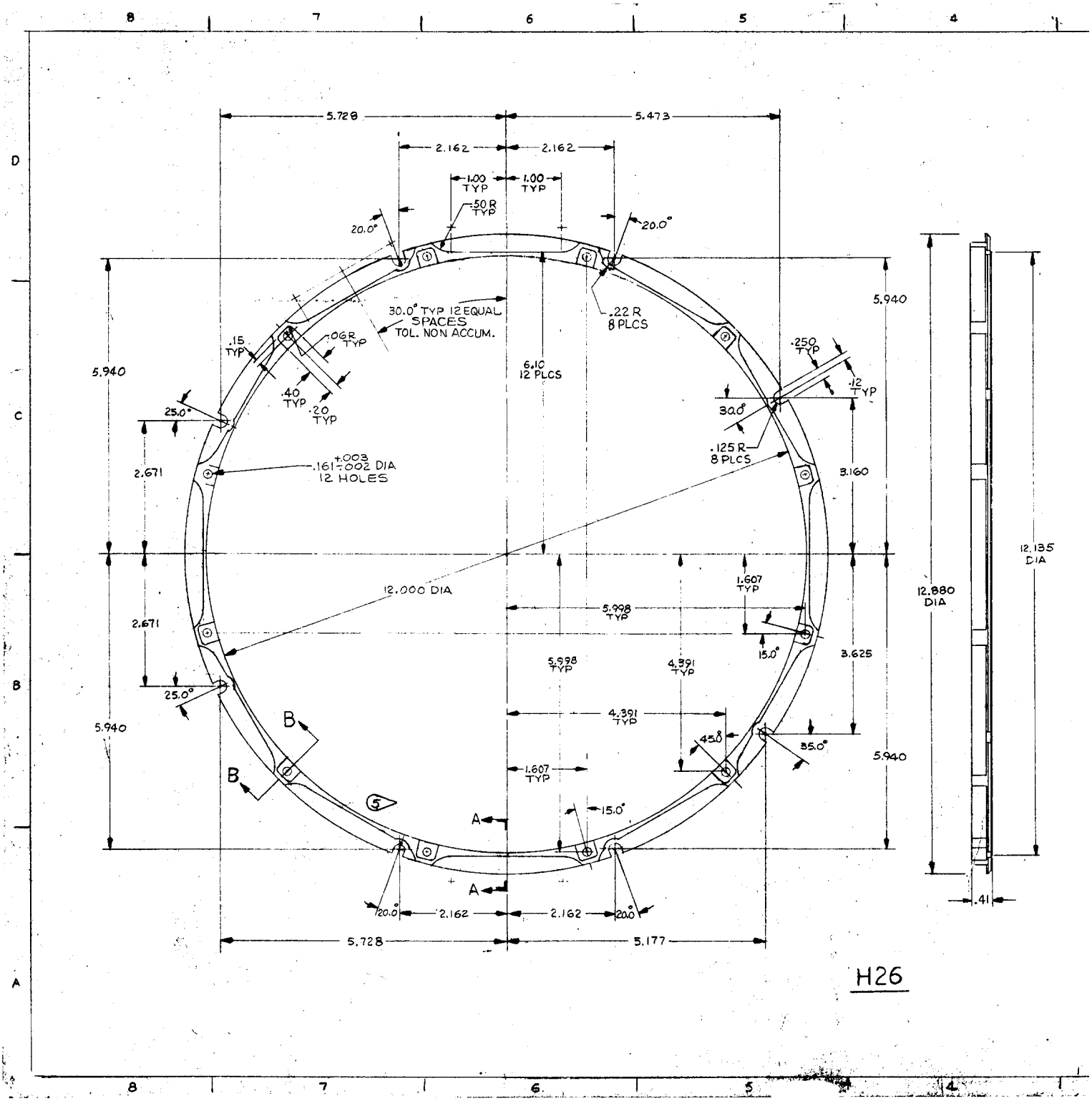
5.728
5.473
2.162
2.162
1.00 TYP
1.00 TYP
.50R TYP
20.0°
20.0°
30.0° TYP 12 EQUAL SPACES TOL. NON ACCUM.
.22 R 8 PLCS
5.940
.15 TYP
.06R TYP
.40 TYP
.20 TYP
6.10 12 PLCS
.250 TYP
.12 TYP
30.0°
.125R 8 PLCS
25.0°
2.671
.161 +.003 -.002 DIA 12 HOLES
3.160
12.000 DIA
1.607 TYP
5.998 TYP
15.0°
2.671
3.625
25.0°
5.998 TYP
4.391 TYP
4.391 TYP
45.0°
35.0°
5.940
1.607 TYP
15.0°
B
B
A
A
20.0°
2.162
2.162
20.0°
5.728
5.177
12.880 DIA
12.135 DIA
.41
H26

DWG NO 687R259 SH 4

REVISIONS

ZONE	REV.	DESCRIPTION	DATE	APPROVED
		DRAWING RELEASED		

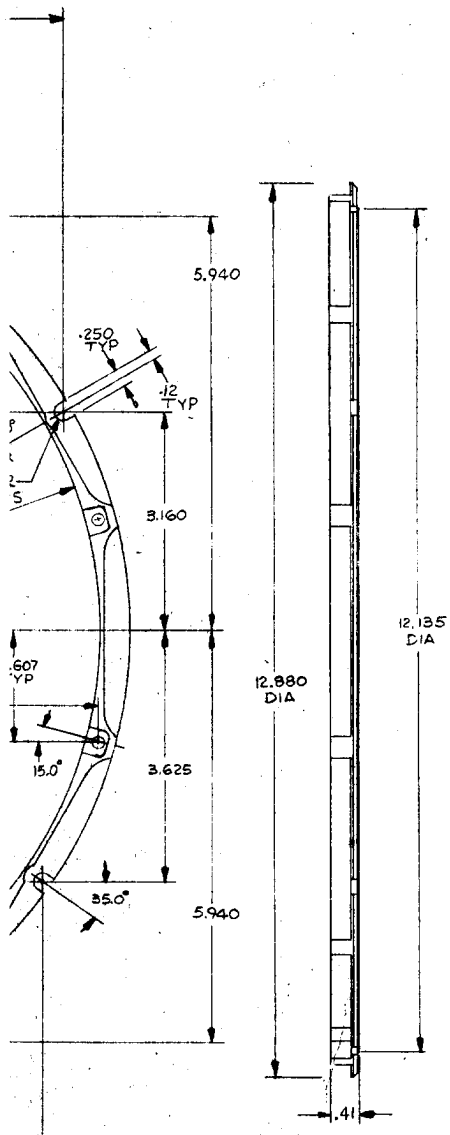

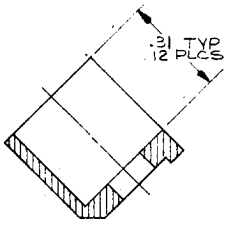

SECTION B-B
TYP 12 PLACES
SCALE 4/1

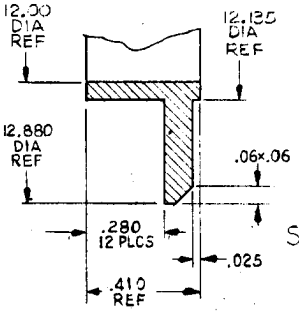

SECTION A-A
TYP 12 PLACES
SCALE 4/1

H26

Westinghouse Electric Corporation	SIZE D	FSCM NO. 97942	DWG NO. 687R259
CONTR NO.			
DFTSMN	SCALE		SHEET 4
RELEASED			

PARENTHETIC IDENTITIES ARE FOR WESTINGHOUSE REFERENCE ONLY

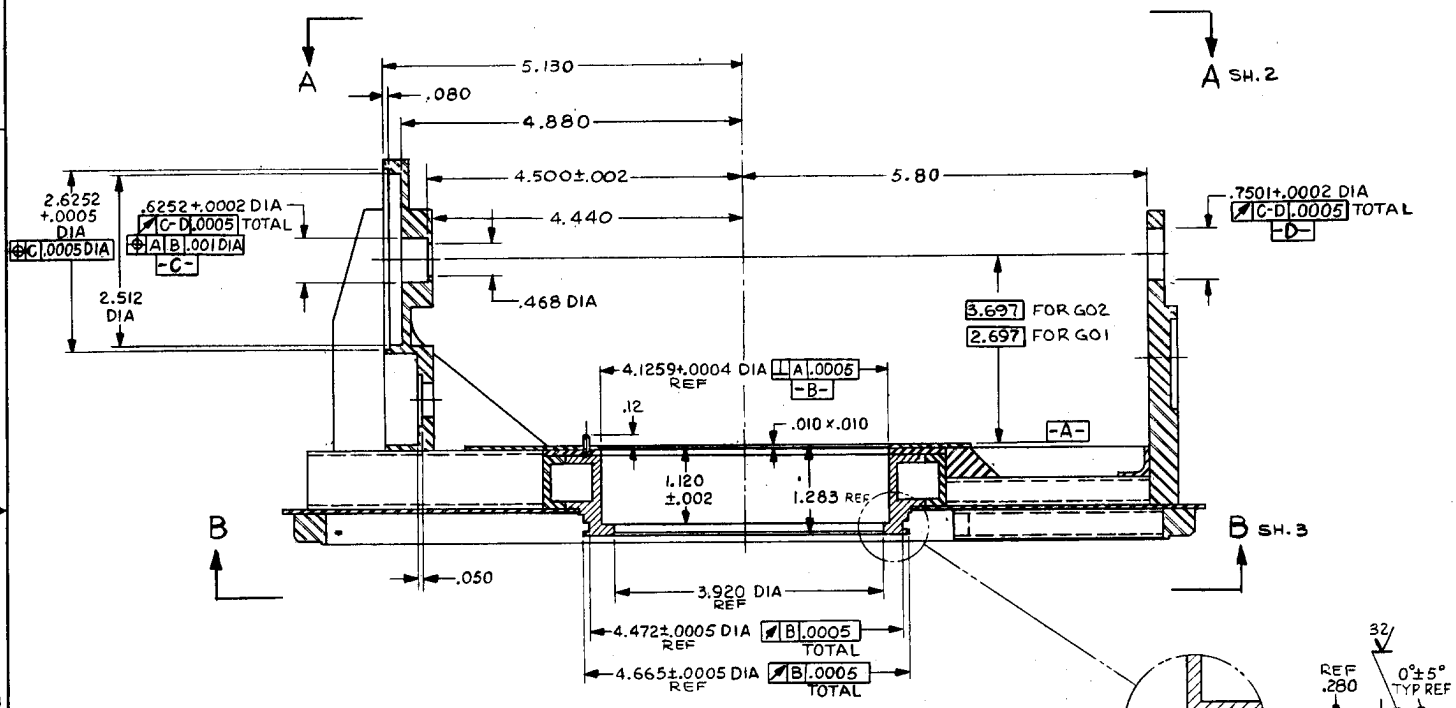

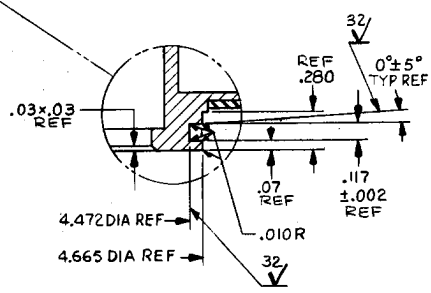

1. ASSEMBLE PER PS 87111 PF
2. BOND WITH FM73 THEN CURE FOR 1 HOUR AT 250°F WITH 40 PSI PRESSURE APPLIED
3. BOND WITH EA9320, CURE AT ROOM TEMP
4. CLEAN BEFORE BONDING PER DOD/NAS STRUCT. COMPOSITES FAB. GUIDE SECTION B-4-2

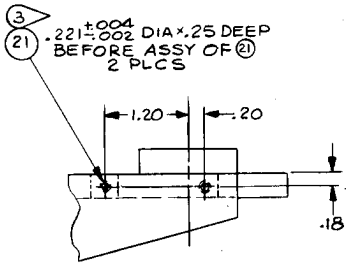

VIEW J-J
TYP 2 PLCS
SCALE 1/1

	COMPOSITES
NEXT ASSY	USED ON
APPLICATION	

DWG NO. 687R260 SH 1

SHEET REVISION STATUS					
5	4	3	2	1	SHEET NO.
	A	A	A	A	REV.

REVISIONS				
ZONE	REV.	DESCRIPTION	DATE	APPROVED
	–	DRAWING RELEASED		
	A	DR DATED 11MAR 81 REV PER ENG INSTR W.A./M.S.	13 MAR 81	

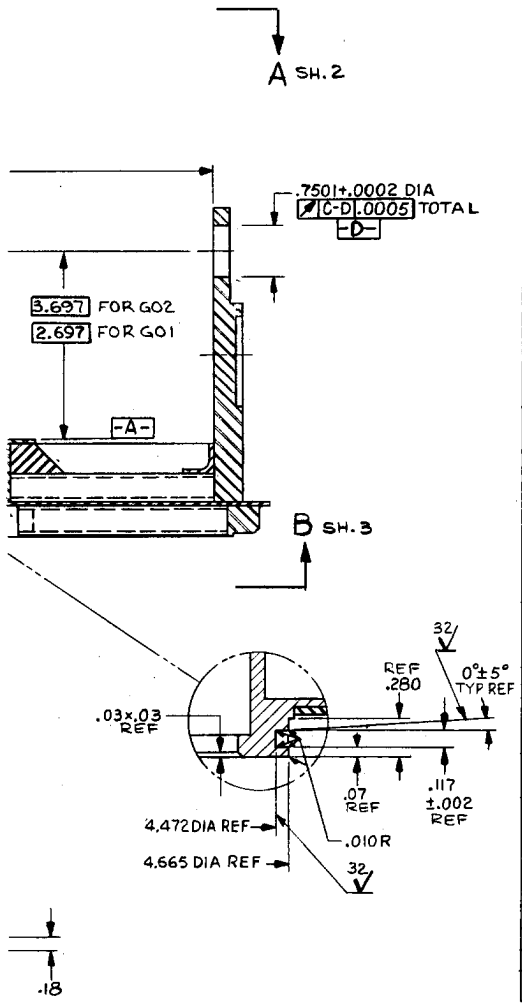

12	12	29372	H111F1C-63-070M		RIVNUT			
8	8	29372	H111F2C-63-070M		RIVNUT			
1	–		687R260H29		DETAIL			31
1	–		687R260H28		DETAIL			30
2	–		687R260H27		DETAIL			29
20	20		NAS620C02		WASHER-FLAT			28
8	8	29372	H111P1C63-230		RIVNUT .138-32			27
1	1		MS16555-618		PIN, DOWEL			26
1	1		687R259H25		DETAIL			25
10	10	29372	H111P1C63-150		RIVNUT .138-32			24
4	4		687R259H23		DETAIL			23
4	4		687R259H22		DETAIL			22
4	4		687R259H21		DETAIL			21
12	12		687R259H20		DETAIL			20
8	8		687R259H19		DETAIL			19
1	1		687R259H18		DETAIL			18
1	1		687R259H17		DETAIL			17
1	1		687R259H16		DETAIL			16
1	1		687R259H15		DETAIL			15
–	1		687R259H14		DETAIL			14
–	1		687R259H13		DETAIL			13
1	1		687R259H12		DETAIL			12
1	1		687R259H11		DETAIL			11
1	1		687R259H10		DETAIL			10
1	1		687R259H09		DETAIL			9
10	10	29372	H111P0C63-110		RIVNUT .112-40			8
1	1		687R259H07		DETAIL			7
–	2		687R259H06		DETAIL			6
1	1		687R259H05		DETAIL			5
2	2		687R259H04		DETAIL			4
1	1		687R259H03		DETAIL			3
1	1		687R259H02		DETAIL			2
1	1		687R259H01		DETAIL			1
G02	G01	FSCM NUMBER	PART NO.	SYM	DESCRIPTION	GOVT SPEC	Ⓦ SPEC	FIND NO.

QTY REQD SYM: B=BULK MATERIAL V=VENDOR ITEM SEE CONTROL DWG — PARTS LIST SEE PL

	COMPOSITES
NEXT ASSY	USED ON
APPLICATION	

UNLESS OTHERWISE SPECIFIED DIMENSIONS ARE IN INCHES DO NOT SCALE. TOLERANCES ON DIM.

2 PLACE	3 PLACE	ANGLES
±.01	±.005	±0.5°

Ⓦ SPEC 9QS01 APPLIES

PROCESS SPEC

CONTR. NO.

ORIGINAL DATE OF DWG

DRAFTSMAN W.J.M. APPD TF

CHECKED APPD

APPD APPD

DESIGN ACTIVITY APPROVAL

PROCURING ACTIVITY APPROVAL

Westinghouse Electric Corporation
AEROSPACE AND ELECTRONIC SYSTEMS DIVISION
BALTIMORE, MARYLAND 21203

AZIMUTH GIMBAL
ADVANCED COMPOSITE STUDY

SIZE	FSCM NO.	DWG NO.
D	97942	687R260

SCALE 1/1 WEIGHT SHEET 1 OF 4

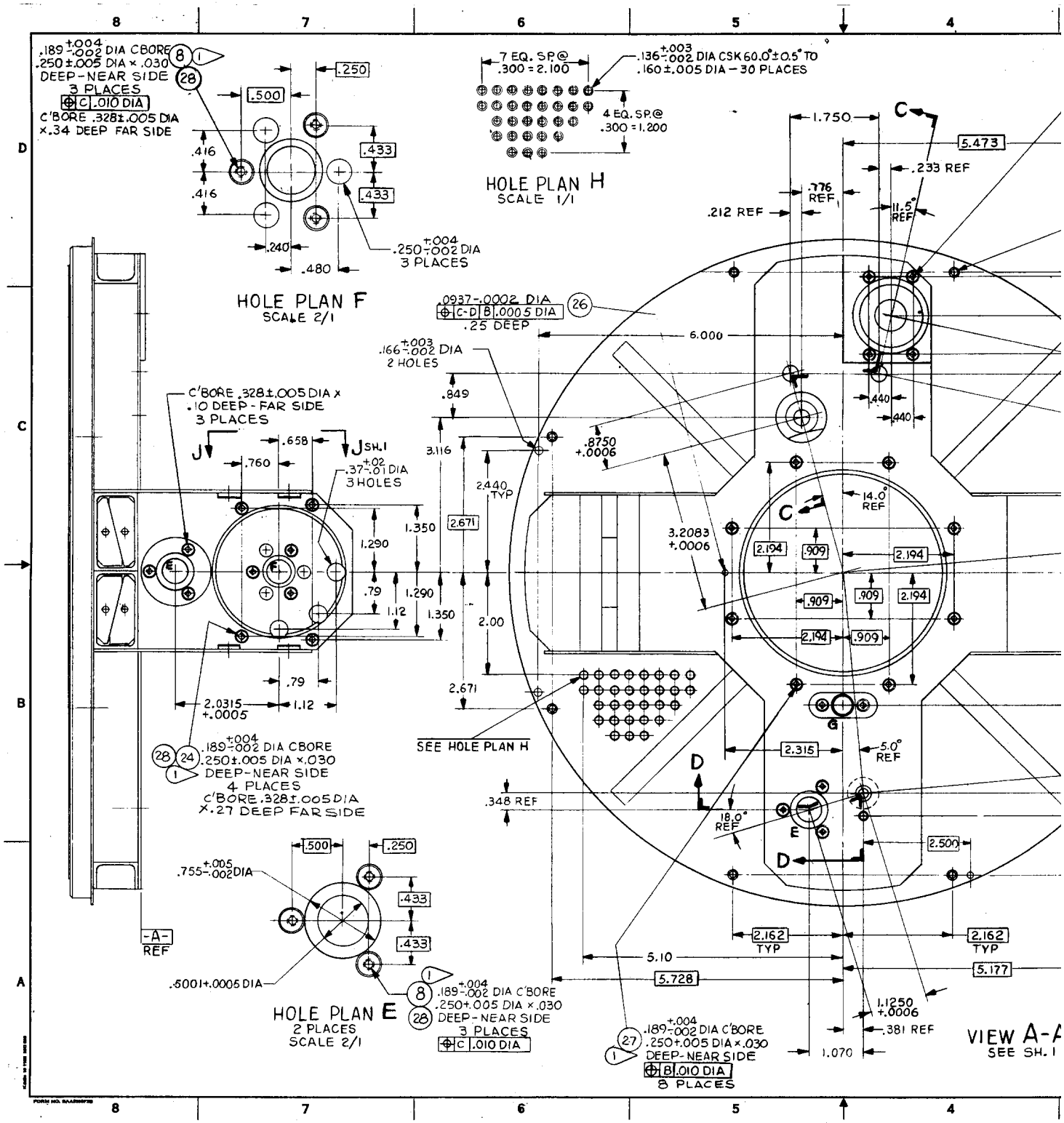
.189 +.004 -.002 DIA CBORE
.250 ±.005 DIA × .030
DEEP - NEAR SIDE
3 PLACES
C .010 DIA
C'BORE .328±.005 DIA
×.34 DEEP FAR SIDE
.500
.250
.416
.433
.240
.480
.250 +.004 -.002 DIA
3 PLACES
HOLE PLAN F
SCALE 2/1
7 EQ. SP. @
.300 = 2.100
.136 +.003 -.002 DIA CSK 60.0° ±0.5° TO
.160 ±.005 DIA - 30 PLACES
4 EQ. SP. @
.300 = 1.200
HOLE PLAN H
SCALE 1/1
1.750
5.473
.233 REF
.776 REF
11.5° REF
.212 REF
.0937 -.0002 DIA
C-D B .0005 DIA
.25 DEEP
6.000
.166 +.003 -.002 DIA
2 HOLES
.849
.440
.440
C'BORE .328±.005 DIA ×
.10 DEEP - FAR SIDE
3 PLACES
.658
.760
J
J SH.1
.37 +.02 -.01 DIA
3 HOLES
3.116
.8750 +.0006
2.440 TYP
2.671
1.350
1.290
.79
1.290
1.12
1.350
2.00
2.671
.79
1.12
2.0315 +.0005
SEE HOLE PLAN H
14.0° REF
3.2083 +.0006
2.194
.909
2.194
.909
.909
2.194
2.194
.909
2.315
5.0° REF
.348 REF
18.0° REF
2.500
.189 +.004 -.002 DIA CBORE
.250±.005 DIA ×.030
DEEP - NEAR SIDE
4 PLACES
C'BORE .328±.005 DIA
×.27 DEEP FAR SIDE
.500
.250
.755 +.005 -.002 DIA
.433
.433
-A-
REF
.5001+.0005 DIA
HOLE PLAN E
2 PLACES
SCALE 2/1
.189 +.004 -.002 DIA C'BORE
.250+.005 DIA ×.030
DEEP - NEAR SIDE
3 PLACES
C .010 DIA
2.162 TYP
2.162 TYP
5.10
5.728
5.177
1.1250 +.0006
.381 REF
1.070
.189 +.004 -.002 DIA C'BORE
.250+.005 DIA ×.030
DEEP - NEAR SIDE
B .010 DIA
8 PLACES
VIEW A-A
SEE SH. 1

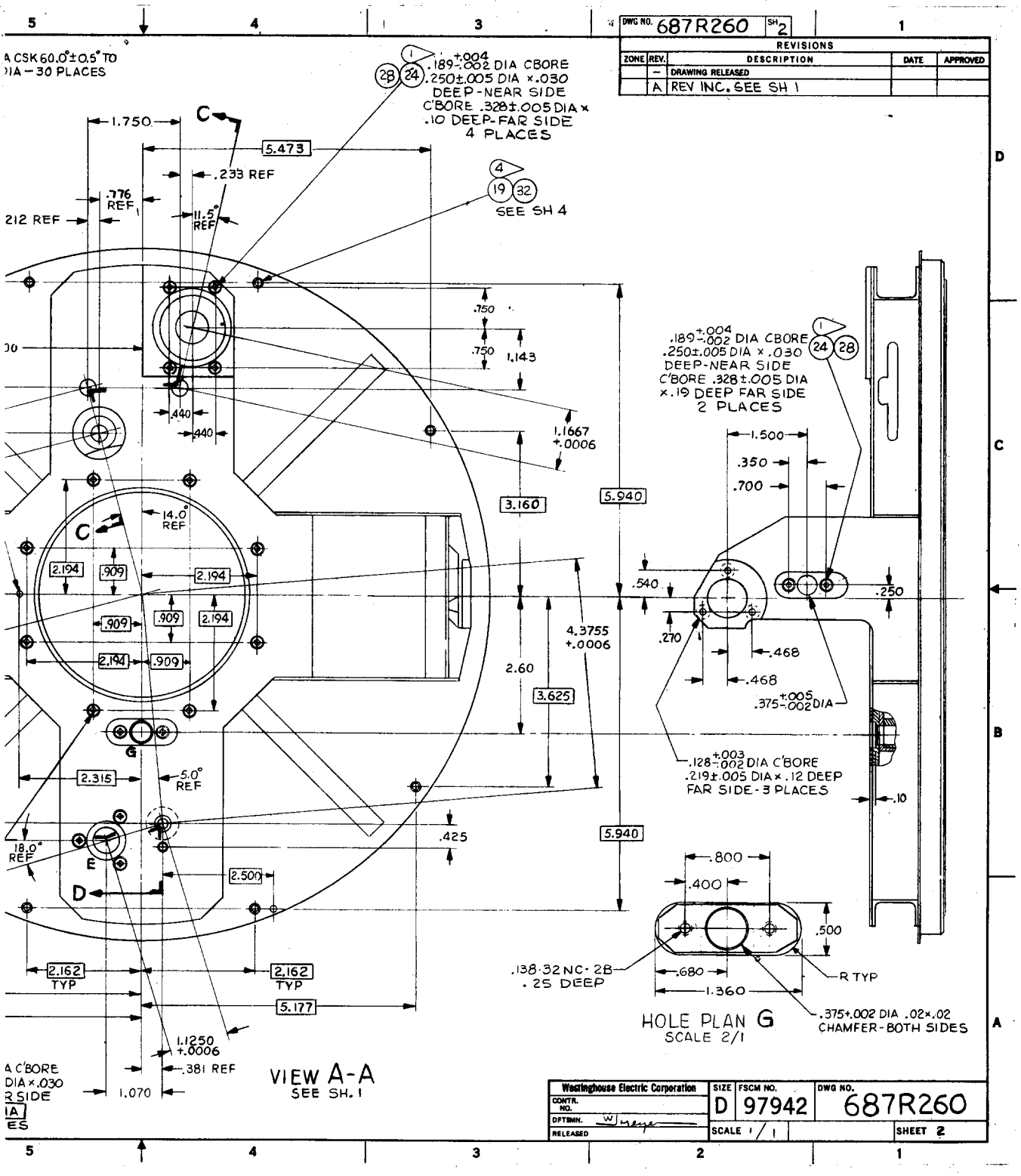
DWG NO. 687R260 SH 2
REVISIONS
ZONE REV. DESCRIPTION DATE APPROVED
– DRAWING RELEASED
A REV INC. SEE SH 1
A CSK 60.0°±0.5° TO DIA – 30 PLACES
.189 +.004 -.002 DIA CBORE .250±.005 DIA x .030 DEEP-NEAR SIDE C'BORE .328±.005 DIA x .10 DEEP-FAR SIDE 4 PLACES
SEE SH 4
1.750
5.473
.233 REF
.776 REF
11.5° REF
212 REF
.750
.750
1.143
.440
.440
1.1667 +.0006
3.160
5.940
14.0° REF
2.194
.909
2.194
.909
.909
2.194
2.194
.909
2.315
5.0° REF
18.0° REF
2.500
.425
5.940
2.60
3.625
4.3755 +.0006
2.162 TYP
2.162 TYP
5.177
1.1250 +.0006
.381 REF
1.070
VIEW A-A
SEE SH. 1
.189 +.004 -.002 DIA CBORE .250±.005 DIA x .030 DEEP-NEAR SIDE C'BORE .328±.005 DIA x .19 DEEP FAR SIDE 2 PLACES
1.500
.350
.700
.540
.250
.270
.468
.468
.375 +.005 -.002 DIA
.128 +.003 -.002 DIA C'BORE .219±.005 DIA x .12 DEEP FAR SIDE - 3 PLACES
.10
.800
.400
.500
.138-32 NC-2B .25 DEEP
.680
1.360
R TYP
.375+.002 DIA .02x.02 CHAMFER-BOTH SIDES
HOLE PLAN G
SCALE 2/1
Westinghouse Electric Corporation
CONTR. NO.
DFTSMN.
RELEASED
SIZE D
FSCM NO. 97942
DWG NO. 687R260
SCALE 1/1
SHEET 2

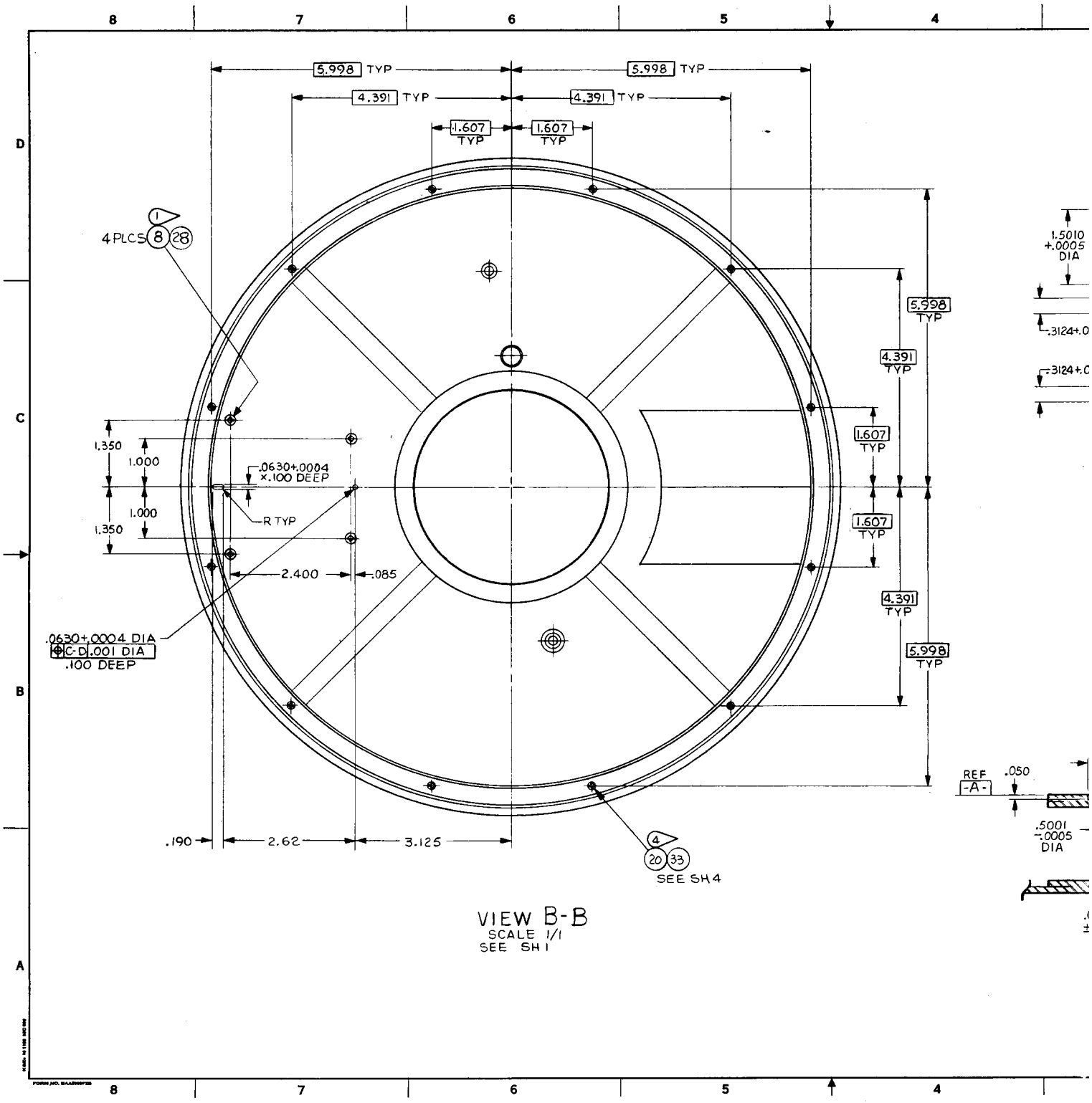

VIEW B-B
SCALE 1/1
SEE SH 1

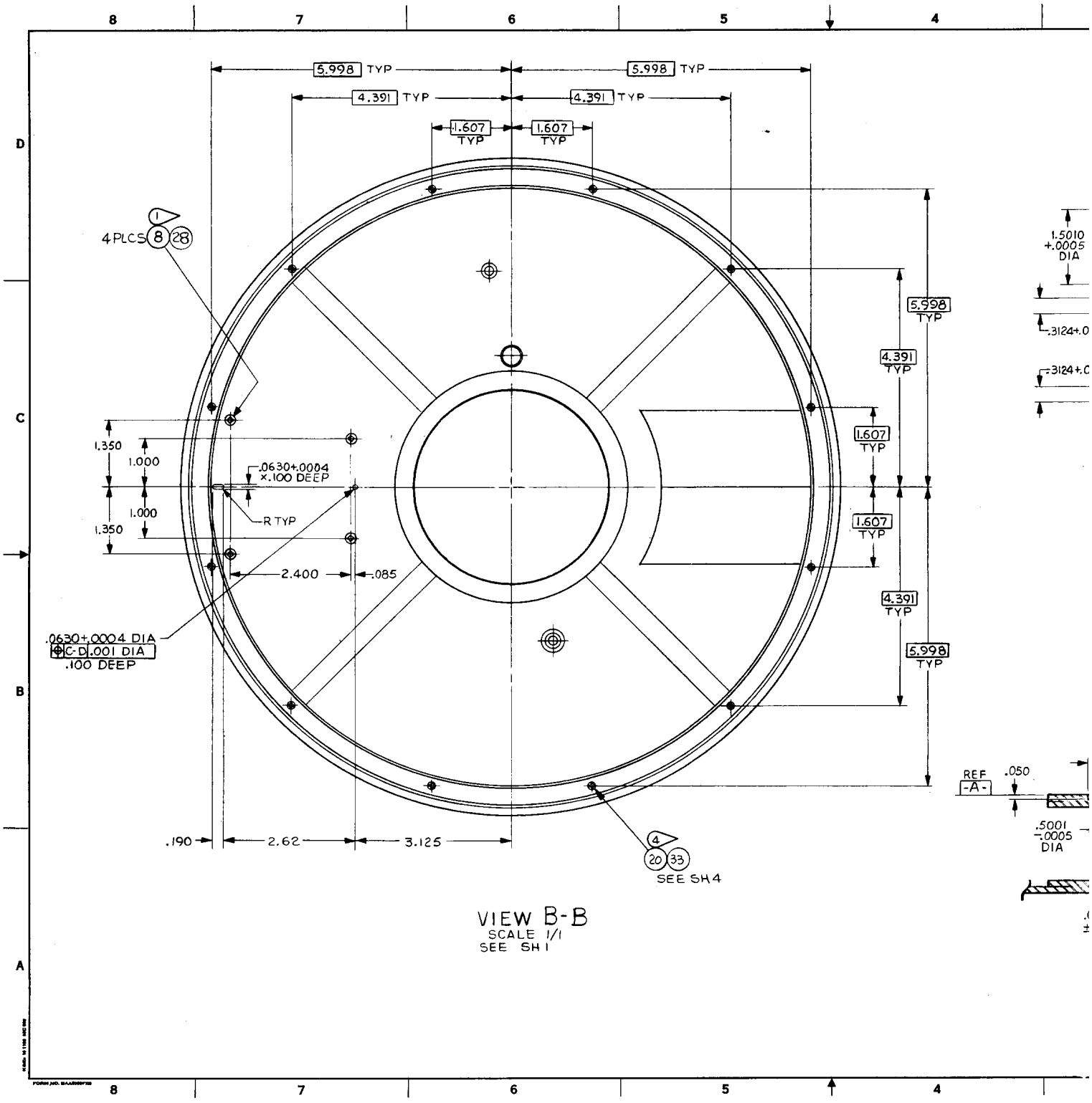

VIEW B-B
SCALE 1/1
SEE SH 1

DWG NO. 687R260 SH 3

REVISIONS				
ZONE	REV.	DESCRIPTION	DATE	APPROVED
	–	DRAWING RELEASED		
	A	REV INC. SEE SH 1.		

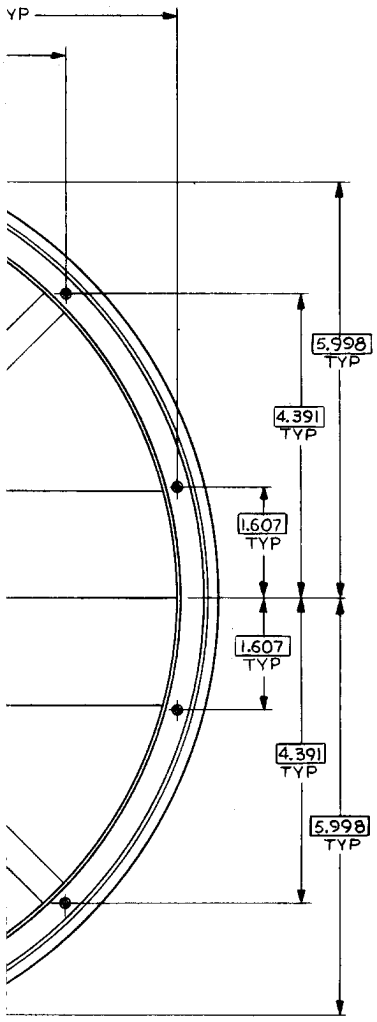

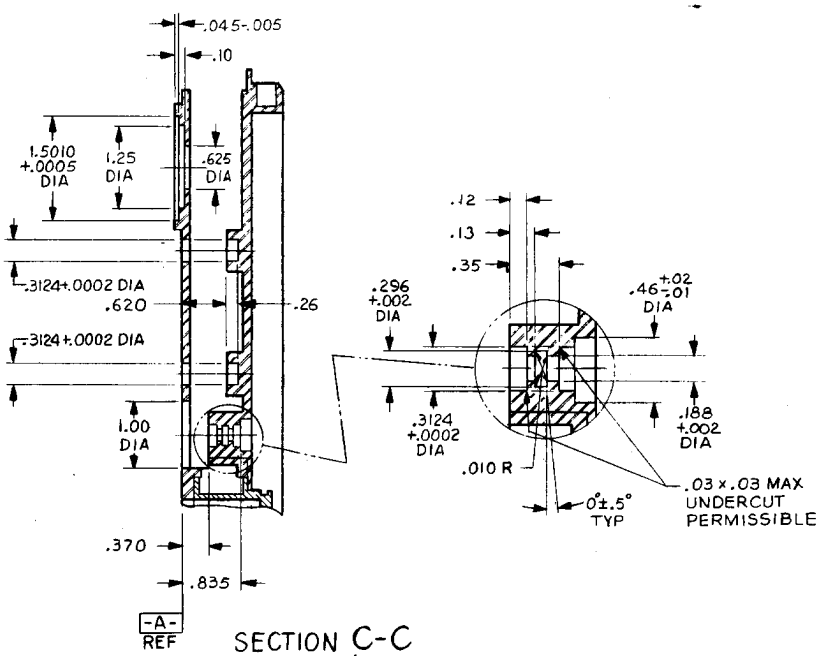

SECTION C-C
SCALE 1/1
SEE SH 2

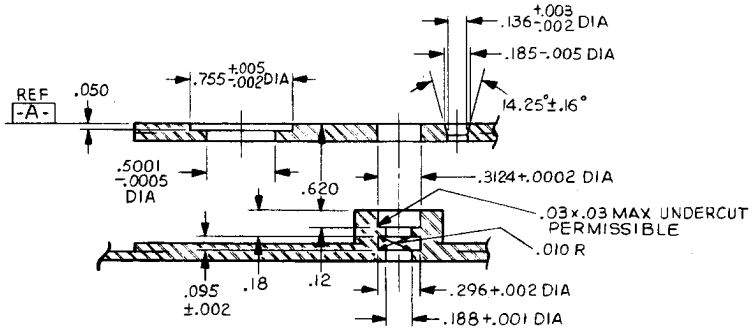

SECTION D-D
SCALE 2/1
SEE SH 2

Westinghouse Electric Corporation	SIZE	FSCM NO.	DWG NO.
CONTR. NO.	D	97942	687R260
DFTSMN. W J Meyer	SCALE 1/1		SHEET 3
RELEASED			

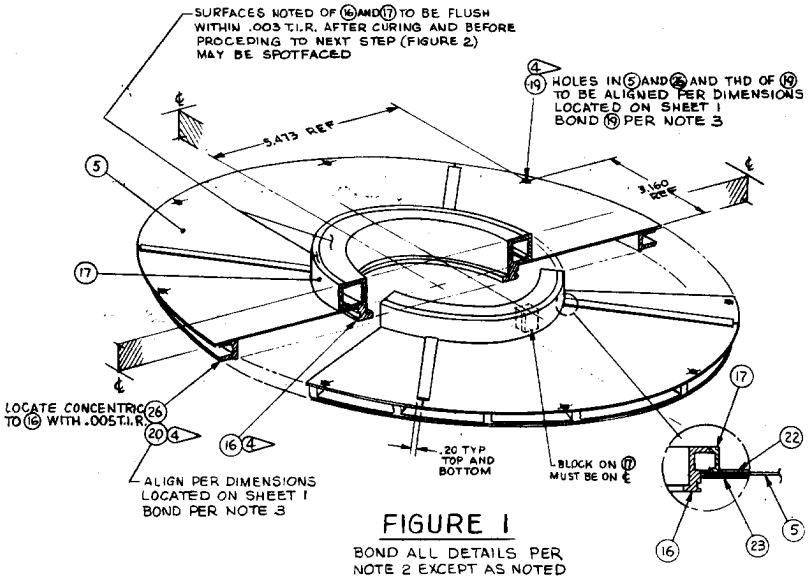

FIGURE 1

BOND ALL DETAILS PER NOTE 2 EXCEPT AS NOTED

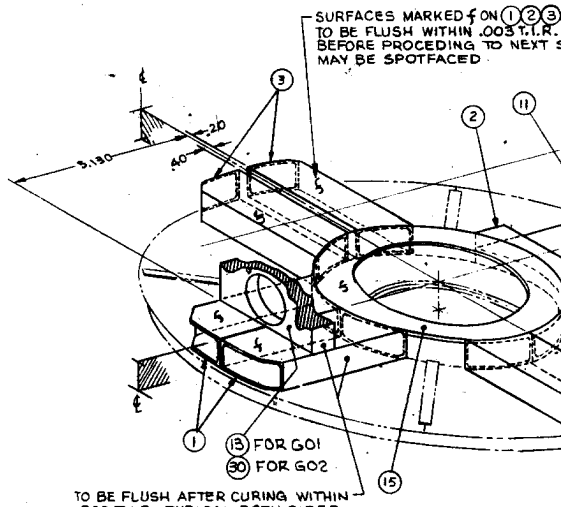

FIGURE 2

BOND ALL DETAILS PER NO

STEP ASSEMBLY PROCEDURE

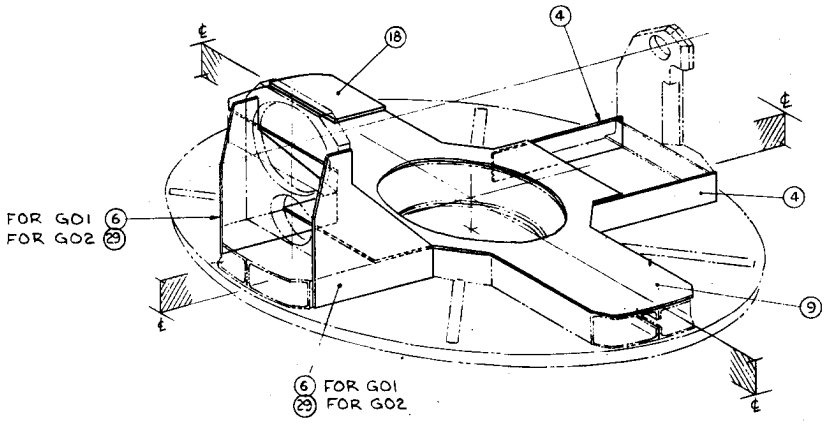

FIGURE 3

BOND ALL DETAILS PER NOTE 2

DWG NO. 687R260 SH 4

REVISIONS

ZONE	REV.	DESCRIPTION	DATE	APPROVED
	–	DRAWING RELEASED		
	A	REV INC. SEE SH 1		

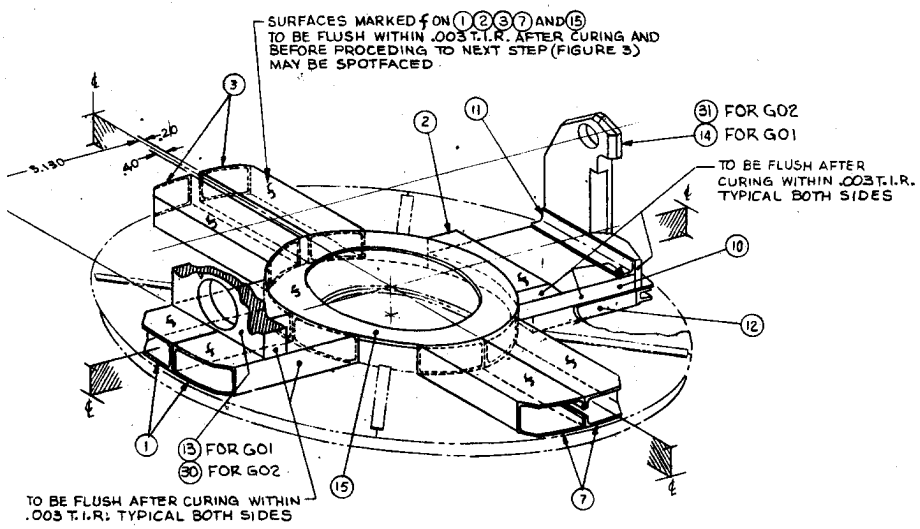

FIGURE 2

BOND ALL DETAILS PER NOTE 2

LY PROCEDURE

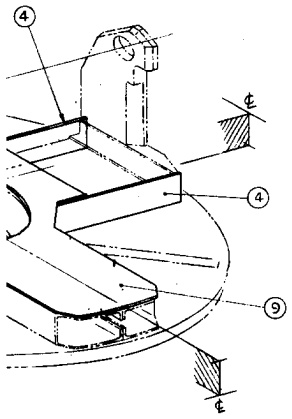

3

5 PER NOTE 2

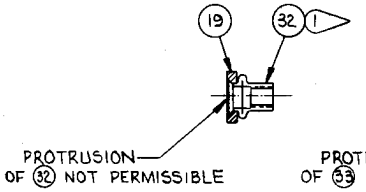

VIEW SHOWING ASSEMBLY OF (19) & (32) PRIOR TO BONDING PER (4)

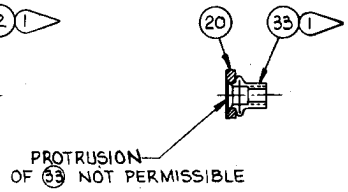

VIEW SHOWING ASSEMBLY OF (20) & (33) PRIOR TO BONDING PER (4)

Westinghouse Electric Corporation	SIZE	FSCM NO.	DWG NO.
CONTR. NO.	D	97942	687R260
OPTIMIN.	SCALE		SHEET 4
RELEASED			

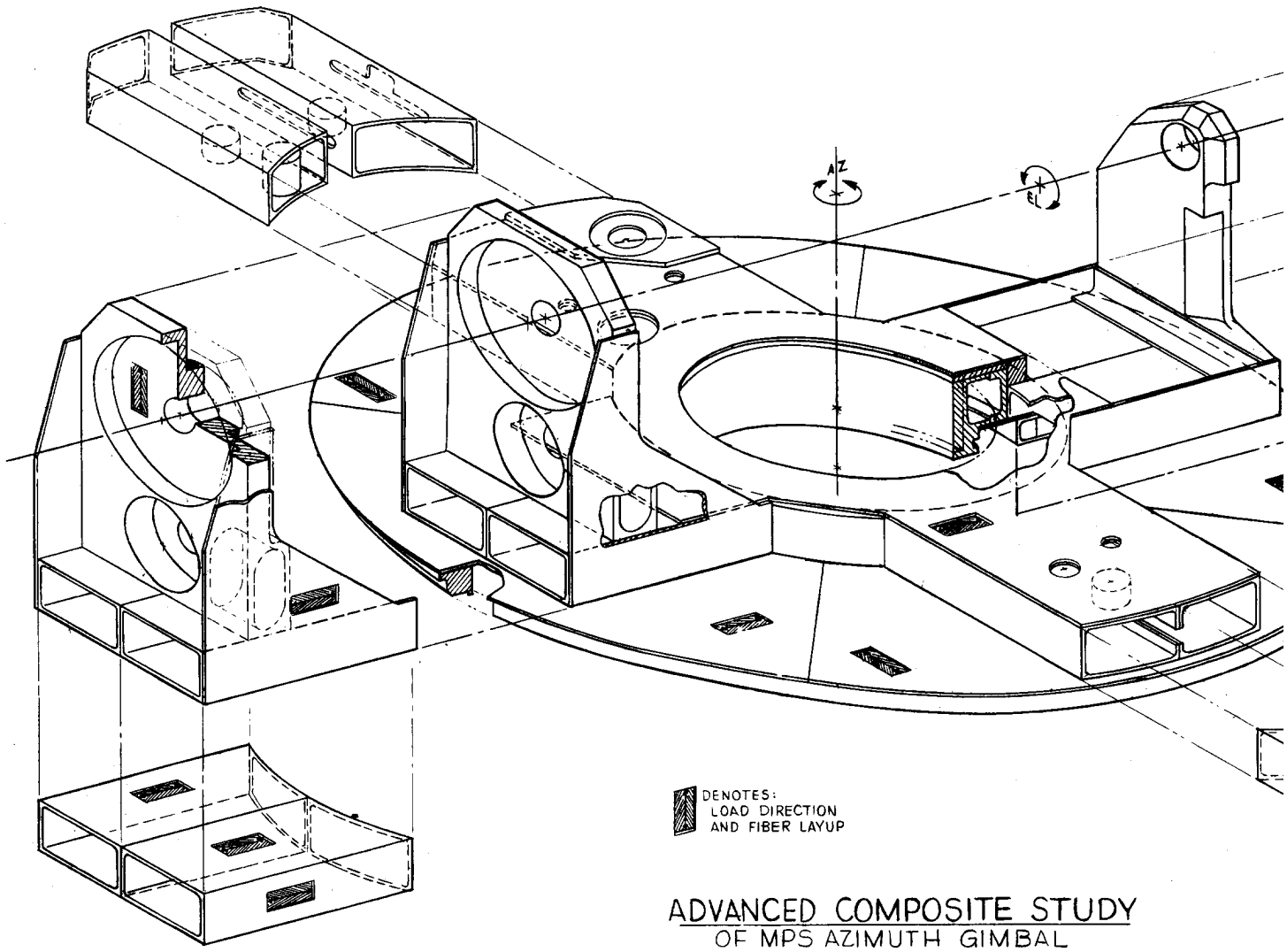

DENOTES:
LOAD DIRECTION
AND FIBER LAYUP

ADVANCED COMPOSITE STUDY
OF MPS AZIMUTH GIMBAL

DWG NO. 687R261 SH 1

REVISIONS

ZONE	REV.	DESCRIPTION	DATE	APPROVED
	–	DRAWING RELEASED		

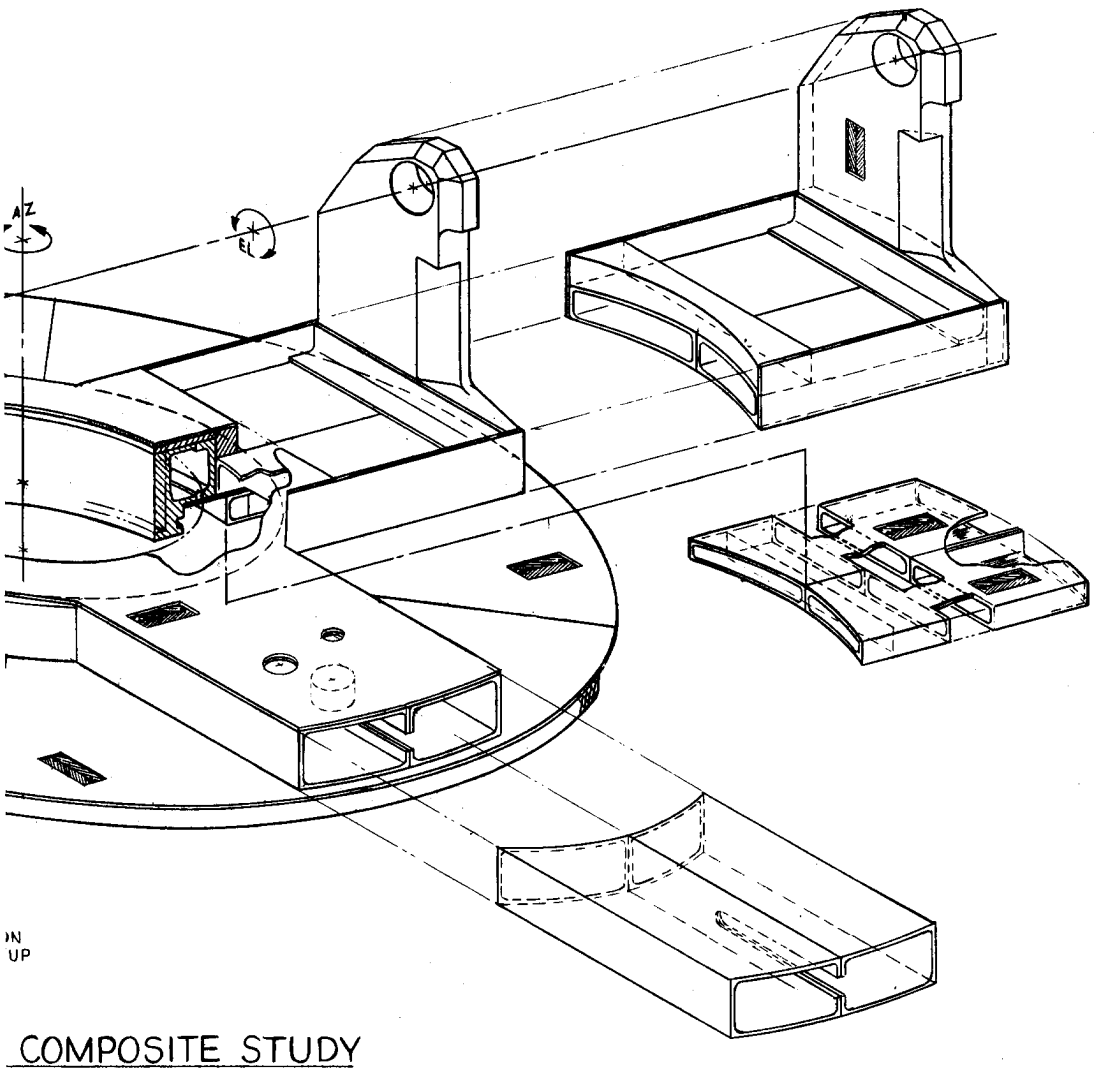

COMPOSITE STUDY
AZIMUTH GIMBAL

Westinghouse Electric Corporation	SIZE	FSCM NO.	DWG NO.
CONTR. NO. ——	D	97942	687R261
DFTSMN: RELEASED 10-1-80	SCALE 1/1		SHEET 1 OF 1

APPENDIX B

TOOLING DRAWING

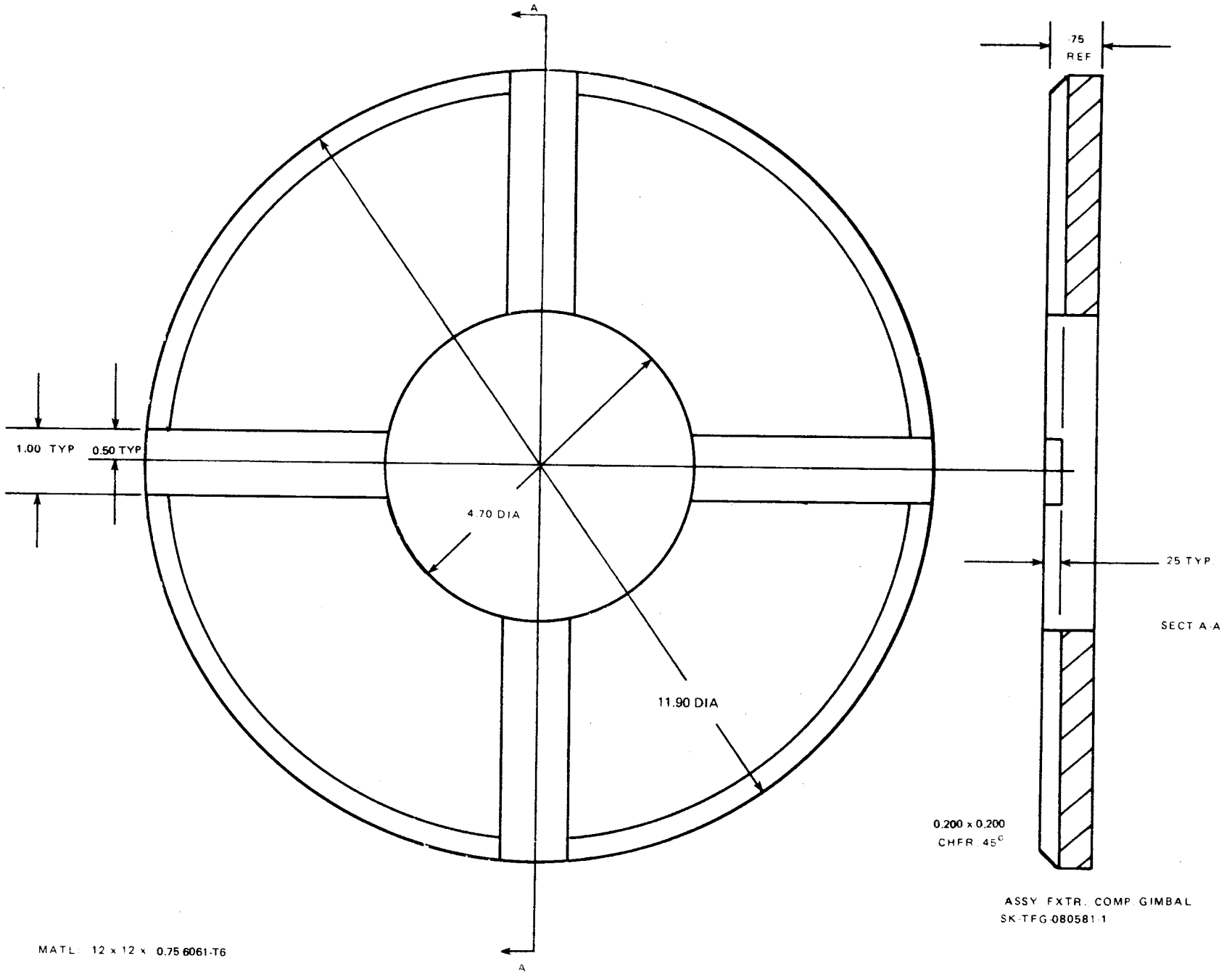

MATL 12 x 12 x 0.75 6061-T6

ASSY FXTR, COMP GIMBAL
SK-TFG-080581-1

82-0344-V-7

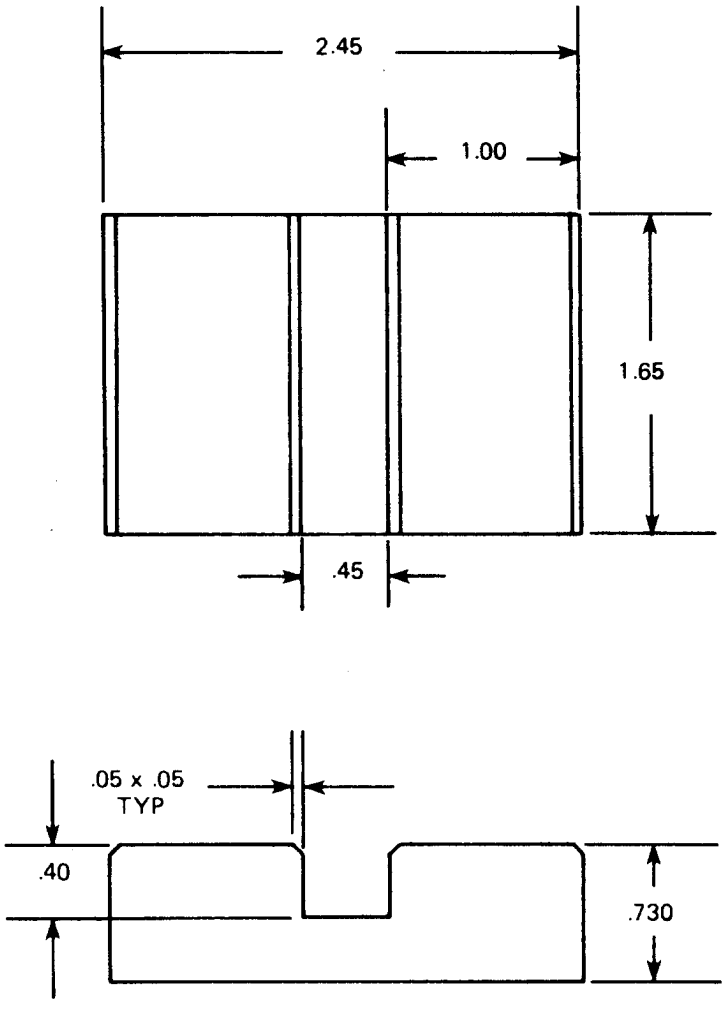

82-0344-V-7

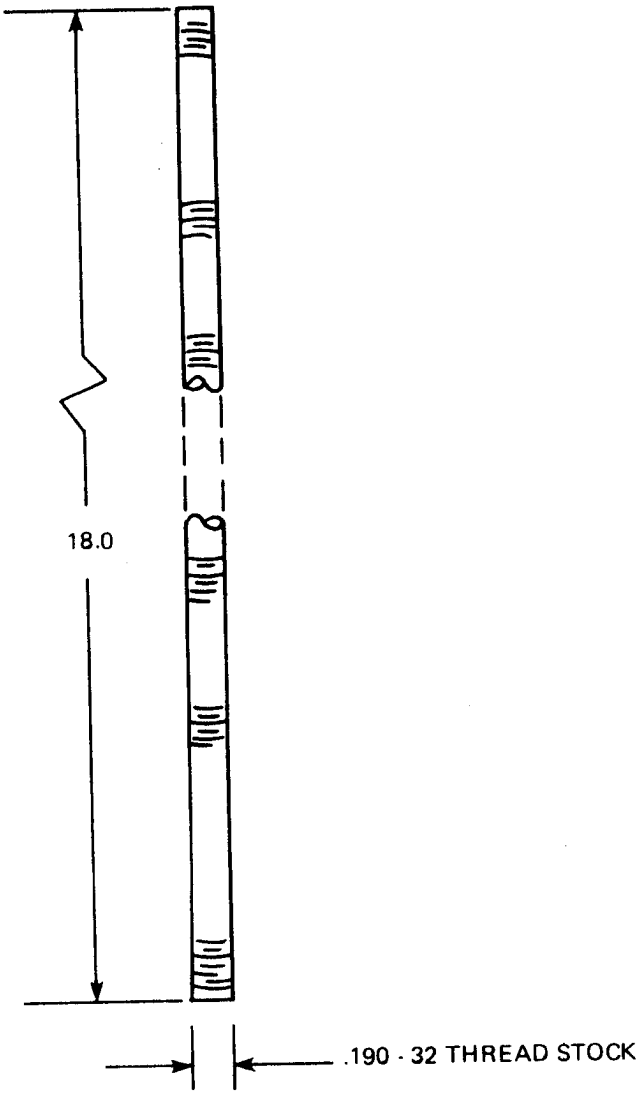

6 NUTS, WASHERS (LARGE)

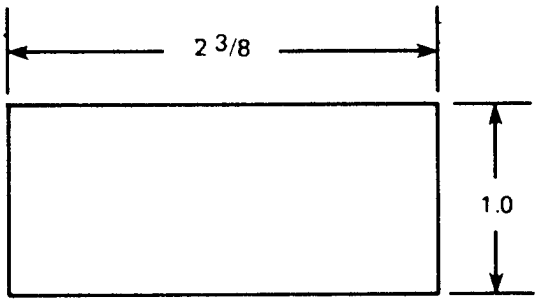

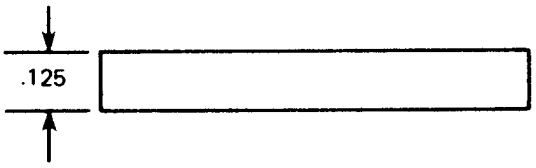

12 PCS

6061 - T6 .125 THICK
SAWCUT

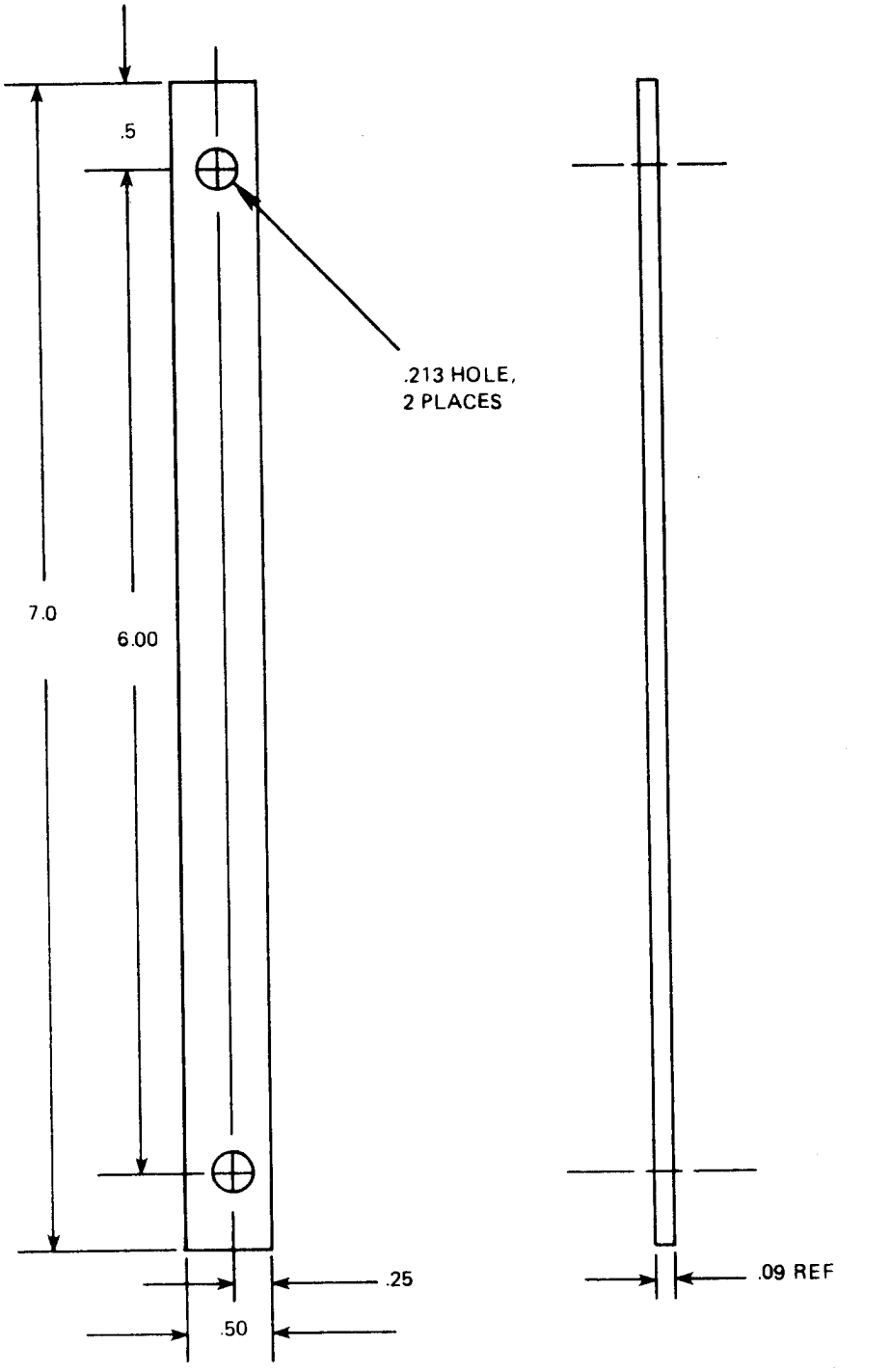

82-0344-V-6

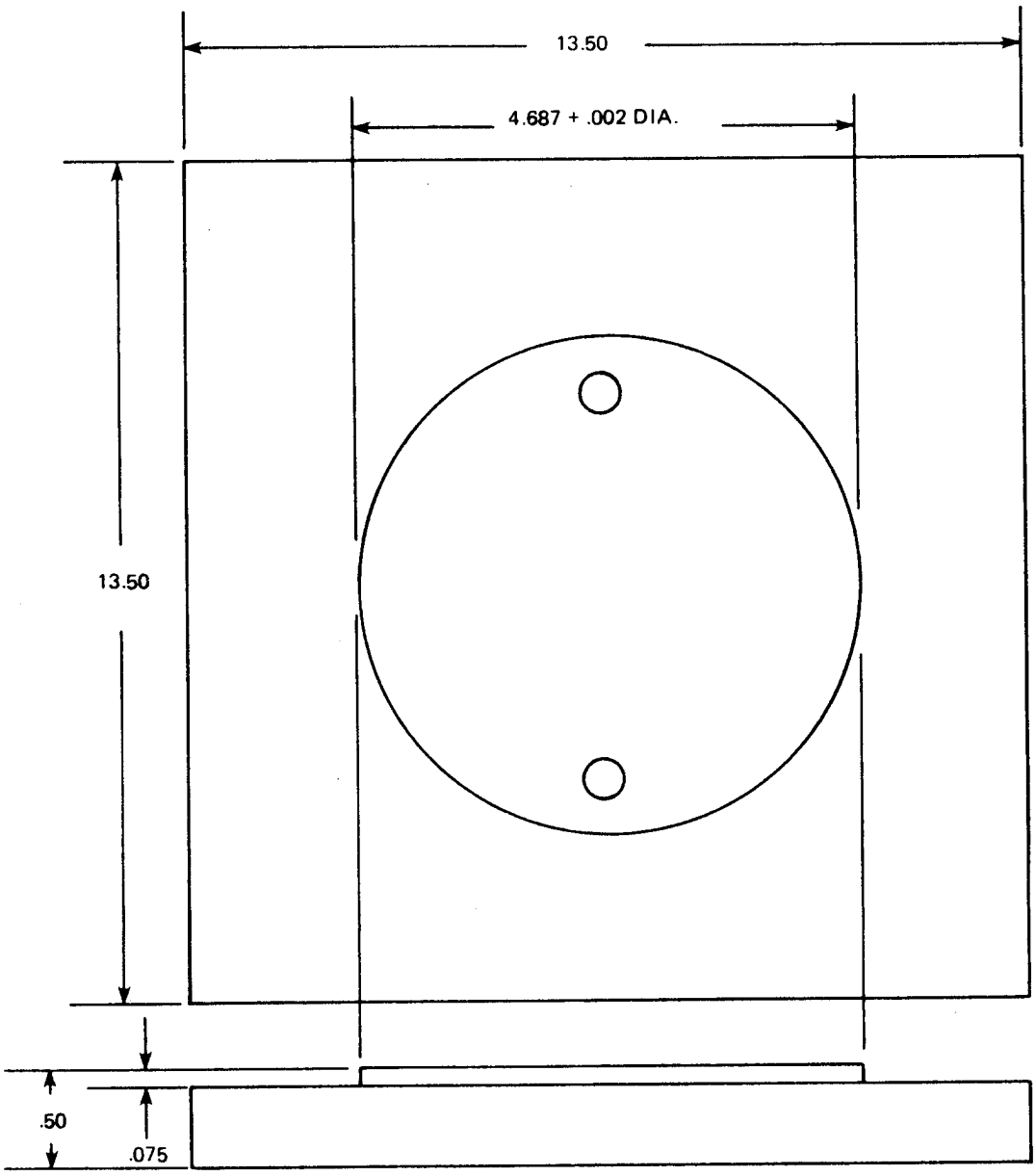

82-0344-V-9

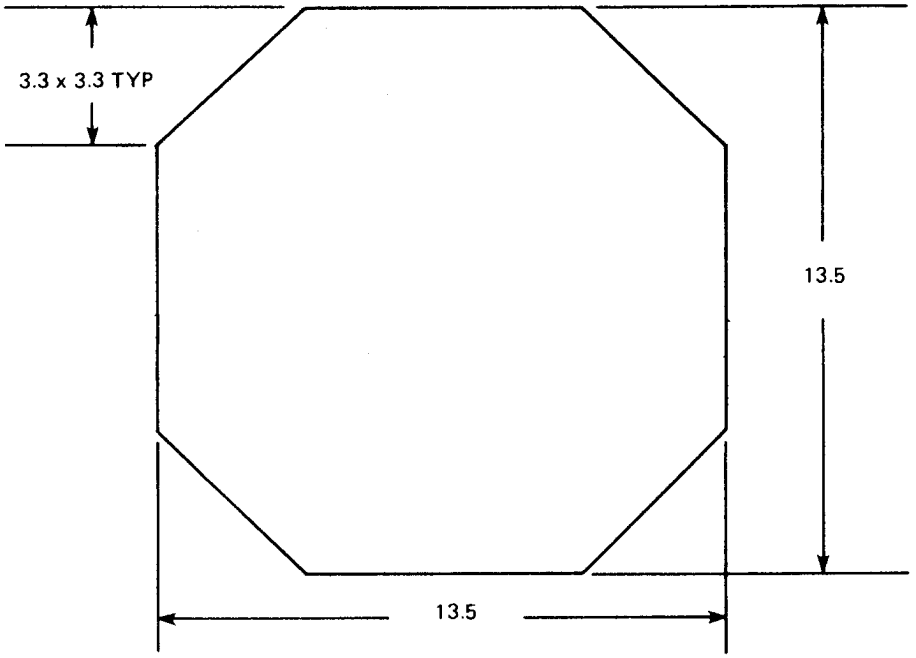

.25 THICK 6061-T6 1 PC

SAWCUT

82-0344-V-12

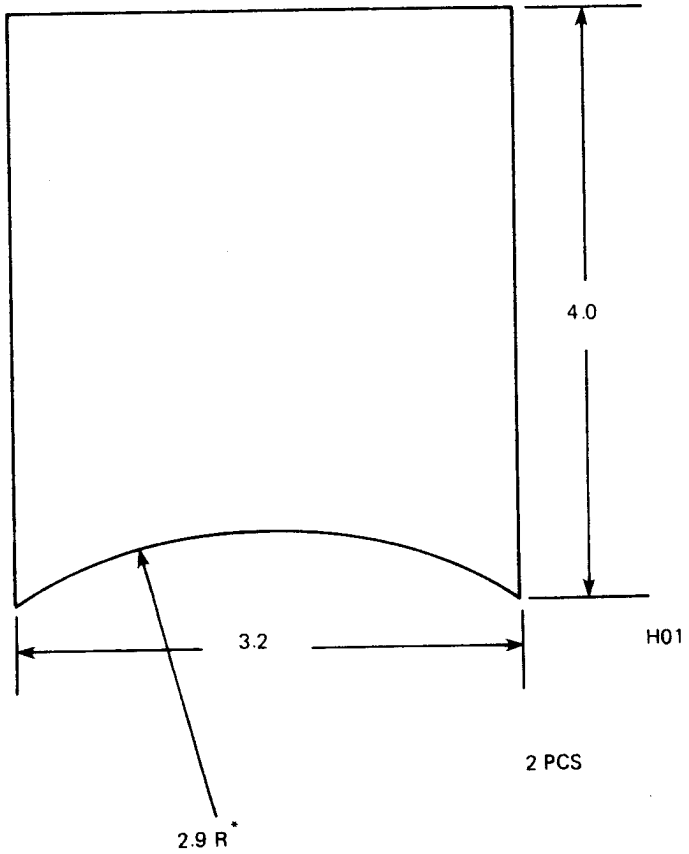

H01

2 PCS

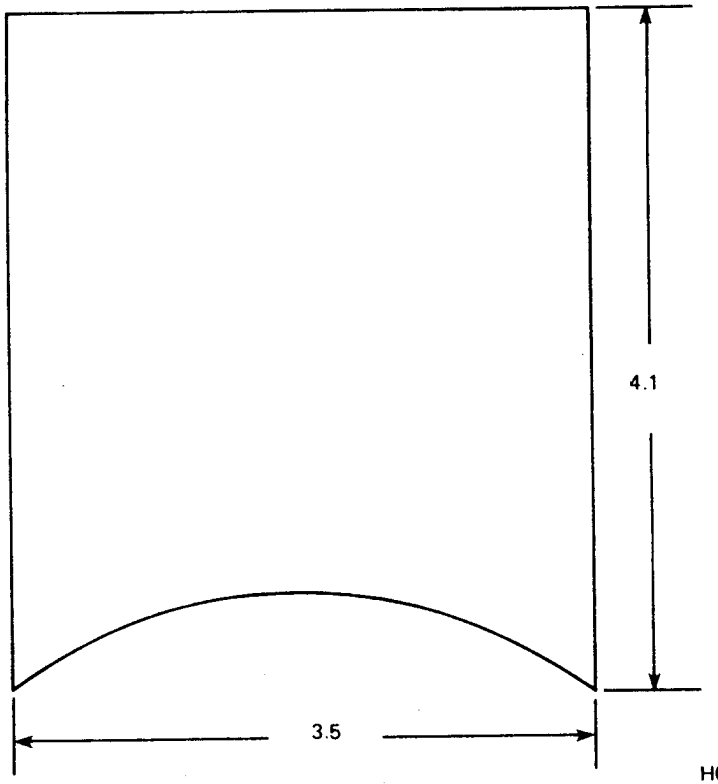

H02

1 PC

* RADIUS TO BE TRACED FROM EXISTING PART

ALL EDGES TO BE SAWCUT H01 & H02

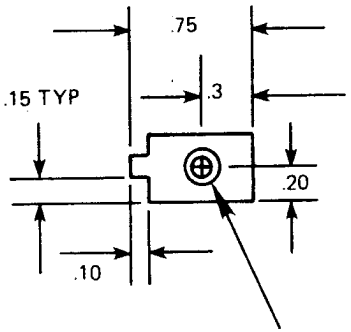

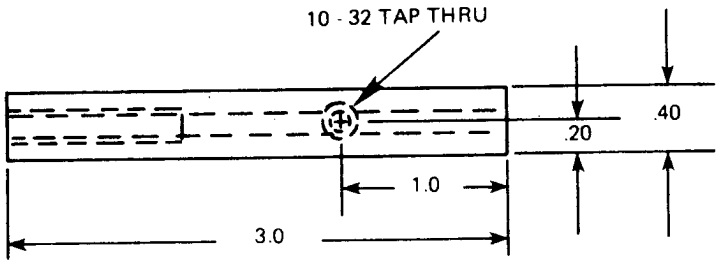

H03

1 PC
6061 T6

82-0344-V-10

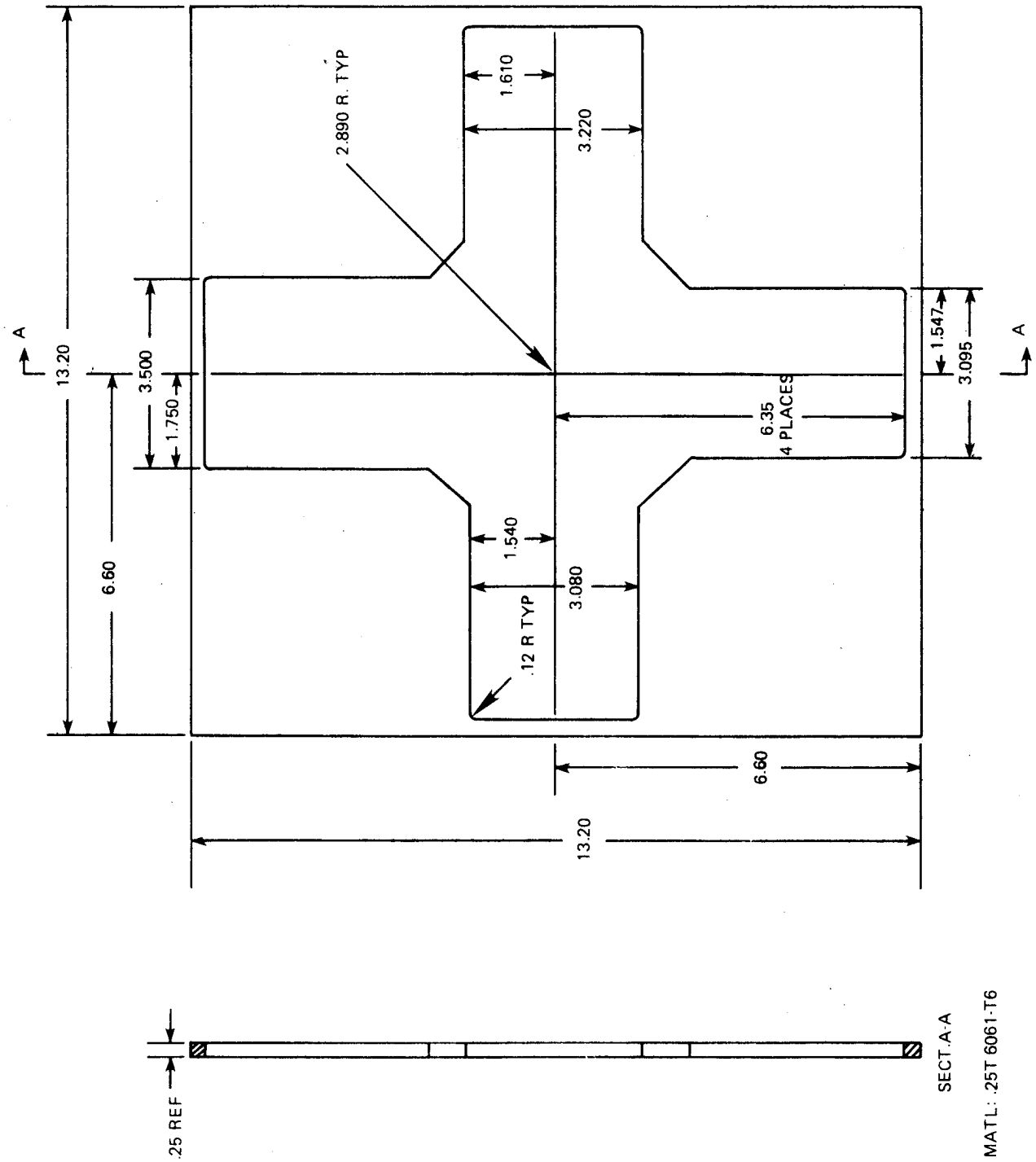
2.890 R. TYP
1.610
3.220
A
13.20
3.500
1.750
6.60
1.547
3.095
A
6.35
4 PLACES
1.540
3.080
.12 R TYP
6.60
13.20
.25 REF
SECT A-A
MATL: .25T 6061-T6

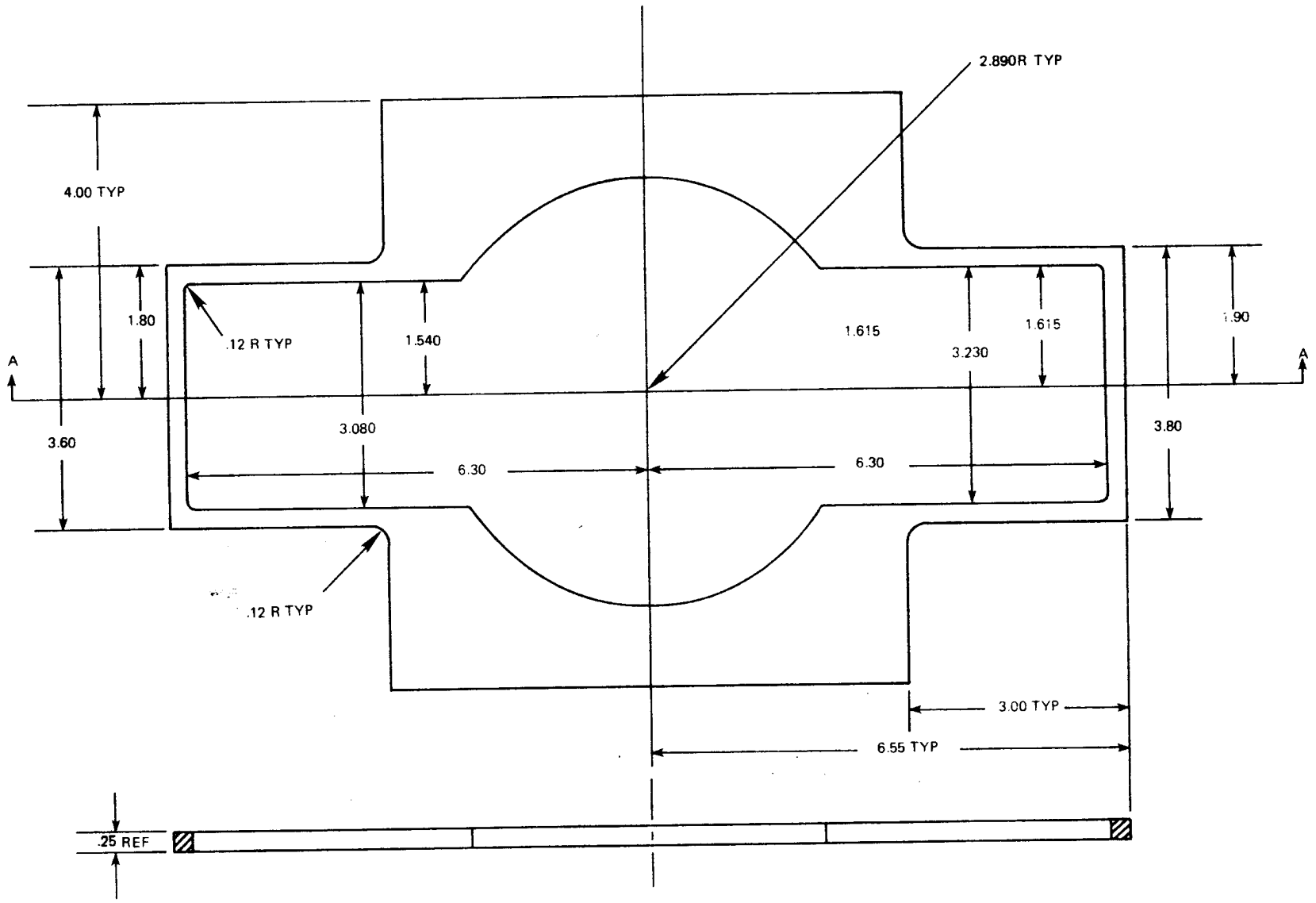

SECT A-A

ALIGNMENT TOOL, COMPOSITE GIMBAL
SK-TFG-073181-1

MATL: .25 THICK 6061 T6

82-0344-V-4

APPENDIX C

TEST FIXTURE DRAWINGS

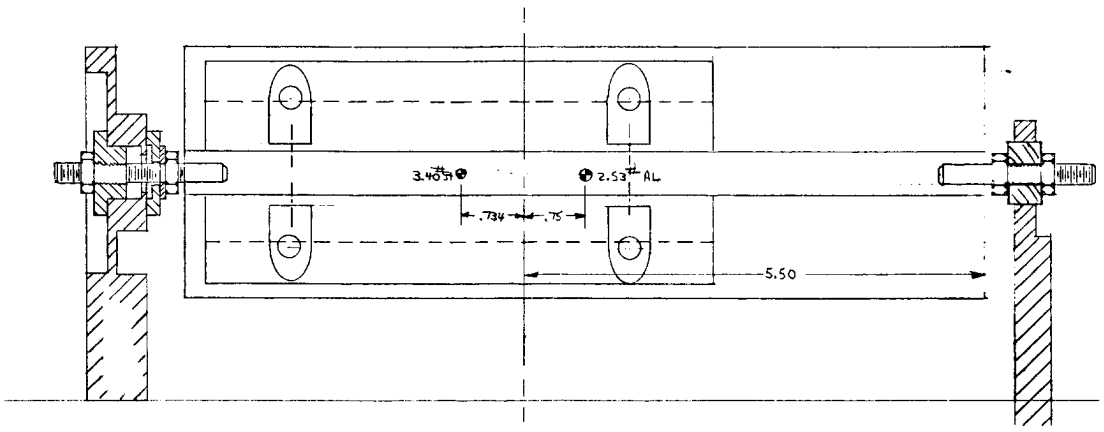

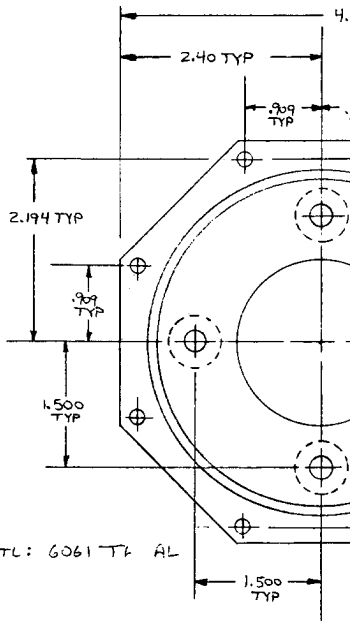

MATL: 6061 T6 AL

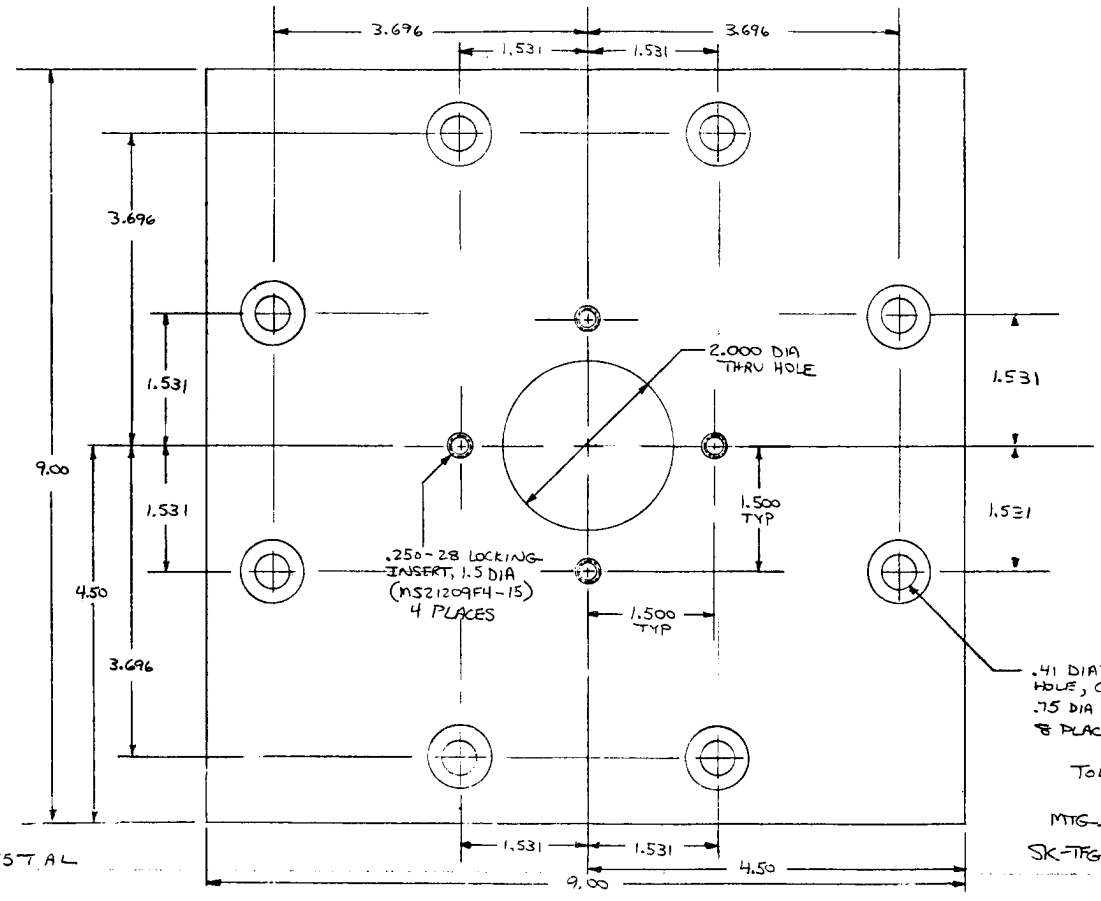

MATL: .75 T AL

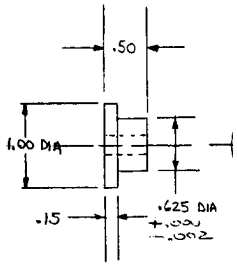

MATL: CARBON STEEL ROD

1 PC

TOL: XX = ±.02
XXX = ±.005

MTG. PLATE

SK-TFG-070281-5

1 PC

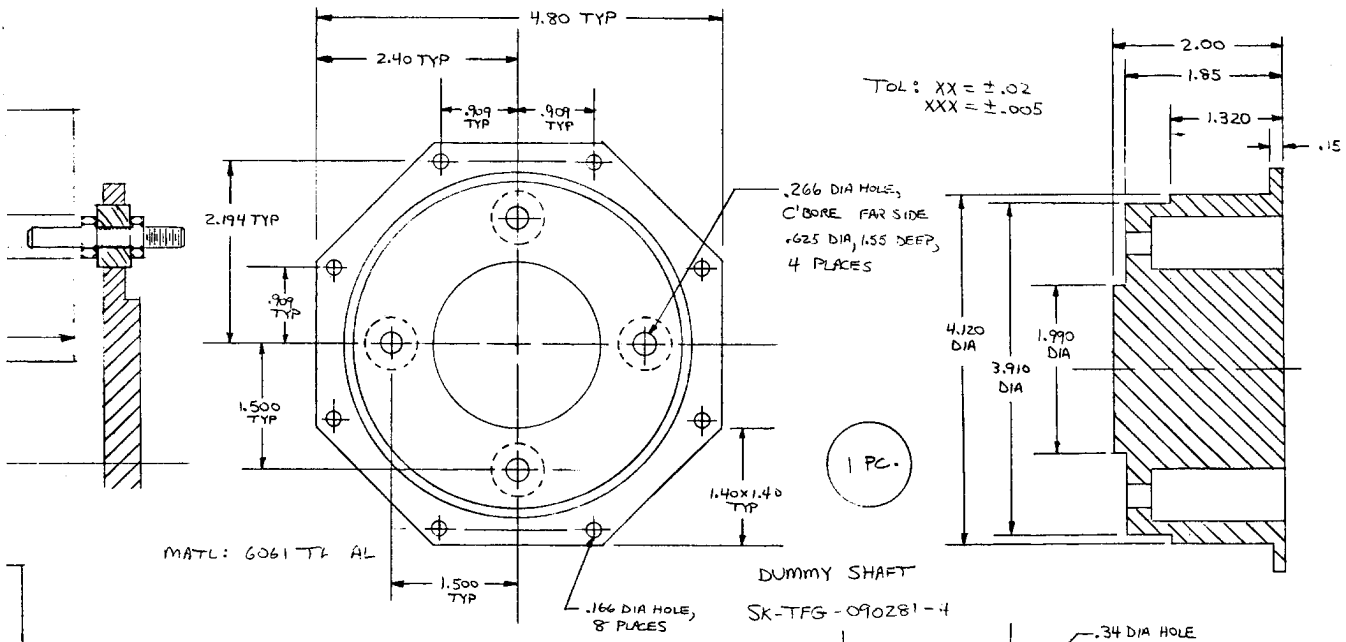

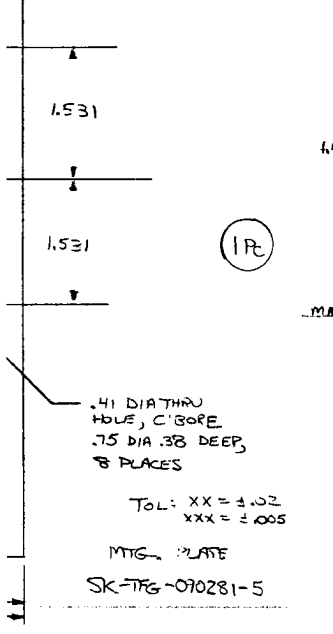

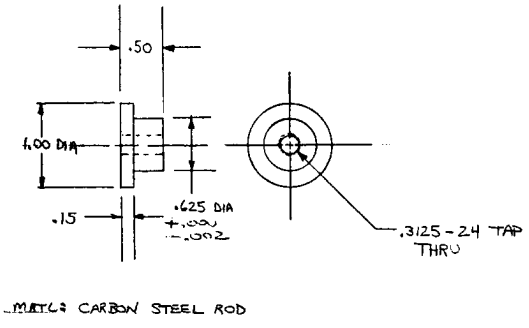

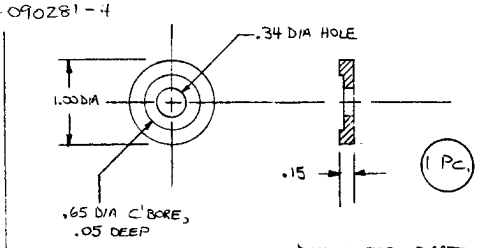

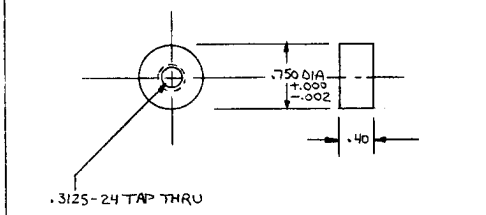

TOLERANCES: ALL PARTS
XX = ±.02
XXX = ±.005

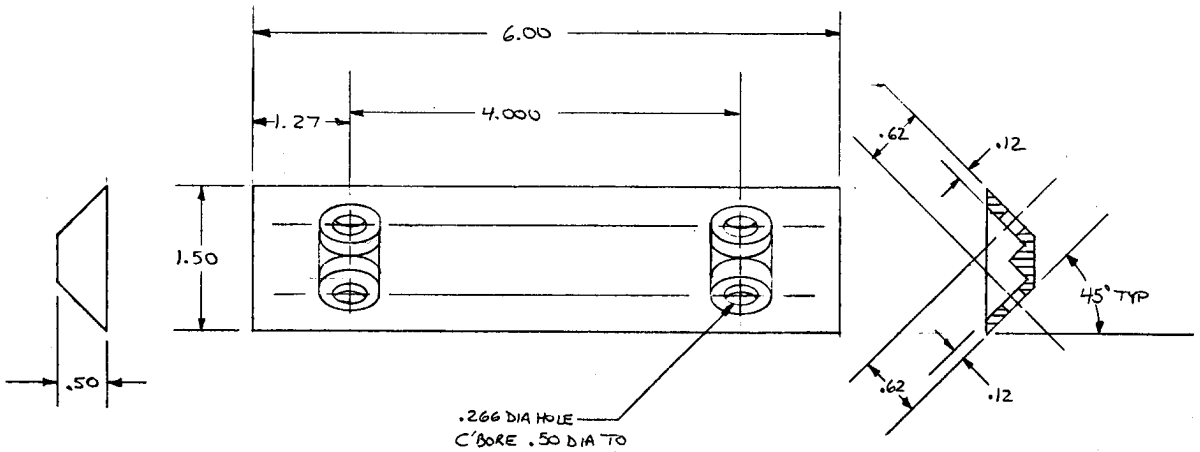

MATL: CARBON STEEL

4 PCS.

EL WEIGHT

SK-TFG-090381-4

TOL: XX = ± .02
XXX = ± .005

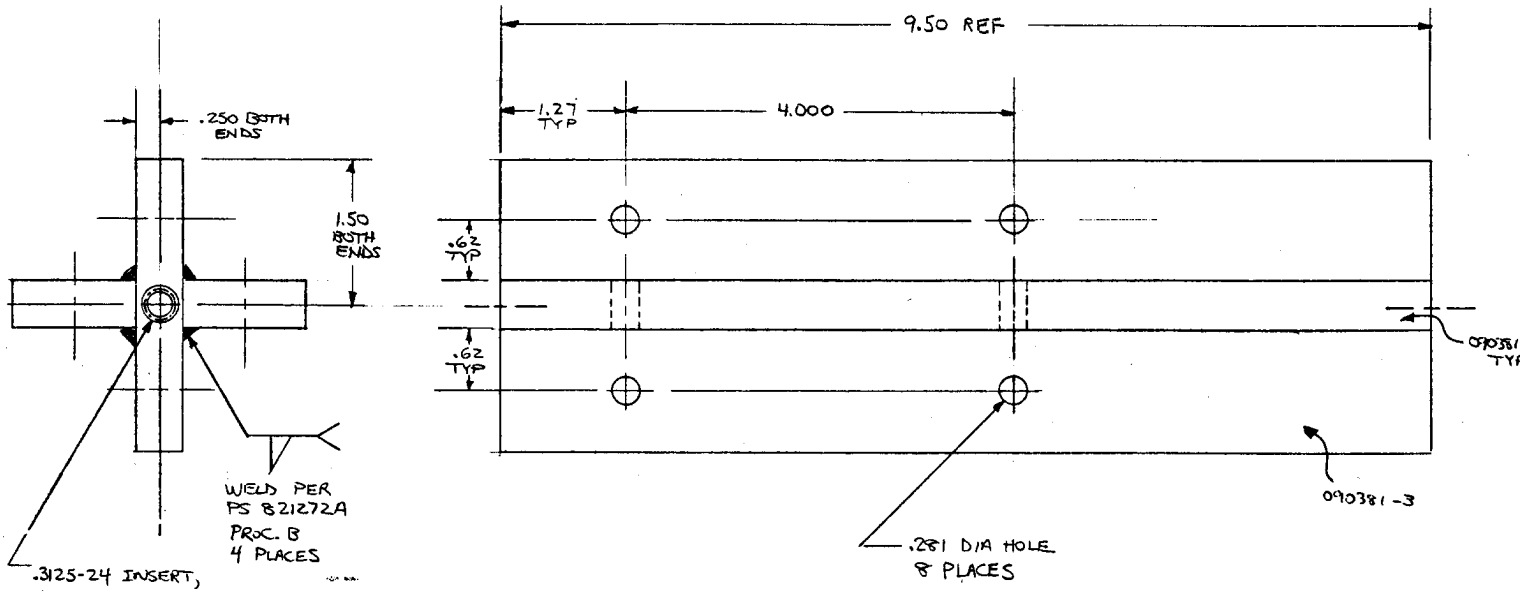

DUMMY EL ASSY.

SK-TFG-090381-1

TOL: XX = ± .02
XXX = ± .005

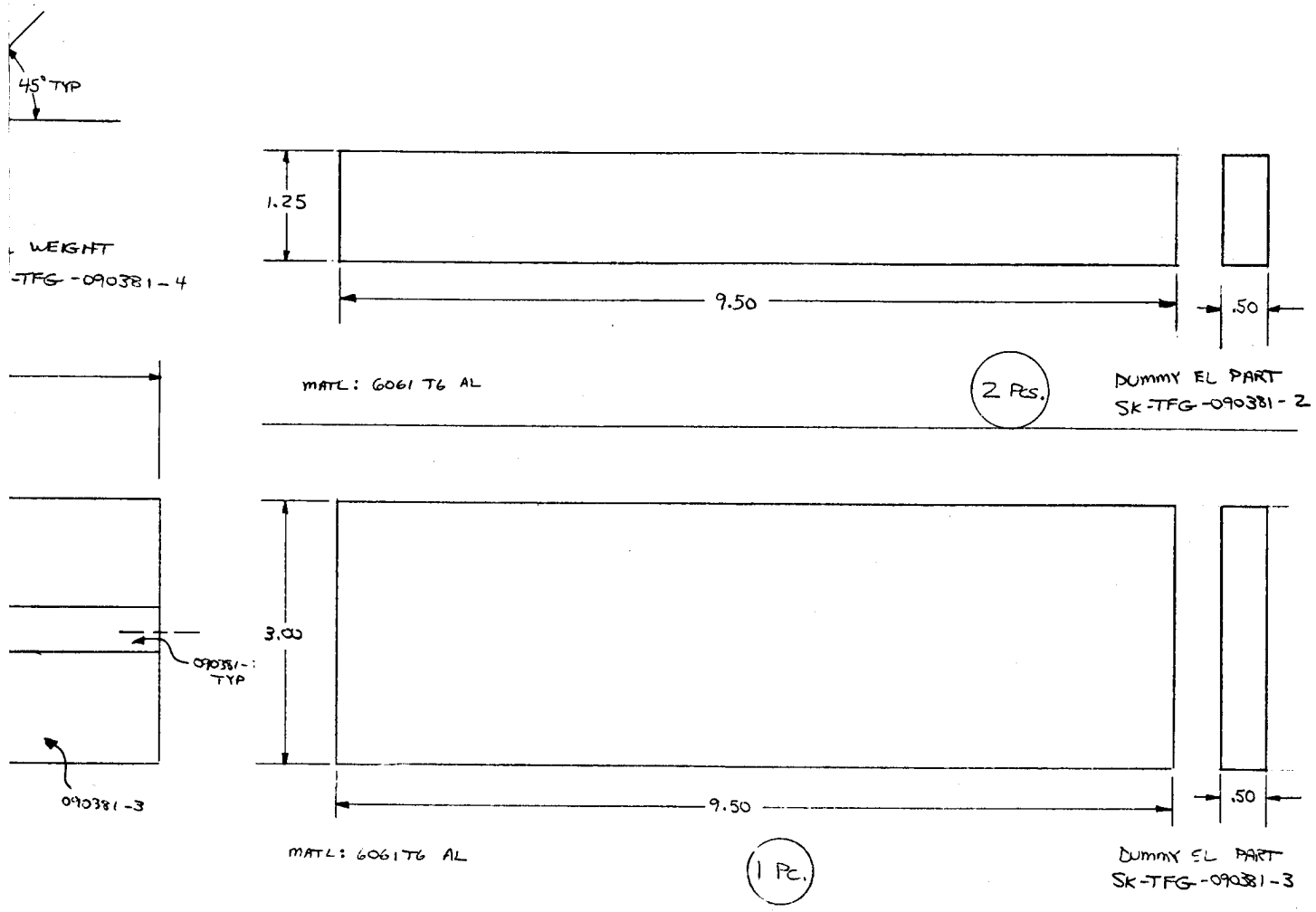
45° TYP
WEIGHT
-TFG-090381-4
1.25
9.50
.50
MATL: 6061 T6 AL
2 Pcs.
DUMMY EL PART
SK-TFG-090381-2
3.00
090381-
TYP
090381-3
9.50
.50
MATL: 6061 T6 AL
1 Pc.
DUMMY EL PART
SK-TFG-090381-3